Quantum states, dynamics and measurement

Build the connection between preparation, time evolution and measurement. Develop the algebra, approximations and scattering theory needed to predict a spectrum or a set of count rates.

Contents

1. **From two-path interference to the geometry of a quantum state**
   Two preparations give the same counts at one analyser. Place a second analyser in a rotated basis and the counts separate. From this experiment develop amplitudes, phase, projective measurement, mixed states and the geometry of distinguishability.
2. **What a momentum eigenstate means in a finite experiment**
   A detector never counts a perfectly sharp momentum eigenket. Derive continuum normalisation from a finite box, change the spectral measure from momentum to energy and predict the full evolution of a normalisable Gaussian packet.
3. **Why an oscillator can move without its packet spreading**
   Start with the measured mass and curvature of a potential. Factor its Hamiltonian, prove the energy ladder, construct a freely moving Gaussian from number states and find when squeezing or anharmonicity changes that prediction.
4. **Adding angular momentum and predicting which lines can appear**
   A three-component orbital wavefunction combines with a two-component spin. Derive the allowed total angular momenta, construct their amplitudes explicitly and predict both forbidden transitions and relative strengths in a polarisation-resolved spectrum.
5. **From a Coulomb orbit to the fine-structure multiplet**
   Separate the hydrogenic Schrödinger equation, identify the origin of its large degeneracy and evaluate the three dominant relativistic corrections. The cancellation among them predicts an equality that spectroscopy can then test.
6. **When a magnetic field changes the quantum numbers of an atom**
   Weak-field Zeeman slopes label total-angular-momentum multiplets. At stronger fields those slopes curve and intensities migrate. Solve an entire orbital-plus-spin manifold and infer coupling constants from measurable line positions and polarisation.
7. **Two electrons, exchange splitting and the cost of localisation**
   Build a two-electron state that respects exchange, derive its charge and spin correlations, and then solve a two-site model exactly. The two examples reveal when a triplet is favoured and when an apparently weak hopping lowers the singlet instead.

8. ## From a finite pulse to a continuum transition rate

Switch a weak perturbation on for a measured duration. Its Fourier transform determines the amplitude of a discrete transition. Summing over a dense set of final states reveals where a time-independent transition rate comes from and where it fails.

9. ## Inferring a short-range interaction from elastic scattering

A beam of neutral particles encounters a weak, localised static potential. Derive differential cross section from current, extract phase shifts by radial matching and compare exact low-energy scattering with the Born approximation and its failure near a bound state.

10. ## Distinguishing entanglement from ordinary shared randomness

Two distant analysers sometimes agree even when individual outcomes look random. Derive which correlations shared classical information can produce, compute the quantum prediction and identify what a finite table of coincidence counts can establish.

11. ## How an unobserved environment changes a quantum state

Model a qubit and a two-state environment by a joint unitary. Derive channels, the continuous-time master equation and the relation between longitudinal and transverse relaxation. A recorded event and an unread detector produce different conditional predictions.

12. ## How a turning point supplies the missing semiclassical phase

Far from a turning point the wavelength follows the classical momentum. At the turning point that approximation becomes singular. Derive the Airy connection, quantise a smooth well, distinguish a hard wall and estimate a tunnelling exponent with a defensible error check.

13. ## Measure geometric phase from three spin overlaps

A numerical eigensolver is free to choose a new complex phase for every eigenvector. A product of three measured overlaps removes these arbitrary choices. Relate its argument to a spherical triangle, then see why a vanishing overlap destroys phase information.

14. ## From electron exchange to atomic shells and molecular binding

An orbital model can explain why a closed atomic shell is special and why a shared electron can bind two protons. Both predictions need an energy as well as a rule for counting states. We construct the energies and check them against their separated-particle limits.

15. ## The scattering integral equation and successive Born terms

A weak potential often produces an angular pattern resembling its Fourier transform. What controls that approximation? A particle can propagate between two interactions with the same potential. Accounting for that propagation builds an integral equation and supplies a calculable second term.

16. ## Spontaneous radiation, stimulated transitions and thermal detailed balance

A coherent laser can drive Rabi oscillations in two atomic levels. A large cavity filled with thermal radiation presents many modes with random phases. In this limit one can infer the ratios of absorption, stimulated emission and spontaneous emission coefficients by requiring the observed equilibrium to be independent of the atoms used to probe it.

17. Which properties of an unknown spin can an instrument copy?

A device calibrated with spin up and down can write two perfectly distinguishable records. Asking what happens to a superposition reveals a limit on information extraction and explains why state tomography needs an ensemble.

Quantum states, dynamics and measurement · 1. From two-path interference to the geometry of a quantum state

Two preparations give the same counts at one analyser. Place a second analyser in a rotated basis and the counts separate. From this experiment develop amplitudes, phase, projective measurement, mixed states and the geometry of distinguishability.

Begin with an experiment that can distinguish two preparations

A single photon enters a lossless interferometer and can take either an upper or a lower path. Think of the paths as two distinguishable spatial modes labelled $0, 1$, with equal travel times unless a phase shifter is inserted. Record one binary result from each freshly prepared photon. Our model predicts outcome frequencies over many repetitions. A preparation that always follows path 0 is represented by $|0\rangle$, one that always follows path 1 by $|1\rangle$. Orthonormality, $\langle i|j\rangle = \delta_{ij}$, encodes perfect distinguishability by a path measurement. A general pure preparation has two complex amplitudes,

$$|\psi\rangle = a|0\rangle + b|1\rangle,$$

with $|a|^2 + |b|^2 = 1$. The probability rule $P(0) = |a|^2$ and its partner for path 1 are physical postulates. Linear algebra lets us derive testable consequences of them; it does not derive probability from arithmetic alone.

Take preparation A with $a = b = 1/\sqrt{2}$. For preparation B choose either path with ordinary probabilities one half using a classical random switch. A detector placed directly in either arm records equal count rates for A and B. One shared probability distribution is therefore insufficient to identify the state. To discriminate the preparations, bring the paths together at a lossless recombiner. Choose its phase references so an incoming $|0\rangle$ emerges as $(|0\rangle + |1\rangle)/\sqrt{2}$, while $|1\rangle$ emerges as $(|0\rangle - |1\rangle)/\sqrt{2}$. The matrix $H = 2^{-1/2}\left(\begin{smallmatrix} 1 & 1 \\ 1 & -1 \end{smallmatrix}\right)$ is unitary because its columns are orthonormal. Other beam-splitter conventions put factors of i on reflection; a consistent set of propagation phases yields the same observed fringes.

Insert a relative phase ϕ on the lower path in preparation A. After recombination the amplitudes are $(1 + e^{i\phi})/2$ and $(1 - e^{i\phi})/2$. Multiplying each by its complex conjugate gives

$$P(0) = \frac{1 + \cos\phi}{2},$$

$$P(1) = \frac{1 - \cos\phi}{2}.$$

For preparation B each possible input produces equal exit probabilities. Averaging those probabilities leaves a constant one half at both ports for every phase. The contrast term results from multiplying the sum of amplitudes by its conjugate. Summing probabilities over alternatives is justified when the alternatives correspond to distinct preparations, or when a physical record distinguishes the two paths and that record is ignored. Confusing these operations predicts a fringe in the random-switch experiment. Counting both outputs checks normalisation independently of visibility, provided detector efficiencies have been calibrated.

At $\phi = \pi/3$, 400 independently prepared photons from A have expected output-0 count 300 and binomial standard deviation $\sqrt{400(3/4)(1/4)} = 8.66$. Preparation B predicts 200 with standard deviation 10. Repeating the measurement at $-\pi/3$ gives exactly the same probabilities: an analyser sensitive only to the cosine cannot determine the sign of the phase. Add a known $\pi/2$ offset before one further run. It converts a

sine into a cosine and removes that ambiguity. This simple experiment is a model of tomography, the recovery of state parameters from several distinct measurement settings.

Remove the phase that no ideal analyser can observe

Let a downstream analyser transmit normalised state $|v\rangle$. Born's rule gives transmission probability $|\langle v|\psi\rangle|^2$. Replacing the entire preparation by $e^{i\gamma}|\psi\rangle$ multiplies the overlap by a phase but leaves its squared modulus invariant for every v. Physical pure states are therefore rays. Relative phases survive because changing the phase of only one term is not multiplication of the whole vector by the same number. A basis vector itself may be assigned an arbitrary phase if its coordinates and every operator matrix are transformed consistently. Such a convention change cannot affect the phase measured relative to an actually inserted optical delay.

A unit vector in two complex dimensions has four real components. Normalisation removes one degree of freedom and the common phase removes another. Away from the coordinate poles a convenient parametrisation is

$$|\psi(\theta,\varphi)\rangle = \cos(\theta/2)|0\rangle + e^{i\varphi}\sin(\theta/2)|1\rangle, \qquad 0 \le \theta \le \pi.$$

Projecting onto $|0\rangle$ gives $(1+\cos\theta)/2$. The corresponding point on the unit sphere has coordinates $\mathbf{r} = (\sin\theta\cos\varphi, \sin\theta\sin\varphi, \cos\theta)$. Orthogonal states sit at opposite ends of a diameter. Their resulting angle in ordinary three-space is π, while their angle defined from the Hilbert-space overlap is $\pi/2$. This factor of two is why the spinor parametrisation contains half angles. At the poles φ drops out of all probabilities. Attempting to estimate an azimuth of an exactly path-localised preparation is a singular parametrisation, rather than a failure of the experiment.

Represent the analyser for the pure direction $\mathbf{n}$ by the projector $P_{\mathbf{n}} = |v\rangle\langle v|$. Projectors satisfy $P^\dagger = P$ and $P^2 = P$. Let $\sigma_x, \sigma_y, \sigma_z$ be the Pauli matrices with products $\sigma_i\sigma_j = \delta_{ij}I + i\epsilon_{ijk}\sigma_k$. Then $P_{\mathbf{n}} = (I + \mathbf{n}\cdot\boldsymbol{\sigma})/2$. Since each Pauli matrix has zero trace and $\operatorname{tr}\sigma_i\sigma_j = 2\delta_{ij}$,

$$\operatorname{tr}(P_{\mathbf{r}}P_{\mathbf{n}}) = \frac{1+\mathbf{r}\cdot\mathbf{n}}{2} = \cos^2(\gamma/2),$$

where γ is the spatial angle between the two directions. Thus transmission through a rotated analyser determines an inner product between real geometric directions, even though the original amplitude was complex. The vector for a path interferometer describes a two-dimensional mode space; rotating it need not mean physically rotating the entire apparatus in the laboratory.

Differentiate a probability from the state after a measurement

For an ideal projective measurement $\{P_j\}$, mutually orthogonal projectors sum to the identity. The probability of result j in a pure state is $\langle\psi|P_j|\psi\rangle$. Conditional on actually observing that result, the state for subsequent predictions in an ideal repeatable experiment is $P_j|\psi\rangle/\sqrt{p_j}$, provided $p_j > 0$. Applying the same measurement immediately gives the same result with probability one, because $P_j^2 = P_j$. Measuring a different observable in between can change the answer. The formula for an ideal repeatable measurement is an assumption about the measuring device as well as about the observable. An absorbing photon counter

ends the photon's trajectory, so a sequential model applies to a nondestructive analyser or to a filtered ensemble prepared in the transmitted state.

Prepare $|0\rangle$ and then sequentially measure a direction tilted 60° from $+z$, followed by z. If one keeps only the positive tilted outcome, three quarters of the original ensemble survive the selection. Among those survivors the fraction with final $+z$ is again three quarters. The joint probability of both positives is $9/16$; reporting $3/4$ for this joint event would discard the probability cost of selection. If all outcomes of the intermediate measurement are retained but unread, half is no longer the right default either. One must add over both paths of recorded outcomes. The final $+z$ probability is

$$(3/4)^2 + (1/4)^2 = 5/8.$$

Without the intermediate device it would be one. Removing data after a measurement and removing the measurement itself are experimentally different operations.

For a broad outcome corresponding to several basis states, a projector can preserve coherence inside the accepted subspace. Suppose a three-mode preparation is $(|0\rangle + |1\rangle + |2\rangle)/\sqrt{3}$. A device that only asks whether the state is in the span of $0, 1$ accepts with probability $2/3$ and ideally transmits $(|0\rangle + |1\rangle)/\sqrt{2}$. A device measuring the individual paths and later combining their labels into “accepted” yields the same acceptance probability but no surviving phase relation between 0 and 1 unless its record is coherently erased. A recombiner acting on the accepted ensemble distinguishes the implementations. An observable's probability table by itself does not specify every disturbance produced by a physical instrument.

Recover a state matrix from three families of counts

For a classical mixture of pure preparations $|\psi_j\rangle$ with weights w_j, average their individual probabilities. The result is $\mathrm{tr}(\rho P)$ with $\rho = \sum_j w_j |\psi_j\rangle\langle\psi_j|$. This matrix has trace one, is Hermitian and has nonnegative expectation on every vector. Changing the ensemble decomposition without changing ρ makes no difference to any measurement performed on the system alone. Preparation B is $I/2$. A 50:50 mixture of the two opposite x-analysed states is the same matrix. Trying to infer which randomisation mechanism was used requires access to its preparation record.

Every Hermitian two-state density matrix of trace one has the form $\rho = (I + \mathbf{r}\cdot\boldsymbol{\sigma})/2$. Diagonalise along $\mathbf{r}$. The eigenvalues are $(1 \pm |\mathbf{r}|)/2$. Positivity is therefore equivalent to $|\mathbf{r}| \le 1$. Interior points correspond to mixtures and surface points to pure states. Measuring σ_i gives $p_i^+ = (1 + r_i)/2$, so three noncoplanar analyser directions suffice to reconstruct an otherwise unknown two-level state given enough identically prepared copies. Noncommutation places no obstacle to using independent copies for these settings.

For 1000 trials per direction take $n_x^+ = 740,\ n_y^+ = 320,\ n_z^+ = 750$. The linear estimates are

$$r_x = 0.48,\ r_y = -0.36,\ r_z = 0.50.$$

Their length is

$$\sqrt{0.61} = 0.7810.$$

The eigenvalues are 0.8905 and 0.1095. The probability for $\mathbf{n} = (3/5, 4/5, 0)$ is $1/2$ even though the state has strong coherence in the path basis. The setting is accidentally perpendicular to its transverse projection.

A fourth such measurement supplies an out-of-sample check of state preparation and analyser calibration. If finite data instead give $|\mathbf{r}| > 1$, a negative estimated eigenvalue signals statistical inconsistency with exact physical probabilities. Fitting all binomial data under $|\mathbf{r}| \leq 1$ retains a physical model. Clipping each Cartesian expectation separately fails to enforce the spherical constraint.

Recover a phase from a closed loop of projections

There is phase information that cannot be associated with any one point on the sphere. For three nonorthogonal preparations A, B, C, the complex product $G = \langle A|B\rangle\langle B|C\rangle\langle C|A\rangle$ is unchanged by independent phase changes of the three state vectors. The phase acquired in each overlap cancels from the complete product. A loop of conditional projections can therefore have an observable phase relative to a reference arm even if every intermediate selection probability depends only on a modulus. The probability of successfully traversing the filtered path also matters for the attainable interference contrast.

Take $A = |0\rangle,\ B = (|0\rangle + |1\rangle)/\sqrt{2},\ C = (|0\rangle + i|1\rangle)/\sqrt{2}$. The overlaps are $1/\sqrt{2}, (1+i)/2, 1/\sqrt{2}$. Their product is $(1+i)/4$, giving phase $+\pi/4$. Traversing the reversed overlap product gives its complex conjugate and changes the sign. The directed path in a laboratory must be matched carefully to the order of bra and ket in the adopted product. If the analysers actually project a state in the order $A \to B \to C \to A$, the amplitude in the reference convention is $\langle A|C\rangle\langle C|B\rangle\langle B|A\rangle = G^*$. A path with a zero overlap has zero surviving interference amplitude and an undefined phase. This condition prevents interpreting a phase jump at a dark output as a measured singular rotation of a physical state.

Design the best analyser for discriminating two known signals

Imagine a source chosen at random from two calibrated preparations ρ_0, ρ_1 with known prior probabilities η_0, η_1. One copy arrives; the task is to guess which preparation was used and minimise the probability of a wrong guess. This differs from estimating all unknown entries of a state matrix from many repetitions. For example, with highly unbalanced priors the best choice may be to guess the more common preparation after many different measured outcomes. A measurement along the direction connecting the two Bloch vectors is optimal for equal priors under the criterion derived below, but generally need not be a universal optimal analyser for other decisions.

Let a binary measurement have two positive effects $E_0, E_1 = I - E_0$, where the eigenvalues of E_0 lie between zero and one. These positive-operator-valued effects give probabilities $\mathrm{tr}(\rho E_j)$, extending projectors to include randomisation or coarse responses. Adopt the decision rule of reporting label j after measurement result j. The average probability of success is then

$$P_{\mathrm{good}} = \eta_0 \,\mathrm{tr}(E_0\rho_0) + \eta_1 \,\mathrm{tr}[(I - E_0)\rho_1] = \eta_1 + \mathrm{tr}(E_0\Delta),$$

$$\Delta = \eta_0\rho_0 - \eta_1\rho_1.$$

Diagonalise the Hermitian Δ. The trace depends only on diagonal elements of E_0 in this basis. Each lies in $[0, 1]$. To maximise the sum, take one for positive eigenvalues and zero for negative ones. The resulting projector is an allowed measurement, proving optimality rather than only providing an upper bound. Zero eigenvalues permit arbitrary treatment without changing average success. Since the sum of positive eigenvalues equals $[\|\Delta\|_1 + \mathrm{tr}\,\Delta]/2$, substitution gives

$$P_{\mathrm{good}}^{\max} = (1 + \|\Delta\|_1)/2.$$

The trace norm here is the sum of singular values; for this Hermitian matrix the singular values are absolute eigenvalues. This operational meaning explains why trace distance between preparations appears repeatedly when comparing quantum processes.

For two equally likely pure states of overlap magnitude $c = |\langle\psi_0|\psi_1\rangle|$, use the two-dimensional span of the states. The eigenvalues of $\Delta = (\rho_0 - \rho_1)/2$ are $\pm\sqrt{1-c^2}/2$. Consequently $P_{\text{good}}^{\max} = [1 + \sqrt{1-c^2}]/2$. Orthogonal states can be perfectly distinguished. Identical preparations attain success one half, exactly the prior random-guess limit. For a concrete optical example let preparation 0 be $|0\rangle$ and preparation 1 be $\cos 30^\circ|0\rangle + \sin 30^\circ|1\rangle$. Their Hilbert-space overlap is $\sqrt{3}/2$, while the Bloch vectors have a spatial separation angle of 60°. The best success probability is $3/4$. Measuring the path basis instead and reporting 0 whenever it transmits yields success $[1 + \sin^2 30^\circ]/2 = 0.625$. The best analyser deliberately allows some errors on both sources to reduce the average error over the pair.

The physical realisation is simple in this example. The difference of Bloch vectors is $(-\sqrt{3}/2, 0, 1/2)$, already of unit length. Use that direction for the positive projector labelled 0. Its dot product with the preparation-0 vector is $+1/2$, and with the preparation-1 vector is $-1/2$, giving correct guess probability $3/4$ for either source independently. The sign of this vector matters because it assigns the outcome label. Reversing the analyser axis and interchanging the decision labels leaves the same performance. An experimental confusion matrix recording each conditional outcome rate checks considerably more than an aggregate fraction of successful guesses, particularly if the priors in the actual source differ from those in the calibration trial.

If two independent copies of the same unknown signal can be stored and measured jointly, the pure-state overlap becomes c^2. The optimum success rises to $[1 + \sqrt{1-c^4}]/2$. For the previous optical example this is about 0.831. The calculation assumes both copies were identically prepared from one shared unknown label. It would be invalid if each copy came from a newly and independently drawn source label. Such a distinction arises naturally when comparing a two-photon coincidence experiment with two unrelated records in a database. Increasing the number of independent preparations for tomography and increasing copies available per individual discrimination decision are different resources.

Calibrate an imperfect path detector with its classical record intact

An ideal path measurement perfectly distinguishes the two modes and destroys their mutual coherence in an unread outcome. A tunable weaker measurement provides an intermediate experiment linking information and disturbance quantitatively. Suppose an instrument reports $+$ or $-$ with operators $M_+ = \mathrm{diag}(\sqrt{(1+d)/2}, \sqrt{(1-d)/2})$ and $M_- = \mathrm{diag}(\sqrt{(1-d)/2}, \sqrt{(1+d)/2})$, in the path basis, with $0 \le d \le 1$. Squaring and summing gives identity, so probabilities normalise for every input. Applied separately to the known 0 and 1 calibration sources, the $+$ result occurs with probabilities $(1+d)/2$ and $(1-d)/2$; their difference measures d. At zero this detector returns an independent coin flip; at one it reads the path without misclassification.

For an input with Bloch component z, the result probability is

$$p_+ = (1 + dz)/2.$$

Conditional on that result, the path-0 and path-1 weights must be renormalised by p_+. The new longitudinal component and transverse coherence satisfy

$$z' = \frac{z + d}{1 + dz}, \qquad (\rho_{01})' = \frac{\sqrt{1 - d^2}}{1 + dz}\,\rho_{01}.$$

If the outcome is unread, the map is the sum of both $M_j \rho M_j^\dagger$. The populations are unchanged and the off-diagonal entry becomes $\sqrt{1 - d^2}\rho_{01}$. A balanced pure input consequently gives a recombiner fringe visibility $\sqrt{1 - d^2}$. This equality links this calibrated detector's ability to distinguish path preparations with the contrast left in a complementary measurement. It depends on the chosen instrument being a minimal diagonal measurement. A device with the same two outcome probabilities can also apply an uncontrolled relative phase, yielding a smaller visibility. The existence of such instruments is why probability effects alone do not determine post-measurement states.

Choose $d = 0.60$ and a balanced pure $+x$ input. Either outcome has probability one half. Given $+$, the new state has $z' = 0.60$ and $x' = 0.80$, so it is pure. The other branch has $z' = -0.60, x' = 0.80$. If the outcomes are ignored their average has $\mathbf{r} = (0.80, 0, 0)$, which is mixed. Feeding each branch through a separate calibrated rotation can align both with the original $+x$ direction, restoring full visibility when the input is known. This feed-forward preparation does not invert arbitrary unknown states through a closed deterministic quantum map; it makes use of the recorded result and knowledge of the preparation. A single fixed rotation cannot increase the purity of the unread mixture because unitaries preserve the eigenvalues of ρ.

There is also a practically important calibration ambiguity. Suppose a perfect projective path detector is followed by a classical reporting error which flips the stored label with probability $(1 - d)/2$. Its outcome rates on every input agree exactly with those of the weak instrument above. But its unrevealed physical interaction has already produced orthogonal environmental records of the true path; unread coherence is then zero for every value of the classical label reliability. Test the distinction by preparing a known balanced superposition, measuring with the candidate instrument and recombining its exits while retaining both count channels. Matching path-classification accuracy cannot substitute for this separate disturbance test. Conversely observing reduced visibility alone does not reveal whether useful path information is accessible in the recorded labels.

Count statistics when the analyser itself has a bias

Suppose the final binary detector has efficiency ϵ_0 at port 0 and ϵ_1 at port 1. If lost events are discarded and only a ratio of recorded clicks retained, the observed fraction is $p_{\mathrm{obs}} = \epsilon_0 p / [\epsilon_0 p + \epsilon_1 (1 - p)]$. At a balanced state unequal efficiencies can imitate a longitudinal preparation bias. For $p = 1/2, \epsilon_0 = 0.90, \epsilon_1 = 0.75$, after selection the recorded port-0 fraction is

$$0.90/1.65 = 0.5455.$$

Treating it as an ideal probability would infer $z = 0.091$. Collecting arbitrarily many photons reduces the scatter about that biased result without reducing the bias itself.

A measured ratio from an independently characterised balanced reference can determine relative efficiency $r = \epsilon_0/\epsilon_1$. In odds form $p_{\mathrm{obs}}/(1 - p_{\mathrm{obs}}) = r\,p/(1 - p)$. If the reference is unavailable but a known unitary exchanges the measurement ports, record a second measurement on the same preparation with that exchange. Its observed odds are $r(1 - p)/p$. Their product is r^2; their ratio is $[p/(1 - p)]^2$. Thus the two

runs can separate relative gain and true probability, provided the gain and preparation remain stable across them. For observed odds 1.8 and 0.8 one obtains $r = 1.2$ and true odds 1.5, hence $p = 0.60$. Stability is testable by alternating the two settings across the acquisition instead of making one long run after the other. This class of self-calibrating measurement is useful far beyond a two-path interferometer; the proposed physical symmetry is built into both the inversion formula and its independent checks.

Reconstruct a state and check positivity

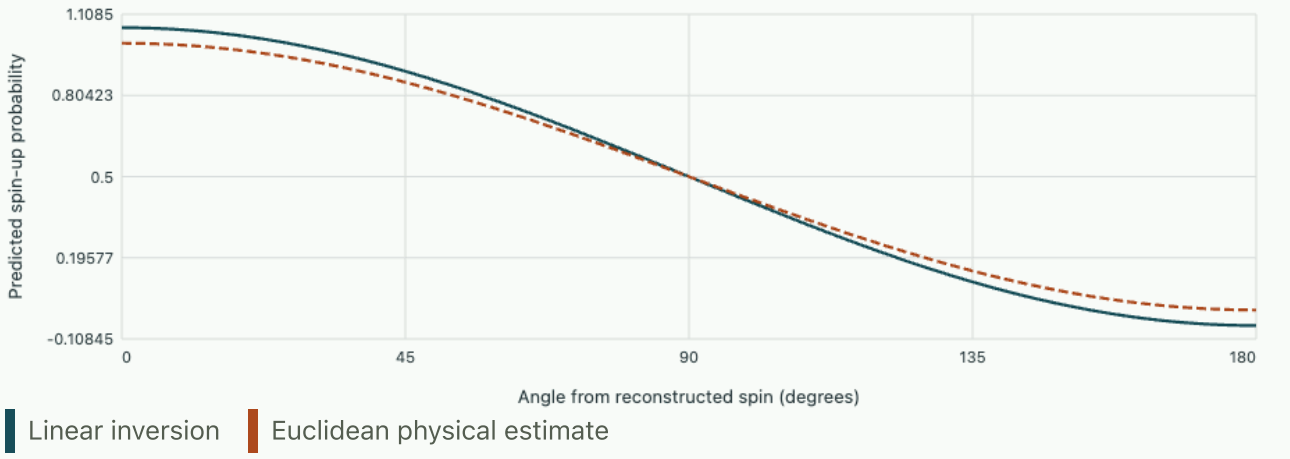
Change the recorded counts along two spin axes. Determine whether the inferred state can predict valid probabilities for every fourth analyser setting.

Open this experiment online

Try the calculation

Up counts along y (out of 25) **19**

Up counts along z (out of 25) **19**



Reconstructed Bloch radius 1.1164. Eigenvalues 1.0582 and -0.058211.

Separate component uncertainty from experimental readout resolution

A variance bound can be proved directly from Hilbert-space geometry without assuming a model of a particular measurement apparatus. For a normalised pure state set $|u\rangle = (A - \langle A\rangle)|\psi\rangle$, $|v\rangle = (B - \langle B\rangle)|\psi\rangle$, for observables and states for which the required products exist. The squared norms are $(\Delta A)^2, (\Delta B)^2$. Cauchy–Schwarz bounds their product below by $|\langle u|v\rangle|^2$. Separating the real and imaginary parts of the inner product gives

$$(\Delta A)^2(\Delta B)^2 \geq \left|\frac{\langle [A,B]\rangle}{2i}\right|^2 + \left|\frac{1}{2}\langle \{\Delta A_{\mathrm{op}}, \Delta B_{\mathrm{op}}\}\rangle\right|^2,$$

where $\Delta A_{\mathrm{op}} = A - \langle A \rangle I$ denotes a centred operator rather than its scalar standard deviation. The real term is the squared symmetrised covariance. The commonly quoted commutator-only inequality drops this nonnegative contribution. The bound describes spreads across identical preparations; the electronics' error in reading a single outcome is a different quantity and enters an experimental analysis through the detection model.

For Pauli measurements $A = \sigma_x, B = \sigma_y$, the elementary lower bound on the product of variances is r_z^2, since $[\sigma_x, \sigma_y] = 2i\sigma_z$. The full covariance is $-r_x r_y$ because their anticommutator vanishes before centring. The actual product is $(1 - r_x^2)(1 - r_y^2)$. Subtracting the full lower bound leaves $1 - r_x^2 - r_y^2 - r_z^2$, directly testing the Hilbert-space positivity constraint on the Bloch vector. Every pure qubit saturates the full inequality for this pair, while a mixed interior state can give strict excess. A zero commutator expectation in a particular state does not prove that the two observables commute or can be jointly assigned precise values there. For $|+x\rangle$ one variance is zero, while the other is maximal.

Decide whether an apparent uncertainty violation is an instrument problem

A device reconstruction reports $r_x = 0.80,\ r_y = 0.60,\ r_z = 0.20$. Test the commutator-only bound, the full covariance inequality and the eigenvalue positivity condition. Why is testing the weaker bound alone insufficient?

▼ **Derive and check the result**

The measured components imply variances 0.36 and 0.64, with product 0.2304. The commutator-only bound is 0.04 and passes. The covariance-squared contribution is $0.8^2\,0.6^2 = 0.2304$, so the full bound is 0.2704 and fails by 0.0400. Independently $|\mathbf{r}|^2 = 1.04$ predicts a slightly negative eigenvalue. Finite count noise or inappropriate calibration can make separate empirical component estimates leave the physical Bloch ball even though every individual estimate lies in its allowed range. Check uncertainty regions jointly and, when fitting a physical state, retain measurement likelihoods and positivity. Satisfying one weaker inequality cannot certify that all estimated outcomes come from a common quantum preparation.

Tutorial · use interference, sequential selection and tomography

Infer visibility and a path-coherence phase

An equal-population path state gives normalised output-0 probabilities 0.80 with zero phase offset and 0.70 after applying $+\pi/2$ to path 1. With the recombiner convention above, find the complex density matrix entry ρ_{01}, its allowed magnitude, and the highest achievable output probability.

▼ **Work through the solution**

The phase plate sends ρ_{01} to $e^{-i\phi}\rho_{01}$, so $p_0 = 1/2 + \mathrm{Re}(e^{-i\phi}\rho_{01})$. The observations give real part 0.30 and imaginary part 0.20. Its magnitude is 0.3606, below the positivity bound $\sqrt{\rho_{00}\rho_{11}} = 0.5$. The maximum exit probability is 0.8606, obtained when the phase offset cancels the argument of ρ_{01}; here $\phi = \arctan(2/3) = 33.7^\circ$. The minimum is 0.1394. The usual fringe visibility $(p_{\max} - p_{\min})/(p_{\max} + p_{\min})$ is 0.721. The shortfall from unity in ideal equal-population data measures reduced path coherence. Unequal

detection efficiencies or an unbalanced recombiner would need an independent calibration before drawing that conclusion from raw counts.

Is a succession of nearly parallel filters an efficient rotator?

Start in $+z$. Place N ideal positive-channel filters whose directions rotate in equal steps from $+z$ to $-z$ along a great circle. Find the transmitted fraction and evaluate it for $N = 2, 10$. Compare with applying a single final filter.

▼ **Work through the solution**

Adjacent directions differ by π/N, so each conditional transmission probability is $\cos^2(\pi/2N)$. All accepted states end at $-z$, with joint transmission $[\cos^2(\pi/2N)]^N$. For one filter overlap is zero. Two filters give $1/4$, whereas ten give about 0.7805. Taking logarithms gives $2N \ln\cos(\pi/2N) = -\pi^2/(4N) + O(N^{-3})$, tending to zero, so the ideal transmission tends to one. Each retained state has been prepared along the new axis by the filtering. Finite loss per filter eventually reverses the trend: multiplying by an efficiency 0.99^N penalises arbitrarily large N. Tracking both conditional and joint rates distinguishes this sequence from a unitary spin rotation.

Set an error bar on a prediction along a new direction

Use the three tomography runs above to predict p_+ for $\mathbf{n} = (3/5, 4/5, 0)$ with an approximate standard error. Test whether observing 535 positives in 1000 new trials is surprising at the level of a few standard deviations.

▼ **Work through the solution**

For a component estimate $r_i = 2n_i^+/N_i - 1$, the plug-in variance is $(1 - r_i^2)/N_i$ for independent binomial trials. Independent settings give $\mathrm{var}(\hat{p}) = \frac{1}{4}[0.36(1 - 0.48^2) + 0.64(1 - 0.36^2)]/1000 = 0.0002085$, or standard error 0.0144. The new fraction has sampling error about 0.0158. Comparing two independent estimates requires adding these variances, giving combined standard error about 0.0214. The discrepancy 0.035 is about 1.6 standard errors. Treating the reconstructed state as exactly known would overstate the evidence of miscalibration. For operational work near the Bloch-sphere boundary, a likelihood analysis handles correlations and positivity more accurately than this linear interior approximation.

Further reading

- Fließbach · Abstrakte Formulierung, Hilbert-space states and observables
- Cambridge · quantum foundations, density matrices and generalised measurements
- Course investigation · spin measurement and joint preparations

Quantum states, dynamics and measurement · 2. What a momentum eigenstate means in a finite experiment

A detector never counts a perfectly sharp momentum eigenket. Derive continuum normalisation from a finite box, change the spectral measure from momentum to energy and predict the full evolution of a normalisable Gaussian packet.

Follow a normalised state as its allowed box grows

Consider a particle moving in one spatial dimension. A periodic box of length L is a mathematical model for an observation made far from any reflecting wall. The inner product is the integral of $\psi^*(x)\chi(x)$ over the box. The momentum operator is $-i\hbar\, d/dx$ with periodic boundary conditions. Integration by parts cancels its boundary form for periodic differentiable functions. Its normalised modes $L^{-1/2}e^{ik_n x}$ have $k_n = 2\pi n/L$ and momenta $p_n = \hbar k_n$. Their overlap is one if the integers coincide and zero otherwise. Increasing L reduces the spacing $\Delta p = 2\pi\hbar/L$ but also reduces the amplitude of each individual box mode at a fixed position. If one simply replaces the Kronecker delta by a Dirac delta while carrying over $L^{-1/2}$, the units and probabilities will fail.

Let c_n be the unit-normalised amplitudes with $\sum_n |c_n|^2 = 1$. For a smooth normalisable packet the probability in an interval dp has a limit $|\phi(p)|^2 dp$. Thus $c_n \simeq \sqrt{\Delta p}\,\phi(p_n)$. Substituting in the synthesis sum and using $L\Delta p = 2\pi\hbar$ produces

$$\psi(x) = \frac{1}{\sqrt{2\pi\hbar}} \int_{-\infty}^{\infty} e^{ipx/\hbar}\phi(p)\, dp,$$

$$\phi(p) = \frac{1}{\sqrt{2\pi\hbar}} \int_{-\infty}^{\infty} e^{-ipx/\hbar}\psi(x)\, dx.$$

The distributions $\langle x|p\rangle = (2\pi\hbar)^{-1/2}e^{ipx/\hbar}$ have $\langle p|p'\rangle = \delta(p-p')$. The delta acts under integration; $\delta(0)$ has no finite interpretation as the probability for a detector. A physical probability is $\int_{p_1}^{p_2} |\phi(p)|^2 dp$. Changing to wave number gives

$$|\phi_k(k)|^2 = \hbar|\phi(\hbar k)|^2.$$

A graph labelled density in k with a vertical axis copied directly from the momentum plot loses the Jacobian and in general ceases to normalise to one.

Change from momentum bins to energy bins

For a free particle $E = p^2/(2m)$. Each positive energy has two distinct momenta $p_\pm = \pm\sqrt{2mE}$. A detector measuring energy but not direction sums over these mutually orthogonal alternatives. Apply the ordinary change-of-variables rule on each monotone half-line:

$$w(E) = \frac{m}{\sqrt{2mE}}\Big[|\phi(+\sqrt{2mE})|^2 + |\phi(-\sqrt{2mE})|^2\Big], \qquad E > 0.$$

The factor $m/|p|$ is $1/|dE/dp|$, with units of momentum per energy. Measuring a finite energy interval around zero can have a density diverging as $E^{-1/2}$ if $\phi(0) \neq 0$, yet the integrated probability is finite because $\int_0^\delta E^{-1/2} dE = 2\sqrt{\delta}$. The same effect appears in a box as relatively dense low-energy modes. Standing-wave box boundary conditions change the counting of travelling directions; include degeneracy once and use the appropriate mode spacing, rather than doubling both.

On an infinite line it is useful to introduce $|E, +\rangle = \sqrt{m/|p|}\,|p\rangle$ at $p > 0$, and a corresponding negative branch. In the overlap,

$$\delta(p(E) - p(E')) = \delta(E - E')/|dp/dE|;$$

the two square-root factors give $\delta(E - E')$. The resolution of identity contains $\sum_{\pm} \int_0^\infty dE\, |E, \pm\rangle\langle E, \pm|$. Measuring energy while coherently manipulating the two degenerate directions requires keeping both amplitudes. Adding their probabilities is sufficient only for an instrument whose outcome identifies energy without mixing the directions before detection.

Integrate the free evolution of a Gaussian

Prepare a minimum-uncertainty wave packet centred at x_0 with average momentum p_0 and initial position standard deviation s:

$$\psi(x, 0) = (2\pi s^2)^{-1/4} \exp[-(x - x_0)^2/(4s^2) + i p_0 (x - x_0)/\hbar].$$

Its squared modulus is a Gaussian with variance s^2, which explains the factor four in the amplitude exponent. Complete the square in the Fourier integral to find a momentum probability Gaussian centred at p_0 of variance $\hbar^2/(4s^2)$. The initial state has zero symmetrised position–momentum covariance. Multiplying by a chirp factor $\exp[i\kappa(x - x_0)^2]$ leaves its initial position density unchanged but changes momentum variance and covariance. A snapshot of one density does not determine its later free spread.

Each momentum component evolves by $e^{-ip^2 t/(2m\hbar)}$. Split $p = p_0 + q$. The constant term in p^2 produces a common phase; the linear term shifts the envelope by $p_0 t/m$; the quadratic term changes the width. Carrying out the remaining Gaussian integral yields

$$|\psi(x, t)|^2 = \frac{\exp[-(x - x_0 - p_0 t/m)^2/(2 s_t^2)]}{\sqrt{2\pi}\, s_t},$$

$$s_t^2 = s^2 \left[1 + \left(\frac{\hbar t}{2 m s^2}\right)^2\right].$$

An independent route uses the Heisenberg operator $x(t) = x(0) + p(0) t/m$. Its variance is $s^2 + (t/m)\langle\{\Delta x, \Delta p\}\rangle + (t/m)^2 (\Delta p)^2$. Inserting zero covariance and the Gaussian momentum width reproduces s_t^2. For a chirped packet the covariance term can be negative; momentary narrowing during free evolution is consistent with uncertainty because momentum width and the phase correlation must be included. The density integral stays one, so spreading lowers the height of the peak without removing particles.

Take a model atom of mass 1.44×10^{-25} kg prepared with $s = 1.00\,\mu\text{m}$. Its spread time $t_s = 2ms^2/\hbar = 2.73$ ms. At $t = t_s$ the standard deviation is 1.41 µm. With mean velocity 2.00 mm/s its mean

has advanced 5.46 µm. At long flight times $s_t \simeq t\Delta p/m$. Measuring position after a known long flight therefore maps the momentum distribution for this free packet. At $0.5t_s$ the neglected initial position variance is still dominant, so the same inference would substantially overestimate Δp.

A detector window and a Fourier grid do different jobs

Suppose the position-sensitive detector has a Gaussian point-spread function of width d. The measured density is a convolution of the true density with that response if detections are independent and gain is uniform. Gaussian variances then add:

$$s_{\mathrm{obs}}^2 = s_t^2 + d^2.$$

This broadening belongs to the observation model; it does not increase the particle's momentum spread before the measurement. For $d = 1.20\,\mu\mathrm{m}$ at $t = t_s$, the observed standard deviation becomes $1.85\,\mu\mathrm{m}$. A fit to a single image with unknown d cannot disentangle the two contributions. A sequence of flight times constrains the coefficient of t^2 independently of a fixed instrument width.

A discrete Fourier propagation represents a periodic interval sampled at spacing Δx. Its wave-number spacing is $2\pi/L$, and the highest resolved wave number is order $\pi/\Delta x$. Enlarging L at fixed Δx samples the momentum profile more finely and delays periodic wraparound. Reducing Δx at fixed L raises the bandwidth without moving the periodic boundary. Either operation alone can leave the other error intact. A norm-preserving FFT propagator can therefore return a perfectly normalised wave packet that has wrapped through an unphysical boundary or whose carrier momentum has aliased. Compare the phase, group velocity and width against independent formulas, then refine the two scales separately.

Why boundary conditions are part of a momentum observable

The expression $p = -i\hbar\, d/dx$ does not by itself specify a complete operator. On a finite interval $[0, L]$, integrate two sufficiently smooth square-integrable functions by parts:

$$\langle f, pg\rangle - \langle pf, g\rangle = -i\hbar[f^*(x)g(x)]_0^L.$$

A symmetric domain makes this boundary form vanish for every pair in the domain. A self-adjoint operator additionally has the same domain as its adjoint. This distinction matters for a physical generator of unitary translations and for assigning sharp spectral outcomes. Imposing a real or imaginary matrix representation in a finite basis can conceal boundary conditions that become essential as the basis is enlarged.

For a ring allow quasi-periodicity $g(L) = e^{i\theta}g(0)$ with fixed θ common to all functions in the domain and square-integrable first derivative. Then the boundary form vanishes. Conversely, for an adjoint candidate f the requirement that it vanish for all possible $g(0)$ forces $f(L) = e^{i\theta}f(0)$, so the same condition reappears. Solving $pg = pg$ yields the momenta $p_n = \hbar(2\pi n + \theta)/L$. Thus boxes with precisely the same local differential expression have momentum spectra shifted by an externally fixed phase. In a physically realised ring such a phase can encode a magnetic flux through a gauge-transformed boundary condition; a gauge consistent with that interpretation must also be used in the Hamiltonian and physical momentum.

Compare with forcing $g(0) = g(L) = 0$ as in a hard-wall well. The boundary form vanishes for all f, g satisfying both zero conditions, so the derivative is symmetric there. But the adjoint boundary form vanishes

for arbitrary endpoint values of f when g vanishes at both ends. Consequently this two-zero derivative domain is smaller than its adjoint domain. There is no ordinary rigid translation that carries every state of a hard-wall interval back into that same interval without assigning what happens at its boundary. Meanwhile the kinetic energy $-\hbar^2 d^2/(2m\,dx^2)$ with suitable Dirichlet domain is self-adjoint and has a well-defined discrete spectrum. The symbol $p^2/(2m)$ in a Dirichlet well does not turn its first derivative with the same two endpoint conditions into a self-adjoint sharp momentum observable.

A release-and-detect experiment makes this distinction concrete. Prepare the first Dirichlet state $\sqrt{2/L}\sin(\pi x/L)$ supported in $0 < x < L$, then remove the walls suddenly and measure momentum on the full line. Its momentum wavefunction is the Fourier transform of the spatial function extended by zero outside. Multiplying the exponential and sine and integrating gives a continuous amplitude proportional to $[1 + e^{-ipL/\hbar}]/[(\pi/L)^2 - (p/\hbar)^2]$. The apparent singularities at $p/\hbar = \pm\pi/L$ are removable because the numerator also vanishes. It is a mistake to predict two delta peaks by replacing the standing wave with the sum of two infinite plane waves. The finite support multiplies that sum by a spatial window and broadens both momentum components.

The mean momentum for this real function is zero. Its second moment after release is $\hbar^2 \int |\psi'|^2 dx = \pi^2\hbar^2/L^2$, consistent with the original kinetic energy. Thus a continuous released momentum distribution can have an rms momentum whose square exactly recovers a discrete energy of the original bounded system. This is a useful quantitative example where the equality of moments across two measurement procedures does not imply equality of their full spectral probability distributions. Adding a short laboratory impulse to every particle after release should translate the whole distribution by the corresponding momentum kick, preserving its width. That response provides an independent check on a momentum detector's sign and scale.

Derive the free propagator with a convergent limiting prescription

Partitioning the free unitary into momentum eigenstates produces its position kernel

$$K(x,t;x',0) = \frac{1}{2\pi\hbar}\int_{-\infty}^{\infty} \exp\left[\frac{i}{\hbar}\left(p(x-x') - \frac{p^2 t}{2m}\right)\right] dp.$$

It is oscillatory rather than absolutely integrable. Define it by first damping $e^{-\varepsilon p^2}$, evaluating a convergent Gaussian and then taking $\varepsilon \downarrow 0$ on smooth normalisable test packets. Completing the square in the exponent gives, for $t > 0$,

$$K = \sqrt{\frac{m}{2\pi i\hbar t}}\exp\left[\frac{im(x-x')^2}{2\hbar t}\right].$$

The phase convention of the square root for positive time follows continuously from the regularised Gaussian. The units are inverse length so $\psi(x,t) = \int K(x,t;x',0)\psi(x',0)\,dx'$ has the same units as the initial wavefunction. As $t \to 0^+$, the kernel does not approach a finite spike pointwise. Its increasingly fast oscillations across x' cancel except near $x' = x$, recovering the initial state in the appropriate strong or distributional sense. For a constant initial amplitude one may recover unity formally, but such an amplitude on the full line is itself not a normalised test state.

Two checks involve no wave packet fitting. Inserting two kernels for t_1, t_2 and integrating over an intermediate position gives the kernel for $t_1 + t_2$, either by another Gaussian integration or, more directly, by composing the momentum phase factors. Complex conjugation and reversing the time arguments yield the inverse evolution. Neither statement holds for an arbitrary choice of magnitude prefactor assigned merely to obtain the correct phase. In Fourier numerics the corresponding checks are unit norm after repeated evolution and recovery of the original sampled complex state after a forward followed by backward propagation. These are necessary algorithm checks, even though a periodic or aliased computational model can still satisfy them exactly.

This kernel also clarifies the long-time momentum mapping. Factor $e^{imx^2/(2\hbar t)}$ from K and identify the Fourier transform of $e^{imx'^2/(2\hbar t)}\psi(x', 0)$ evaluated at $p = mx/t$. If the occupied initial region is narrow enough that $mx'^2/(2\hbar t)$ varies little across it about the selected origin, the extra phase can be neglected and

$$|\psi(x,t)|^2 \simeq \frac{m}{t}\left|\phi\Big(\frac{mx}{t}\Big)\right|^2.$$

The factor m/t is the Jacobian dp/dx. When the initial packet is displaced, use a suitable shifted origin or account for the induced linear phase explicitly. This derivation applies well beyond Gaussians and gives a scale for testing the approximation before interpreting a flight image as a momentum histogram. The quadratic residual phase provides the matter-wave analogue of the near-field correction in diffraction.

Distinguish a detector crossing from a snapshot in space

A detector counts particles passing through an aperture over time. Its signal is related to flux, whereas a camera image of identical preparations at one time probes a position distribution. For a one-dimensional free wavefunction the continuity equation is $\partial_t|\psi|^2 + \partial_x j = 0$ with $j = (\hbar/m)\,\mathrm{Im}(\psi^*\partial_x\psi)$. Integrating over the region $x < X$ gives the change in probability to the left of a fixed plane. If there is no flux at negative infinity, the net integrated current through X equals the reduction in that probability. A positive-reading counter with absorption is a more detailed instrument and cannot in general be identified with a signed current in the presence of reflected waves or interference.

For a minimum-uncertainty Gaussian initially at x_0, the exact phase in the freely expanding envelope has a quadratic term. Differentiating the phase gives the local velocity entering current,

$$\frac{j(x,t)}{|\psi(x,t)|^2} = \frac{p_0}{m} + \frac{t}{t_s^2 + t^2}\left(x - x_0 - \frac{p_0 t}{m}\right).$$

At the centre this equals the group velocity p_0/m, but ahead of the centre it is larger and behind it smaller. A single constant velocity multiplying density is inadequate for a significantly spreading packet. For the earlier atom at $t = t_s$, one current-standard-deviation distance ahead corresponds to $1.41\ \mu\mathrm{m}$ and the additional speed is about 0.259 mm/s. The trailing side gives the opposite correction. Direct differentiation of its Gaussian density verifies that this current satisfies continuity. A code reproducing s_t but evolving the wrong complex phase may fail this current test; judging an entire propagation by the changing width alone would miss the error.

A useful inverse question is whether two time-of-flight images suffice to recover an unknown complex wavefunction. In the long-time limit the image yields $|\phi(p)|^2$, which contains no direct momentum-dependent

phase. Translation of the initial wave packet changes $\phi(p)$ by a linear phase, leaving the momentum density unchanged. Complex conjugate or chirped preparations can also share particular intensity records. Additional calibrated evolution, known reference interference or structural assumptions can provide phase information. Even an exact free propagator only defines the forward map; its invertibility on complex amplitudes does not imply intensity-only data identify every possible input. The experiment must specify which class of preparations and which measurement settings render the desired parameters estimable.

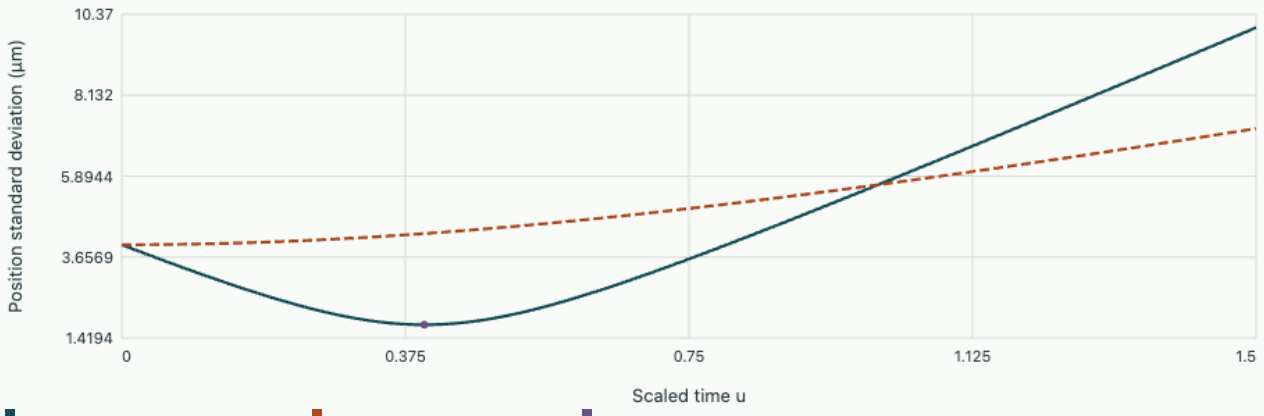
Track a continuous superposition through focus

Change a position-momentum correlation and compare the full packet width with an initially unchirped packet. A narrow width at one time does not determine its subsequent spread.

Open this experiment online

Try the calculation

Initial phase curvature b -2



For u ≥ 0 the minimum width is 1.789 µm at u = 0.4.

Plan an FFT comparison using physical position and momentum resolution

A grid propagator can track the same packet analytically solved earlier, then carry over its verified conventions to less elementary potentials. A common trap is to regard the number of points N as a single accuracy parameter. Define a periodic interval of physical length $L = N\Delta x$. Discrete Fourier modes have $k_j = 2\pi j/L$, with negative wave numbers represented by negative indices after reordering. Their spacing is $\Delta k = 2\pi/L$; the largest distinct magnitude is close to $\pi/\Delta x$. A narrow structure in momentum requires large L. A high carrier momentum requires small Δx. These conditions can fail independently even when the norm stays exactly one.

If $\psi_l = \psi(x_l)$ is a sampled wavefunction in inverse square-root metres and the forward transform sums without $1/N$, the approximated continuum k-amplitude is

$$\phi_k(k_j) \simeq \Delta x \sum_l \psi_l e^{-ik_j x_l}/\sqrt{2\pi}.$$

The phase includes the physical coordinate origin adopted for the grid. Parseval then gives

$$\Delta k \sum_j |\phi_k(k_j)|^2 = \Delta x \sum_l |\psi_l|^2.$$

A library returning a unitary discrete transform instead assigns a factor $1/\sqrt{N}$ to both directions; multiplying its output by $\sqrt{\Delta x/\Delta k}$ converts sample units. Plotting a library output directly against physical momentum without these scale factors is especially misleading when comparing two meshes. Total discrete ℓ^2 norm and continuum probability density are different normalisations of the same samples.

For the atom of mass 1.44×10^{-25} kg, $s = 1.00$ µm and $v_0 = 2.00$ mm/s,

$$k_0 = mv_0/\hbar = 2.73\,\mu\mathrm{m}^{-1},$$

$$\Delta k_{\mathrm{rms}} = 1/(2s) = 0.50\,\mu\mathrm{m}^{-1}.$$

A box 80 µm wide gives spacing $0.0785\,\mu\mathrm{m}^{-1}$, about 6.4 modes per rms momentum width. With $N = 256$, grid spacing is 0.3125 µm and Nyquist wavenumber is $10.05\,\mu\mathrm{m}^{-1}$, exceeding $k_0 + 5\Delta k_{\mathrm{rms}} = 5.23\,\mu\mathrm{m}^{-1}$. This comfortably samples the initial carrier distribution. It is still necessary to check that the envelope remains inside the periodic box at the desired final time.

At $t = 10$ ms the packet centre has moved 20 µm and $s_t \simeq 3.80$ µm. Starting at the centre of an interval spanning -40 to 40 µm, its five-standard-deviation front approaches 39 µm and begins testing the boundary margin. At 20 ms the centre alone reaches the periodic boundary. A perfectly unitary calculation will show it reappearing on the opposite side. This is correct for a ring and incorrect for a free-space flight image. Enlarging N while keeping the same L improves the Nyquist limit but does nothing to postpone this crossing. An open-boundary absorber can delay reflected artefacts but attenuates norm; a lost norm in that model should be compared with counted escape rather than naively enforced to zero.

Infer displacement and speed from a wrapped packet without mistaking periodicity for reflection

A code on a periodic box of length 80 µm reports a sharp packet peak at $+35$ µm in one frame and -36 µm in the next frame 4.50 ms later. Find a consistent uniform drift and identify the ambiguity if no speed prior is available.

▼ Derive and check the result

The smallest forward displacement is $+9$ µm after adding one full box length to the second position. It corresponds to 2.00 mm/s and agrees with the earlier preparation. Direct subtraction without unwrapping would give -71 µm, or -15.8 mm/s, an apparent reversal. All displacements $9 + 80n$ µm for integer n yield the same wrapped pair, so the frames alone cannot identify the number of turns. A momentum measurement or a bound on speed relative to frame spacing resolves the branch. For an extended packet crossing a seam, use a periodic circular moment such as $\langle e^{2\pi i x/L} \rangle$ so an ordinary spatial mean does not spuriously jump

toward the box centre. If that circular moment is nearly zero, even its angular centre is ill-defined and a full density comparison is preferable.

Tutorial · design a momentum measurement

Distinguish an unresolved line from a finite-width packet

A periodic calculation of length $L = 100\,\mu\mathrm{m}$ contains mode n. A detector bins momentum in intervals $1.0 \times 10^{-29}\,\mathrm{kg\,m/s}$. How many box-mode spacings fit into a bin? What changes if the box length doubles at fixed physical packet?

▼ Work through the solution

Here $\Delta p = h/L = 6.626 \times 10^{-30}\,\mathrm{kg\,m/s}$, so the detector bin spans about 1.51 spacings. The precise number of grid points falling within a bin depends on its endpoints. Doubling L gives roughly 3.02 spacings per bin. Each corresponding coefficient squared decreases approximately in proportion to Δp, while the number included increases. The total probability should approach a stable integral on a progressively finer grid. If a graph compares $|c_n|^2$ across the boxes, divide by the corresponding Δp before calling the ordinate a continuum density.

Calculate a threshold energy interval without evaluating a delta at zero

A packet's momentum density is nearly constant w_0 over $-p_c < p < p_c$. Obtain the probability for $0 < E < E_c = p_c^2/(2m)$ by two different integrations. What changes when only positive-momentum particles reach the counter?

▼ Work through the solution

Direct integration in momentum gives $2p_c w_0$. In energy the two branches contribute $2mw_0/\sqrt{2mE}$. Its integral gives $4mw_0\sqrt{E_c}/\sqrt{2m} = 2p_c w_0$ as required. A positive-direction selector halves this particular probability when applied to the original ensemble. If the entire subsequent experiment is renormalised to the selected particles, divide again by the total positive-momentum probability. Those two reported probabilities correspond to different conditioning and should be labelled explicitly.

Infer the packet width from two images

The model atom has an initial measured width 1.56 µm and a width 1.85 µm after 2.73 ms. Assume a time-independent Gaussian instrument response and a freely evolving unchirped minimum-uncertainty state. Infer s and d, and identify an additional check.

▼ Work through the solution

Subtract squared widths to remove the detector:

$$s_{\mathrm{obs}}(t)^2 - s_{\mathrm{obs}}(0)^2 = \hbar^2 t^2 / (4 m^2 s^2).$$

The observed difference is about $0.99\,\mu\mathrm{m}^2$, giving $s \simeq 1.0\,\mu\mathrm{m}$ and $d = \sqrt{s_{\mathrm{obs}}(0)^2 - s^2} \simeq 1.2\,\mu\mathrm{m}$, within rounding. A third flight time tests the predicted quadratic in t. A term linear in time would point to a nonzero initial correlation or to measurement drift. Independent calibration of the point-spread function distinguishes those interpretations from a nonminimum momentum width.

Further reading

- Fließbach · Eigenwerte und Eigenfunktionen
- TUM · Theoretische Physik 3, representations and momentum states
- Course investigation · probability density and current

Quantum states, dynamics and measurement · 3. Why an oscillator can move without its packet spreading

Start with the measured mass and curvature of a potential. Factor its Hamiltonian, prove the energy ladder, construct a freely moving Gaussian from number states and find when squeezing or anharmonicity changes that prediction.

Use the equilibrium length and momentum scales

Near a stable minimum a smooth one-dimensional potential has expansion $V(x) = V(0) + m\omega^2 x^2/2 + O(x^3)$ after the origin is shifted to the minimum. Choose the arbitrary zero $V(0) = 0$. The fitted curvature is $m\omega^2$, not ω itself; measuring both the oscillation frequency and restoring slope separately identifies the effective mass. The classical energy ellipse becomes a circle if position and momentum are rescaled consistently. Define $X = \sqrt{m\omega/\hbar}\, x$ and $P = p/\sqrt{m\hbar\omega}$, so $[X, P] = i$ and $H = \hbar\omega(X^2 + P^2)/2$. Since position and momentum fail to commute, multiplying two linear factors must retain their order.

Set $a = (X + iP)/\sqrt{2}$ and $a^\dagger = (X - iP)/\sqrt{2}$. Then

$$a^\dagger a = (X^2 + P^2 + i[X, P])/2 = (X^2 + P^2 - 1)/2.$$

Thus $H = \hbar\omega(N + 1/2)$, $N = a^\dagger a$ and $[a, a^\dagger] = 1$. For every normalised state in the relevant domain $\langle N\rangle = \|a|\psi\rangle\|^2 \geq 0$. The additive half quantum is an energy contribution that survives in a state with vanishing classical means of x, p; discarding the commutator would lose it. Transition frequencies within an ideal ladder measure energy differences, so those frequencies alone cannot determine an absolute zero of energy.

Prove discreteness and construct the ground state

Using the product rule for commutators gives

$$[N, a] = -a,$$
$$[N, a^\dagger] = a^\dagger.$$

If a normalisable energy eigenstate has N eigenvalue ν, application of a either annihilates it or yields an eigenstate of eigenvalue $\nu - 1$ and norm squared ν. Repeated lowering cannot yield a state of negative norm squared. For noninteger nonnegative ν the chain would reach $0 < \nu' < 1$ with nonzero image at a negative eigenvalue. Therefore the chain must terminate at an integer step in an annihilated ground state. This argument uses the bound oscillator's spectrum and states in the ladder operators' domains. Existence and completeness can also be checked by solving the one-dimensional differential equation with decaying boundary conditions.

In coordinate representation $P = -i\, d/dX$, so $a\psi_0 = 0$ reduces to

$$d\psi_0/dX = -X\psi_0.$$

Its square-integrable solution is

$$\psi_0(X) = \pi^{-1/4} e^{-X^2/2}.$$

Normalised excited states follow by $|n\rangle = (a^\dagger)^n|0\rangle/\sqrt{n!}$. Orthogonality follows from the self-adjoint number operator with distinct eigenvalues. The coordinates in metres have ground variance $\sigma_x^2 = \hbar/(2m\omega)$, momentum variance $\sigma_p^2 = m\hbar\omega/2$, and zero symmetrised covariance. The geometric ground-state width is thus fixed by mass and trap stiffness. A semiclassical estimate minimising $\hbar^2/(8m\sigma_x^2) + m\omega^2\sigma_x^2/2$ gives $E_{\min} = \hbar\omega/2$, because the Gaussian saturates the uncertainty inequality used in that estimate.

In a number state both $\langle x\rangle$ and $\langle p\rangle$ vanish. Their fluctuations do not. Substitute $x = \sigma_x(a + a^\dagger)$. Terms $a^2, (a^\dagger)^2$ change the occupation by two and have zero diagonal element, whereas $aa^\dagger$ and $a^\dagger a$ contribute $n + 1$ and n. Hence $\langle x^2\rangle_n = (2n + 1)\sigma_x^2$; similarly $\langle p^2\rangle_n = (2n + 1)\sigma_p^2$. The mean kinetic and potential energies each equal half the total. Measuring a nonzero rms displacement does not imply that the oscillator centre is undergoing a coherent motion.

Find a state whose centre follows the classical trajectory

Search for a normalised eigenstate of a with complex eigenvalue α. It is permissible for this non-Hermitian operator to have complex eigenvalues; they label states rather than directly observable outcomes. Expand $|\alpha\rangle = \sum_n c_n|n\rangle$. Matching every number-state coefficient yields

$$c_{n+1} = \alpha c_n/\sqrt{n + 1}.$$

Using the exponential series to normalise gives

$$|\alpha\rangle = e^{-|\alpha|^2/2}\sum_{n=0}^{\infty}\frac{\alpha^n}{\sqrt{n!}}|n\rangle,$$

$$P(n) = e^{-|\alpha|^2}\frac{|\alpha|^{2n}}{n!}.$$

The mean and variance of occupation are both $|\alpha|^2$. Different coherent states are nonorthogonal: summing the overlap yields

$$|\langle\beta|\alpha\rangle|^2 = e^{-|\alpha-\beta|^2}.$$

At displacement difference one in this dimensionless complex plane the overlap probability is still $e^{-1} = 0.368$. A measurement that distinguishes all such nearby coherent preparations perfectly from one copy would contradict this overlap.

Each coefficient acquires $e^{-i(n+1/2)\omega t}$. Take the common zero-point phase outside the sum, leaving exactly the same expansion with $\alpha(t) = \alpha e^{-i\omega t}$. Hence $\langle x(t)\rangle = 2\sigma_x \operatorname{Re}\alpha(t)$ and $\langle p(t)\rangle = 2\sigma_p \operatorname{Im}\alpha(t)$. The centred operator $a - \alpha$ annihilates the state, so its centred quadrature variances match those of the ground state. The packet moves on the classical phase-space ellipse without spreading. In a free particle the quadratic momentum phase causes spreading; in the bound oscillator equally spaced energy levels preserve this particular relative-phase structure.

For a vibrational mode with $m = 2.00 \times 10^{-25}$ kg and $\omega = 2\pi \times 100$ kHz, $\sigma_x = 20.5$ nm. Prepare $\alpha = 1.5i$. Initially the average position is zero and the momentum is positive; a quarter period later the centre reaches $3\sigma_x = 61.5$ nm. The mean occupation is 2.25 and the ground probability is 0.1054. This ensemble has a nonzero ground-state probability even though its position oscillation is clearly resolved by repeated

measurements. A pure number state of average energy near this value could give similar rms positions but would show no time-dependent centre.

Background · Which measurement distinguishes two oscillators of equal mean energy?

Compare the first excited number state with a coherent state of amplitude $\alpha = 1$. Both have mean occupation one and hence the same mean energy $3\hbar\omega/2$. For a number state the expectation of the lowering operator vanishes because it connects orthogonal levels. For a coherent state its expectation equals α and evolves with the oscillator phase.

$$\langle x(t)\rangle_{\mathrm{coh}} = \sqrt{\frac{2\hbar}{m\omega}}\,\mathrm{Re}(\alpha e^{-i\omega t}),$$

$$\langle x(t)\rangle_{n=1} = 0.$$

Synchronous position measurements on freshly prepared states distinguish the moving centroid from the stationary one. A repeated energy measurement also separates the preparations. The number state always gives one quantum, whereas the coherent state gives a Poisson distribution with mean and variance both equal to one. A mean energy by itself omits both distinctions.

Rotate an uncertainty ellipse and test a nonideal trap

A sudden frequency change provides an experimentally meaningful way to generate a state with unequal quadrature fluctuations. Prepare the ground state at frequency ω_i, then instantaneously change to ω_f. The state in the position representation is continuous through an ideal sudden change. Relative to the final oscillator,

$$\langle X_f^2\rangle = \omega_f/(2\omega_i),$$

$$\langle P_f^2\rangle = \omega_i/(2\omega_f);$$

their product remains $1/4$. Their sum exceeds one unless the two frequencies coincide. Thus the state is a squeezed vacuum for the new trap, with mean occupation $\frac{1}{4}(\omega_f/\omega_i + \omega_i/\omega_f - 2)$. Unlike a coherent displacement its centre remains zero. Measuring a variance as the ellipse rotates distinguishes these preparations even if their average energies match.

For $\omega_f = 2\omega_i$ the mean occupation is 0.125. Since $X_f(t) = X_f(0)\cos\omega_f t + P_f(0)\sin\omega_f t$, variance oscillates between 1 and 0.25 in these units with angular frequency $2\omega_f$. The ground variance for the final trap would be 0.5, so part of the cycle lies below it. Momentum variance rises correspondingly, and at intermediate angles a nonzero covariance is needed in the uncertainty determinant. Abrupt changes also inject work via the time-dependent Hamiltonian. Energy measured before and after the sudden change need not agree even though the state vector at the switching instant is unchanged.

Real traps eventually depart from exact harmonic confinement. Write a model diagonal spectrum $E_n/\hbar = \omega(n + 1/2) + \chi n(n-1)/2$ for weak amplitude-dependent spacings over the occupied range. Coherent-state sums give

$$\langle a(t)\rangle = \alpha e^{-i\omega t}\exp[|\alpha|^2(e^{-i\chi t} - 1)].$$

Its magnitude is $|\alpha|\exp[-|\alpha|^2(1-\cos\chi t)]$. The collapse of the centre can occur under strictly unitary evolution while the number probabilities stay fixed. Their phases reassemble at $2\pi/|\chi|$ in this ideal spectrum. Irreversible noise and uncontrolled fluctuations can suppress a measured revival; loss of the mean alone does not diagnose dissipation. A position trace and a number-resolved distribution probe complementary parts of the dynamics.

Factor a measured displacement into force history and oscillator response

A linear force couples to position,

$$H(t) = \hbar\omega(N + 1/2) - F(t)x.$$

Even if the force time series is irregular, this driven oscillator is exactly soluble within the harmonic approximation. In the Heisenberg picture use $\dot{a} = (i/\hbar)[H, a]$. Since $[x, a] = -\sigma_x$, the equation is

$$\dot{a} = -i\omega a + i\sigma_x F(t)/\hbar.$$

Multiply by $e^{i\omega t}$ and integrate:

$$a(t) = e^{-i\omega t}\left[a(0) + \frac{i\sigma_x}{\hbar}\int_0^t F(t')e^{i\omega t'}dt'\right].$$

A force therefore displaces the rotating oscillator according to one complex Fourier component of its history. Its phase determines which final quadrature changes. The centred operator still evolves as in free oscillation. Thus a known linear drive displaces a ground state into a coherent state without squeezing it. The same formula shifts a thermal state without removing its thermal fluctuations. The statement about pure coherence requires knowing the initial state as well as measuring the final displacement.

Take a constant force F_0 switched on for time T then off. For an initially stationary ground state the final amplitude, measured at switch-off in the original oscillator basis, is $\alpha_F = F_0\sigma_x[1 - e^{-i\omega T}]/(\hbar\omega)$. The corresponding mean position is $F_0(1-\cos\omega T)/(m\omega^2)$, agreeing with the classical step response of a mass on a spring. Its excitation number is $4(F_0\sigma_x/\hbar\omega)^2\sin^2(\omega T/2)$. A constant force applied for exactly a full period creates zero residual excitation at switch-off even though the oscillator moved substantially during the pulse. Motion of the trap centre and persistent excitation after the trap returns must be experimentally distinguished.

For $m = 2.00\times10^{-25}$ kg and 100 kHz as above, let $F_0 = 2.00\times10^{-21}$ N. Its static equilibrium displacement is

$$F_0/(m\omega^2) = 25.3\,\mathrm{nm}.$$

A half-period pulse leaves the mean at 50.7 nm with zero mean momentum and $|\alpha| = 50.7/(2\times20.5) \simeq 1.24$. Its mean added occupation is roughly 1.53. The elastic energy $m\omega^2\langle x\rangle^2/2$ at switch-off matches $\hbar\omega|\alpha|^2$, independently of any counting argument. This check subtracts the unchanged zero-point energy. Using the total energy including zero point in the comparison would incorrectly attribute a half quantum to the drive even when the applied force vanishes.

The sudden impulse limit provides another independent test. Let a short pulse deliver total impulse $J = \int F dt$ over a time much shorter than $1/\omega$. The amplitude increment is approximately $i\sigma_x J/\hbar$ in the appropriate rotating phase. Since $2\sigma_p\sigma_x = \hbar$, the mean momentum changes by J. For a smooth pulse spread around one period the same total impulse can produce a much smaller residual excitation because the force acts at different phases of the oscillator. A force sensor based on final occupation measures the squared magnitude of a windowed resonant integral. Reconstructing a complete time-dependent force from that single energy measurement is generally impossible. Varying the drive start time or measuring both final quadratures gives additional information.

Use operator ordering to predict a phase with zero final displacement

Define the displacement operator $D(\alpha) = \exp(\alpha a^\dagger - \alpha^* a)$. Its generator is anti-Hermitian, so it is unitary. The commutator of $\alpha a^\dagger - \alpha^* a$ with a is a constant. Differentiating $D^\dagger(s\alpha) a D(s\alpha)$ with respect to s and integrating gives

$$D^\dagger(\alpha) a D(\alpha) = a + \alpha.$$

Consequently $D(\alpha)|0\rangle$ is an annihilation eigenstate of eigenvalue α, giving an independent physical construction of the number expansion. The normal-order factorisation $D = e^{-|\alpha|^2/2} e^{\alpha a^\dagger} e^{-\alpha^* a}$ follows from the Baker–Campbell–Hausdorff formula because the relevant commutator is a scalar. Acting on the ground state recovers the Poisson coefficients directly. Omitting the scalar prefactor gives a state with the wrong norm.

Two displacements do not commute as operators despite their effects on the mean phase-space position adding in either order. Their scalar commutator gives

$$D(\alpha) D(\beta) = e^{(\alpha\beta^* - \alpha^*\beta)/2} D(\alpha + \beta).$$

The product around a closed displacement loop is

$$D(\alpha) D(\beta) D(-\alpha) D(-\beta) = e^{\alpha\beta^* - \alpha^*\beta} I.$$

For $\alpha = 1,\ \beta = i/2$ the phase is -1 rad in this written operator order. Reversing the physical order conjugates the phase. The oscillator returns to its initial phase-space position and, apart from this phase, to its initial state. In a single isolated preparation the common phase is invisible. To observe it, place the oscillator interaction under coherent control of one branch of a separate two-level reference, recombine the reference and compare the branch that went around the loop with the branch that did not. Surviving coherence of the reference is essential. The same result can be described as an oriented area in the $\mathrm{Re}\,\alpha, \mathrm{Im}\,\alpha$ plane and ultimately follows from $[x, p] = i\hbar$.

It is useful to trace the actual motion before interpreting a claimed geometric phase. Operators act from right to left on kets, so plotting a particular rectangular loop in time can correspond to the conjugate of a product written left to right. A lab comparison should specify the four pulse phases in chronological order and the ordinary free rotation occurring between them. In the rotating frame the displacement vectors are simple complex increments; in the laboratory frame the oscillator itself continually advances in phase. An uncompensated delay can leave a residual displacement rather than a closed loop. The overlap of that

residual displaced ground state with the reference branch is $e^{-|\Delta\alpha|^2/2}$ in amplitude, reducing observed fringe contrast as well as shifting its phase.

Measure displaced parity to distinguish a number state from a mixture

The number parity operator $\Pi = (-1)^N$ gives $+1$ for even and -1 for odd occupation. It implements the coordinate reflection $x \to -x$ for the harmonic oscillator. A position-space Wigner distribution may be sampled by displacing the state and measuring its parity. In the complex phase-space convention used here define $W(\beta) = (2/\pi)\,\mathrm{tr}[D(-\beta)\rho D^\dagger(-\beta)\Pi]$; it integrates to one in $d^2\beta$. At $\beta = 0$ it is just twice the even-minus-odd probability divided by π. Its sign is determined by observable population statistics, but its value at a point is not the probability that a particle occupies a sharp simultaneous position and momentum.

For a coherent input $|\alpha\rangle$, displacement produces $|\alpha - \beta\rangle$ up to a phase. Summing the even-minus-odd Poisson occupations gives $e^{-2|\alpha-\beta|^2}$. Hence $W(\beta) = 2e^{-2|\alpha-\beta|^2}/\pi$, a positive Gaussian. A first excited number state instead has $W(0) = -2/\pi$. Mix that state with ground-state population,

$$\rho = p|1\rangle\langle 1| + (1-p)|0\rangle\langle 0|.$$

Then $W(0) = (2/\pi)(1-2p)$, negative only when $p > 1/2$. An observed lack of negativity at one displacement does not imply a Gaussian state or a globally classical description. It may simply mean that the probe is examining a positive region or that losses have mixed the odd preparation with the ground state.

Suppose an experimental detector distinguishes only “zero excitations” from “one or more”. A measured nonzero fraction of 0.80 does not determine parity without further information: all those events might contain one excitation or a substantial even population might be present. Number resolution or a separate calibrated parity mapping is needed. If only ground and first excited population are independently established, an observed $p_1 = 0.70 \pm 0.02$ gives $W(0) = -0.255 \pm 0.025$ in these dimensionless units. Propagating that uncertainty requires the assumption about higher occupations. Combining a displacement scan with number-resolved or parity-sensitive data therefore tests both the preparation and the adequacy of a finite oscillator basis.

Recover a thermal occupation from two independent observables

For an oscillator in thermal equilibrium at inverse temperature β_T, the occupation probabilities are $P_n = (1-q)q^n$ with $q = e^{-\beta_T\hbar\omega}$. The geometric series gives $\bar{n} = q/(1-q)$ and variance $\bar{n}(\bar{n}+1)$. Unlike a coherent state with the same mean occupation, the number distribution is broader and the free mean displacement is zero. The symmetrised position variance is $(2\bar{n}+1)\sigma_x^2$. A variance measurement alone cannot distinguish a thermal distribution from an incoherent nonthermal mixture with the same mean energy. Resolving more than the variance probes the full probability law.

For example, at $\bar{n} = 2$ thermal equilibrium predicts ground occupation $1/3$, number variance 6 and parity $1/(2\bar{n}+1) = 1/5$. A coherent state with $|\alpha|^2 = 2$ gives ground probability 0.1353, variance 2 and parity $e^{-4} = 0.0183$. A uniform randomisation of the coherent phase removes the mean displacement but leaves these Poisson number statistics unchanged. It can therefore resemble the thermal state on a quadrature average while differing sharply in ground population and parity. A displaced thermal preparation adds a

classical centre motion on top of the thermal fluctuations; fitting only its energy would confuse displacement with temperature. Centre, centred variance and at least one independent number statistic make a coherent experimental set of observables for these physically different preparations.

Follow a coherent oscillator state in phase space

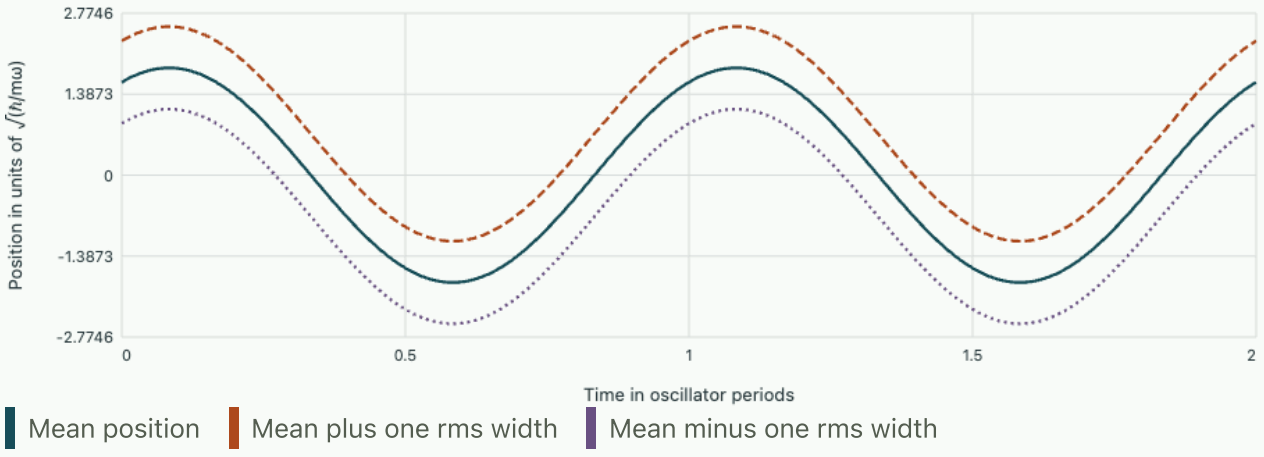
Change the magnitude and phase of a coherent amplitude independently. Predict which control changes the mean occupation and which shifts the timing of the position measurement.

Open this experiment online

Try the calculation

Coherent amplitude magnitude **1.3**

Preparation phase (degrees) **30**



Mean occupation 1.69 quanta, standard deviation 1.3. Ground-state probability 0.18452. Position variance in the plotted units is 1/2.

Recover individual transition probabilities after a sudden trap change

The sudden-frequency experiment predicted mean occupation from the second moments. Number-resolved probabilities provide a stronger test. The initial ground-state wavefunction is even, and changing the trap curvature about the same centre preserves parity. The initial state therefore overlaps only even eigenstates of the final trap. A measured odd population beyond readout uncertainty diagnoses a displaced minimum, parity-breaking drive or imperfect initial preparation. The vanishing of odd occupation is stronger than knowing only the mean and variance of a quadrature.

Write the old annihilator in terms of the new operators,

$$a_i = \cosh r\, a_f - \sinh r\, a_f^\dagger,$$

with $r = \frac{1}{2}\ln(\omega_f/\omega_i)$ for this choice of sign. This follows directly by expressing both in the same x, p and comparing coefficients. The relative sign can change under a different convention for defining the squeeze parameter but all probabilities below are invariant. The old vacuum obeys $(a_f - \tanh r\, a_f^\dagger)|0_i\rangle = 0$. In the final number basis $c_n = \langle n_f|0_i\rangle$, the coefficient of $|n\rangle$ gives

$$\sqrt{n+1}c_{n+1} = \tanh r\sqrt{n}\, c_{n-1}.$$

The $n = 0$ equation forces $c_1 = 0$, and iteration gives

$$c_{2j} = c_0 \frac{\sqrt{(2j)!}}{2^j j!}(\tanh r)^j,$$

$$c_{2j+1} = 0.$$

To normalise, use the central-binomial series $\sum_j \binom{2j}{j} q^j/4^j = (1-q)^{-1/2}$ at $q = \tanh^2 r$. Thus

$$|c_0|^2 = 1/\cosh r.$$

A separate coordinate-space check follows by integrating the overlap of two Gaussian ground states, giving $P_0 = 2\sqrt{\omega_i\omega_f}/(\omega_i + \omega_f)$. This agrees with $1/\cosh r$, independently of the operator recursion. Differentiating the normalisation-generating series gives $\bar{n} = \sinh^2 r$, agreeing with the energy inferred from the sudden change of the Hamiltonian.

For a doubling of frequency, $\tanh r = 1/3,\ \cosh r = 3/(2\sqrt{2})$, so

$$P_0 = 0.9428,\ P_2 = P_0/18 = 0.05238,$$

$$P_4 = P_0(3/8)(1/81) = 0.00436.$$

Higher even levels contain the remaining probability. At a mean excitation of 0.125, a coherent state would instead have $P_1 = 0.1103$. Even imperfect number resolution discriminating odd versus even can strongly distinguish a pure curvature quench from a coherent displacement with equal final energy. A finite switching time can reduce excitation if the oscillator tracks the moving ground state adiabatically. A shift of trap centre during a nominal curvature change adds a displacement and can populate odd levels. Measure the mean and parity along with the energy estimate before inferring a squeeze strength solely from a single occupation number.

Separate temperature from a parity-preserving quench

Before a sudden centred frequency doubling, a calibrated trap has thermal mean occupation 0.10. Predict the fraction of odd-number results after the quench and its final mean occupation. How might an experiment mistakenly interpret the odd results?

▼ **Derive and check the result**

In the initial thermal ensemble parity expectation is

$$1/(2\bar{n}+1) = 1/1.2 = 0.8333.$$

Parity commutes with both centred trap Hamiltonians, and measuring even or odd final occupation measures that same parity operator. The odds fraction is therefore $(1 - 0.8333)/2 = 0.0833$, unchanged by the quench. The final energy fluctuations scale with the initial quadrature variances multiplied by $2\bar{n} + 1$, giving $\bar{n}_f + 1/2 = (\bar{n}_i + 1/2)(\omega_f/\omega_i + \omega_i/\omega_f)/2 = 0.75$. Thus $\bar{n}_f = 0.25$. Assuming a perfectly cold initial state might turn the observed odd fraction into a false diagnosis of trap displacement. Measure initial parity and post-quench parity independently to isolate processes that actually break the symmetry. The increase of mean occupation alongside unchanged parity is the predicted signature of a centred quench.

Tutorial · analyse a state from amplitude and fluctuation data

Test two preparations with the same mean energy

Take a coherent state with $|\alpha|^2 = 3$ and number state $|3\rangle$. Compare energies, number variance, ground probability and the largest possible mean displacement.

▼ Work through the solution

Both have $\langle H \rangle = 3.5\hbar\omega$. The coherent number variance is 3 while the number-state variance is zero. Ground probabilities are $e^{-3} = 0.0498$ and zero. By selecting a suitable oscillator phase, the coherent state reaches $2\sqrt{3}\sigma_x$; the number state has zero centre at every time. An energy average alone leaves these preparations indistinguishable. The event of measuring exactly three quanta has probability $e^{-3}3^3/3! = 0.224$ in the coherent case and unity in the number case. Repeated shots allow this comparison without assuming a single shot reveals the input state.

Estimate numerical truncation before trusting a simulated coherent state

Expand a coherent state with $\alpha = 2$ in number states $0, \ldots, 8$. Is the missing probability negligible at a desired accuracy of one part in a thousand?

▼ Work through the solution

Generate probabilities successively from $p_0 = e^{-4}$, $p_{n+1} = 4p_n/(n+1)$; summing through 8 gives 0.97864, leaving 0.02136 above the cutoff. Renormalising the retained vector hides this discarded probability from a norm check and distorts quantities weighted by n. Through $n = 11$ the tail is about 0.00092, just below the specified probability tolerance. Energy moments require a separate tail weighted by n; a probability bound alone can be inadequate for them. Vary the cutoff while monitoring both number statistics and the centre motion to separate truncation artefacts from real dephasing.

Infer the coherent displacement and a squeezing test

At a known phase, measurements give

$$\langle x \rangle = 1.2\sigma_x, \ \langle p \rangle = -1.6\sigma_p.$$

Infer the coherent amplitude consistent with those means, then say what must still be measured to confirm a coherent preparation.

▼ **Work through the solution**

The means imply $\mathrm{Re}\,\alpha = 0.60,\ \mathrm{Im}\,\alpha = -0.80$, so $|\alpha| = 1$ and the putative coherent mean occupation is one. They do not fix the variances. A displaced thermal or squeezed state can produce the same means with different fluctuations. Measure the variance along independent quadratures, including a rotated axis to infer covariance. In an ideal normalised state the expectation of the positive operator $(a-\alpha)^\dagger(a-\alpha)$ equals $\langle N\rangle - |\alpha|^2$. If it vanishes exactly, the support is in the kernel of $a-\alpha$, giving the coherent state. With finite uncertainty a near-zero value instead bounds extra excitation in the displaced frame.

Further reading

- Fließbach · Operatorenmethode
- Course experiment · operators and oscillator spectra
- TUM · quantum mechanics, harmonic oscillator and operator formulation

Quantum states, dynamics and measurement · 4. Adding angular momentum and predicting which lines can appear

A three-component orbital wavefunction combines with a two-component spin. Derive the allowed total angular momenta, construct their amplitudes explicitly and predict both forbidden transitions and relative strengths in a polarisation-resolved spectrum.

Read the angular momentum algebra as a statement about rotations

Rotate a prepared quantum state through a small angle $\delta\theta$ about a unit laboratory direction $\mathbf{n}$. A continuous norm-preserving transformation has form $U = I - i\delta\theta\,\mathbf{n}\cdot\mathbf{J}/\hbar + O(\delta\theta^2)$, with Hermitian generators J_i. Rotations about different axes need not commute. Comparing the commutator of two infinitesimal rotations with the rotation around the third axis gives

$$[J_i, J_j] = i\hbar\epsilon_{ijk}J_k.$$

The sum $J^2 = J_x^2 + J_y^2 + J_z^2$ commutes with each component. One can therefore label eigenstates of J^2 and one chosen component J_z simultaneously, while generally leaving the other components uncertain.

Define $J_\pm = J_x \pm iJ_y$. Their commutators with J_z are $\pm\hbar J_\pm$; with J^2 they vanish. If $J_z|m\rangle = \hbar m|m\rangle$, the two ladder operations change m by one without changing total angular momentum. To determine their coefficients, use $J_-J_+ = J^2 - J_z^2 - \hbar J_z$ and $J_+J_- = J^2 - J_z^2 + \hbar J_z$. Nonnegative squared norms bound the ladder above and below. Let j be its maximum magnetic quantum number. Vanishing raising norm there fixes the J^2 eigenvalue at $\hbar^2 j(j+1)$; vanishing lowering norm at the bottom gives

$$m_{\min} = -j.$$

The number of unit steps between the two endpoints is $2j$, so j is an integer or half-integer. With a consistent phase convention

$$J_\pm|j,m\rangle = \hbar\sqrt{j(j+1) - m(m\pm1)}\,|j,m\pm1\rangle.$$

Spatial orbital eigenfunctions on an ordinary single-valued scalar wavefunction carry integer orbital l. Spin-$\frac{1}{2}$ has two states that cannot be modelled by adding another spatial coordinate angle to a scalar orbital. The operator algebra describes both. In $|j,j\rangle$, J_z is definite but J_x, J_y fluctuate. Their variance sum is $\hbar^2 j(j+1) - \hbar^2 j^2 = \hbar^2 j$; rotational symmetry around z splits it evenly. Drawing a classical vector with precisely fixed components perpendicular to the axis would miss these fluctuations.

Construct a coupled basis from the stretched state

For independent angular momenta $\mathbf{L}, \mathbf{S}$, the total generator is $\mathbf{J} = \mathbf{L} + \mathbf{S}$. Operators on different factors commute. In the product basis $|m_l, m_s\rangle$, J_z is diagonal with eigenvalue $\hbar(m_l + m_s)$. The Hamiltonian may instead depend on J^2, for example through $\mathbf{L}\cdot\mathbf{S}$. Then states with the same $m_l + m_s$ can mix. Resolving that degeneracy requires a unitary change of basis, whose entries are Clebsch–Gordan coefficients.

Take $l = 1, s = 1/2$. The unique state $m = 3/2$ is $|1,\uparrow\rangle$, so it must be $|3/2, 3/2\rangle$. Lower once with $J_- = L_- + S_-$. The left side is $\hbar\sqrt{3}|3/2, 1/2\rangle$; the right side is $\hbar(\sqrt{2}|0,\uparrow\rangle + |1,\downarrow\rangle)$. Normalising and constructing an orthogonal state in the same m plane gives

$$|3/2,1/2\rangle = \sqrt{2/3}|0,\uparrow\rangle + \sqrt{1/3}|1,\downarrow\rangle,$$

$$|1/2,1/2\rangle = \sqrt{1/3}|0,\uparrow\rangle - \sqrt{2/3}|1,\downarrow\rangle.$$

The sign of an entire coupled vector is conventional. The relative sign of its two components matters whenever a later measurement recombines amplitudes. Applying J_+ to the second combination gives zero, which verifies the top of the $j = 1/2$ multiplet independently of orthogonality. Lowering produces four states for $j = 3/2$ and two for $j = 1/2$, exhausting the six-dimensional product space. Merely listing both possible j's does not supply the amplitude with which a prepared product state belongs to each, which is what spectroscopy needs.

There is a counting derivation for arbitrary j_1, j_2. Start with one stretched state at $m = j_1 + j_2$ and remove its entire ladder. The next highest unused m supplies the next multiplet and so on down to $|j_1 - j_2|$. The identity $\sum_{j=|j_1-j_2|}^{j_1+j_2}(2j+1) = (2j_1+1)(2j_2+1)$ checks completeness. Distinct coupling schemes for three angular momenta are different bases of a common space. An intermediate angular momentum may be a reliable state label when a corresponding interaction dominates, yet cease to be conserved if an external field favours another axis or coupling.

Derive magnetic and parity selection rules

Consider a weak optical field coupled by the electric dipole interaction $-\mathbf{d}\cdot\mathbf{E}$, where $\mathbf{d}$ transforms as a vector and has odd parity. Its spherical components relative to z are

$$d_0 = d_z,\; d_{\pm1} = \mp(d_x \pm i d_y)/\sqrt{2}.$$

For a definite tensor component $[J_z, d_q] = q\hbar d_q$. Sandwiching the commutator between initial and final J_z eigenstates yields

$$(m_f - m_i - q)\langle f|d_q|i\rangle = 0.$$

Thus nonzero amplitudes require

$$m_f = m_i + q.$$

Coupling j_i with a rank-one tensor also requires $|j_i - 1| \le j_f \le j_i + 1$, and $0 \to 0$ is excluded. Parity gives a separate test: under inversion the matrix element gains factor $-\pi_f\pi_i$, so it vanishes for equal initial and final parity in a parity-symmetric Hamiltonian. For purely orbital motion with parity $(-1)^l$, the triangle condition plus odd parity gives

$$\Delta l = \pm 1.$$

A direction label on a photon depends on propagation and polarisation conventions. Stating the driven operator component q is less ambiguous than calling a beam “right circular” without defining the viewing direction.

For a spin-independent dipole transition the spin factor is $\langle m_s'|m_s\rangle$. Begin in $l_i = 0, m_l = 0, m_s = +1/2$ and drive $q = 0$ to $l_f = 1, m_l = 0$. In the product basis there is one equally normalised orbital amplitude D. Its projections on the two coupled final levels have squared amplitudes $2|D|^2/3$ and $|D|^2/3$, giving a 2:1 line-strength ratio under equal field intensity, comparable detection and negligible population saturation. For $q = +1$ the product state is $|1, \uparrow\rangle$. The transition to final $j = 1/2$ vanishes because no $m = 3/2$ belongs to that multiplet. These statements predict relative angular factors. Actual count rates can also depend on frequencies, radial matrix elements, initial populations and how fluorescence is collected.

As an explicit orbital check,

$$Y_{00} = 1/\sqrt{4\pi},$$

$$Y_{10} = \sqrt{3/(4\pi)}\cos\theta.$$

The angular factor of $d_0 \propto r\cos\theta$ is $\int Y_{10}^* \cos\theta Y_{00}\, d\Omega = 1/\sqrt{3}$, while for $Y_{1,\pm1}$ the azimuthal integral vanishes. A radial integral can still vanish accidentally even when all angular tests permit the transition. Symmetry rules predict zeros robust to changes preserving that symmetry; a permitted channel has an amplitude that must still be calculated.

Separate atomic structure from analyser orientation with a reduced matrix element

The angular selection rule from the J_z commutator identifies which transitions are forced to zero but does not alone give their relative strengths. A rotationally covariant way to connect the allowed amplitudes is to view an irreducible tensor component $T_q^{(k)}$ as carrying angular momentum rank k. Under rotations its $2k+1$ components transform among themselves with the same representation matrices as the magnetic substates of an angular momentum k. Coupling $T_q^{(k)}$ to an initial $|jm\rangle$ therefore furnishes the same product representation as coupling $|jm\rangle$ to $|kq\rangle$. The component projecting onto a final j' must transform as j'. When this representation occurs once in the product, its relative magnetic amplitudes are fixed by Clebsch–Gordan coefficients up to one common factor independent of m, q, m'.

In one standard convention the Wigner–Eckart theorem writes

$$\langle \alpha' j' m'|T_q^{(k)}|\alpha j m\rangle = \frac{\langle jm; kq|j'm'\rangle}{\sqrt{2j'+1}}\langle \alpha' j'\|T^{(k)}\|\alpha j\rangle.$$

Additional labels α, α' specify the radial, spin or configuration information absent from the angular labels. Conventions placing a different square-root factor in the reduced element are equally common, so a table of reduced strengths should be checked before combining it with an external coefficient table. The theorem predicts ratios within a fixed j, j' multiplet. It does not remove differences in radial integrals between unrelated configurations, nor does it assert the reduced element is nonzero. This factorisation explains why angular data alone may fix a branching ratio while offering no absolute radiative lifetime.

For a vector operator connecting j to the same j, there is an especially transparent example. Within a given irreducible j space, any vector operator has matrix elements proportional to the corresponding J_q matrix elements, provided additional degeneracies are separated. For the conventional spherical components $J_0 = J_z$, $J_{+1} = -J_+/\sqrt{2}$, ask for the ratio of line strengths out of $j = 2, m = 1$ into $m' = 2$ via $q = +1$

and into $m' = 1$ via $q = 0$, with equal field amplitudes in the specified components. The squared matrix elements of J_q are $\hbar^2[6 - 1(2)]/2 = 2\hbar^2$ and $\hbar^2$, hence the ratio is two. The same numerical angular ratio can apply to any appropriate nonzero reduced vector coupling between these specified manifolds. For an electric dipole transition parity must still allow the initial and final configurations; using J_q here computes angular ratios and does not turn angular momentum itself into an electric dipole operator.

Summing over a complete set of final magnetic substates and all tensor components supplies a useful normalisation audit. For a fixed initial m, rotational invariance of the scalar sum $\sum_q T_q^\dagger P_{j'} T_q$ makes its diagonal expectation independent of m. A detector with a preferred polarisation or direction samples only a subset and may exhibit strong dependence on m. This difference is essential in interpreting “unpolarised” line strengths: an unpolarised pump that populates all m equally, an unanalysed detector that sums final polarisations, and a source with a definite m viewed along one axis are three different experimental ensembles.

Compare successive Stern–Gerlach measurements with addition of spin

Two spin-$1/2$ particles provide a minimal addition experiment with no spatial angular wavefunction needed. The coupled triplet basis is $|1,1\rangle = |\uparrow\uparrow\rangle$,

$$|1,0\rangle = (|\uparrow\downarrow\rangle + |\downarrow\uparrow\rangle)/\sqrt{2},$$
$$|1,-1\rangle = |\downarrow\downarrow\rangle;$$

the singlet is $(|\uparrow\downarrow\rangle - |\downarrow\uparrow\rangle)/\sqrt{2}$. An apparatus measuring the total z component alone cannot distinguish the two $m = 0$ states. Measuring J^2 along with J_z can. Their local one-spin reduced matrices are both $I/2$, so even complete tomography of either spin alone fails to reveal the difference. The distinction lies in a joint correlation.

The singlet projector can be obtained as a polynomial in $\mathbf{S}_1 \cdot \mathbf{S}_2$. That scalar has eigenvalues $-3\hbar^2/4, +\hbar^2/4$, so $P_s = I/4 - \mathbf{S}_1 \cdot \mathbf{S}_2/\hbar^2$. Expressing $\mathbf{S}_i = (\hbar/2)\boldsymbol{\sigma}_i$ gives

$$P_s = [I - \sum_i \sigma_i \otimes \sigma_i]/4.$$

If three independently prepared ensembles yield measured same-axis correlations $(-0.80, -0.78, -0.82)$, their inferred singlet fraction is

$$(1 + 2.40)/4 = 0.85.$$

This result uses all three axes. Perfect z-anticorrelation alone constrains the population to a two-dimensional $m = 0$ space but says nothing about the relative phase within it. If each measurement has uncertainty 0.03 and the estimates are independent, the resulting statistical uncertainty in singlet fraction is $\sqrt{3}(0.03)/4 = 0.013$, before calibration uncertainties.

For a coherent initial product $|\uparrow\downarrow\rangle$, a Hamiltonian $H = J_{\mathrm{ex}}\mathbf{S}_1 \cdot \mathbf{S}_2/\hbar^2$ evolves the singlet and triplet amplitudes with distinct phases. Writing the initial state as $(|1,0\rangle + |0,0\rangle)/\sqrt{2}$, the probability to find spins reversed later is $\sin^2(J_{\mathrm{ex}}t/(2\hbar))$. The total m remains exactly zero at all times. If $J_{\mathrm{ex}}/h = 5.00$ MHz, the

first full reversal occurs at $t = 1/(2 \times 5\,\mathrm{MHz}) = 100$ ns. An incoherent mixture with the same singlet and triplet populations has a constant reversal probability one half. This calculation makes the signs in the coupled basis observable and distinguishes a true exchange evolution from random spin flips inferred solely from individual populations.

Rotate the quantisation axis without changing the atomic Hamiltonian

A transverse magnetic or polarisation analyser can interrogate a state prepared relative to z along a different laboratory axis. For spin $1/2$, $e^{-i\theta S_y/\hbar} = \cos(\theta/2)I - i\sin(\theta/2)\sigma_y$, from $\sigma_y^2 = I$. To obtain the rotation probabilities for a spin-one state without memorising a rotation matrix, represent its stretched state as the symmetric product of two up spinors. Under a common rotation each spinor transforms as $\cos(\theta/2)|\uparrow\rangle + \sin(\theta/2)|\downarrow\rangle$. Expanding the two-spin product gives the triplet amplitudes $\cos^2(\theta/2), \sqrt{2}\cos(\theta/2)\sin(\theta/2), \sin^2(\theta/2)$ for the three m values. This construction exploits the representation and applies to any angular momentum one, regardless of its microscopic origin.

At $\theta = \pi/2$, a stretched $m = 1$ state projected on the rotated axis gives probabilities $(1/4, 1/2, 1/4)$. The expectation of its rotated component vanishes, but outcomes $+\hbar$ and $-\hbar$ still occur and the variance is $\hbar^2/2$. A source prepared in $m = 0$ along z gives a different test. Rotate its symmetrised up–down form on both spins and project on $m = 0$; the amplitude is $\cos\theta$ and the probability $\cos^2\theta$. At a right angle the “zero” outcome is absent, although the mean along either axis is zero. A single mean value cannot distinguish alignment from an unpolarised mixture. Measuring the full resolved substate distribution, or its quadrupole moment, can.

The general stretched state $|j, j\rangle$ can be represented by $2j$ symmetrised spinors all up. Its rotated m outcome distribution is binomial:

$$P(m) = \binom{2j}{j-m} \cos^{2(j+m)}(\theta/2)\sin^{2(j-m)}(\theta/2).$$

Its mean angular momentum component is $\hbar j\cos\theta$, with variance $\hbar^2(j/2)\sin^2\theta$. At fixed nonzero $\cos\theta$, the relative fluctuation falls like $j^{-1/2}$ as j grows. This supplies a precise sense in which a large stretched state can approximate a classical oriented angular momentum while retaining quantum projection noise. A state with the same large j but $m = 0$ need not resemble an oriented classical arrow. The representation dimension alone does not determine the suitability of a classical approximation.

Distinguish an angularly forbidden line from coherent cancellation

Suppose two degenerate lower magnetic states $|g_1\rangle, |g_2\rangle$ both couple to one excited state $|e\rangle$ under controlled coherent drives. In a rotating-frame model the raising part is $|e\rangle(\Omega_1\langle g_1| + \Omega_2\langle g_2|)\hbar/2$, with the lowering term its adjoint. A normalised superposition proportional to $\Omega_2|g_1\rangle - \Omega_1|g_2\rangle$ has zero excitation amplitude because the two terms cancel. Each angular channel can be individually allowed and strong, yet this particular coherent combination is dark. Its orthogonal bright state is proportional to $\Omega_1^*|g_1\rangle + \Omega_2^*|g_2\rangle$ and has effective Rabi coupling $\sqrt{|\Omega_1|^2 + |\Omega_2|^2}$.

For equal real drives and an initially balanced antisymmetric superposition, the transition ideally vanishes. A randomly prepared mixture of the same two basis states populates the bright and dark subspaces equally. If a resonant pulse transfers the bright component completely, that mixture produces 50% excitation. Changing the relative optical phase changes which superposition is dark but does not change the selection rule for either individual transition. Preparing a calibrated ground-state phase and scanning the drive phase can therefore distinguish coherent cancellation from a forbidden angular matrix element or a disconnected drive channel. Two-photon detuning, magnetic splitting of the lower states and dephasing can spoil the destructive interference even if every angular coefficient is exactly known.

Track a spin while rotating the preparation axis

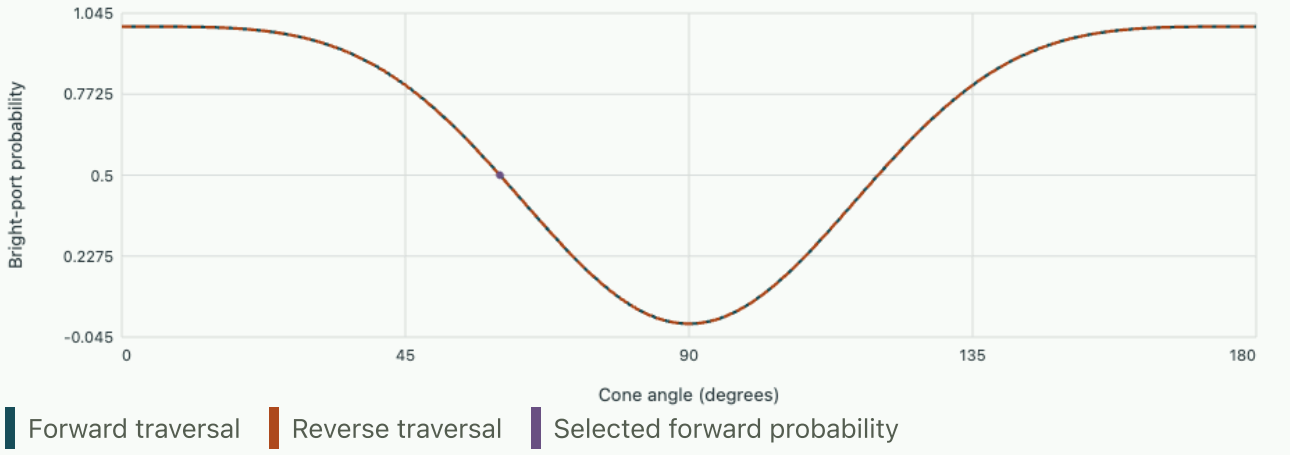
Change the path of a spin direction and compare a change in its geometric phase with an ordinary dynamical phase.

Open this experiment online

Try the calculation

Cone angle (degrees) **60**

Reference phase (degrees) **0**



Forward geometric phase -0.5π radians. Forward port probability 0.5, reverse 0.5.

Predict which perturbation can make a dark transition visible

Electric dipole selection rules use the approximation that the driving field is essentially uniform across the atom. Expand a monochromatic plane wave $e^{i\mathbf{k}\cdot\mathbf{r}} = 1 + i\mathbf{k}\cdot\mathbf{r} + \cdots$. For a source of size a the next spatial term is suppressed in amplitude by a factor of order ka when $ka \ll 1$. Consistently expanding the light–matter Hamiltonian yields higher electric multipoles and magnetic couplings with their own symmetry. The electric quadrupole is a rank-two even-parity tensor. Thus it can connect same-parity states with $|j_i - 2| \le j_f \le j_i + 2$. A magnetic dipole is a rank-one operator of even spatial parity, permitting some same-parity transitions denied to an electric dipole. A line forbidden to one specified multipole need not vanish in all experimental conditions.

Take a model atom with a lower $j = 0$ even state and an upper $j = 2$ even state. Electric dipole fails both parity and angular-momentum tests. Magnetic dipole has the right parity but still cannot supply total angular rank two. Electric quadrupole has the correct parity and satisfies the triangle condition; its actual reduced matrix element and the applied field gradient still determine strength. In a $j = 0 \to j' = 2$ transition with $m_i = 0$, each spherical quadrupole component q excites only $m_f = q$. A simple claim that changing circular to linear polarisation opens an electric dipole line in this field-free atom would be inconsistent with both global selection rules. A static field that mixes opposite parity or different angular momentum can change the states themselves and thereby modify that conclusion.

For a 600 nm wavelength and characteristic radius $a = 0.10$ nm,

$$ka = 2\pi a/\lambda = 1.05 \times 10^{-3}.$$

The squared geometric factor is about 1.1×10^{-6} relative to a typical allowed electric dipole strength in comparable units, before distinct radial and angular factors. This is an order estimate, not a quantitative branching ratio for two arbitrary lines. In particular, dividing a finite quadrupole amplitude by a strictly zero dipole amplitude of the same ideal transition is meaningless. Compare with a separate reference line whose dipole matrix element and detection efficiencies are known if a rate ratio is needed.

An independent way to brighten an otherwise forbidden line is mixing through a perturbation W. Suppose an upper state $|u\rangle$ has zero electric dipole amplitude from $|g\rangle$, while a nearby state $|v\rangle$ allows amplitude D. If $|\langle v|W|u\rangle| \ll |E_u - E_v|$, the perturbed upper state contains coefficient $\epsilon = \langle v|W|u\rangle/(E_u - E_v)$ of $|v\rangle$, and its borrowed dipole intensity scales as $|\epsilon|^2|D|^2$. Where W is proportional to a reversible static field, borrowed intensity typically begins quadratically in that field for a previously dark isolated line. A native higher-multipole contribution may already be present at zero field and can interfere if it feeds the same final channel with coherent angular dependence.

Use polarisation and bias sweeps to identify borrowed intensity

In a two-state model the bright level is 2.00 GHz away and a perturbation mixes it with the dark state at off-diagonal $W/h = 20$ MHz. Predict relative borrowed intensity, assess the leading approximation, and identify an independent spectroscopic consequence.

▼ **Derive and check the result**

The small parameter is

$$20/2000 = 0.010.$$

The leading borrowed intensity is 10^{-4} of the corresponding bright reference, with corrections of relative order 10^{-4} in the ideal two-level mixing expansion. The dark state's energy shifts by approximately $W^2/(E_u - E_v)$, whose magnitude expressed as ordinary frequency is

$$20^2/2000 = 0.20\,\mathrm{MHz}.$$

Its sign is away from the neighbouring bright level. Measuring this level repulsion together with the same polarisation pattern as the borrowed bright transition tests the mixing explanation. Changing the perturbing field by a factor of two should increase both the leading borrowed intensity and the magnitude of the second-

order level shift by a factor of four while the coupling remains weak. A field-independent residual or a different polarisation dependence motivates examining other multipoles or additional states.

Tutorial · infer the state that a spectrum actually selects

Measure the orbital label after total angular momentum preparation

Prepare $|j = 1/2, m = 1/2\rangle$ in the coupled p manifold. Predict m_l outcomes, the spin expectation and the sum $\langle L_z + S_z \rangle$. Is either product component a state with definite J^2?

▼ **Work through the solution**

The probabilities are $1/3$ for $m_l = 0$ with spin up, $2/3$ for $m_l = 1$ with spin down. Thus $\langle L_z \rangle = 2\hbar/3$, $\langle S_z \rangle = -\hbar/6$ and the sum is $\hbar/2$. The product vectors in this two-dimensional plane are each superpositions of both j's, as can be checked by inverting the two orthogonal combinations. A joint measurement of orbital and spin labels can therefore disturb a previously exact J^2. The total m remains fixed in every outcome, stronger than merely having the correct mean.

Determine a spin–orbit interval without an angular integral

Within $l = 1, s = 1/2$, take $H' = A\,\mathbf{L}\cdot\mathbf{S}/\hbar^2$ with $A/h = 8$ GHz. Find level shifts, degeneracies and their degeneracy-weighted centre. Check the result from a product-basis trace.

▼ **Work through the solution**

Use $2\mathbf{L}\cdot\mathbf{S} = J^2 - L^2 - S^2$. For $j = 3/2$ the factor is $+1/2$; for $j = 1/2$ it is -1. Shifts are $+4$ and -8 GHz, with degeneracies four and two; their interval is 12 GHz and their weighted centre is zero. The product-basis trace of each $L_i S_i$ is $\mathrm{tr}\, L_i \;\mathrm{tr}\, S_i = 0$, which predicts that centre independently. If a measured centroid is weighted by optical intensity instead of counting every substate once, it need not equal this trace centre.

Distinguish resolved lines from a coherent pulse

A short $q = 0$ pulse prepares the product final state $|0, \uparrow\rangle$ above. If its spectrum covers both j levels coherently, find the later return probability to that same product state for a level angular-frequency splitting Δ. What would an incoherent population mixture give?

▼ **Work through the solution**

The return amplitude is $(2/3)e^{-iE_{3/2}t/\hbar} + (1/3)e^{-iE_{1/2}t/\hbar}$. Its squared modulus is $5/9 + (4/9)\cos\Delta t$, between $1/9$ and 1. The corresponding incoherent mixture gives a constant $5/9$. At $t = 0$ both constructions share the same energy-measurement probabilities, yet only the coherent preparation returns with certainty to the original product state. Temporal resolution, controlled pulse phase and bandwidth sufficient to cover both

lines are part of the proposal. If the emitted or absorbed field records distinguishable frequencies, the observed beat can be suppressed.

Further reading

- Fließbach · Operatorenmethode, angular momentum algebra
- Cambridge · atoms in electromagnetic fields and electric dipole selection rules
- Course investigation · angular momentum and atoms

Quantum states, dynamics and measurement · 5. From a Coulomb orbit to the fine-structure multiplet

Separate the hydrogenic Schrödinger equation, identify the origin of its large degeneracy and evaluate the three dominant relativistic corrections. The cancellation among them predicts an equality that spectroscopy can then test.

Separate centre-of-mass and relative motion

A light particle of mass m_e and charge $-e$ interacts with a pointlike nucleus $+Ze$ of mass M. Use centre of mass $\mathbf{R} = (m_e\mathbf{r}_e + M\mathbf{r}_N)/(m_e + M)$ and separation $\mathbf{r} = \mathbf{r}_e - \mathbf{r}_N$. Expanding the sum of the two kinetic energies cancels all cross terms and gives a free centre-of-mass kinetic energy plus relative energy $p^2/(2\mu)$, with reduced mass $\mu = m_eM/(m_e + M)$. The relative potential is $-k/r,\ k = Ze^2/(4\pi\epsilon_0)$. Its rotational symmetry implies $[H, L_i] = 0$. Use a spherical harmonic Y_{lm} and write $\psi = u(r)Y_{lm}/r$, so the probability in a thin radial shell is $|u(r)|^2dr$ for angular harmonics of unit norm.

Substituting in the Laplacian separates the radial equation

$$-\frac{\hbar^2}{2\mu}u'' + \left[\frac{\hbar^2 l(l+1)}{2\mu r^2} - \frac{k}{r}\right]u = Eu.$$

For the regular three-dimensional solution $u(0) = 0$ and a bound state also decays at infinity. The centrifugal term is an effective energy associated with angular variation, not a separate force added by hand. For $E < 0$ define $\kappa = \sqrt{-2\mu E}/\hbar,\ \rho = 2\kappa r$, and $a = \hbar^2/(\mu k)$. The small-radius behaviour of u is r^{l+1}; the large-radius tail contains $e^{-\kappa r}$. Pull both out by $u = \rho^{l+1}e^{-\rho/2}v(\rho)$. Straight differentiation leaves

$$\rho v'' + (2l + 2 - \rho)v' + (1/\kappa a - l - 1)v = 0.$$

For $v = \sum c_j\rho^j$, coefficient matching gives

$$c_{j+1}/c_j = (j + l + 1 - 1/\kappa a)/[(j + 1)(j + 2l + 2)].$$

The regular series must terminate to avoid an exponential asymptotic part that defeats the decaying prefactor. Thus $1/(\kappa a) = n_r + l + 1 = n$, and $E_n = -\mu k^2/(2\hbar^2 n^2)$. The normalised radial polynomials are associated Laguerre functions. This gives $l = 0, \ldots, n - 1$ and $\sum_l(2l + 1) = n^2$ states before including spin. Rotational symmetry guarantees the degeneracy in m, but a different central potential can split levels of different l. The additional equality is specific to the Coulomb potential.

Calculate the radial moments needed for a correction

To isolate the leading relativistic corrections now take an infinitely heavy nucleus and set $m = m_e$, $a = \hbar^2/(mk)$. Including reduced mass in the leading energy is straightforward; a complete recoil correction to the fine structure requires additional interactions. A useful identity is $\langle 1/r\rangle = 1/(an^2)$, obtained by differentiating E_n with respect to k. The derivative of an eigenvalue equals the expectation of $\partial H/\partial k = -1/r$ for the normalised eigenstate, which follows by differentiating $H|\psi\rangle = E|\psi\rangle$ and cancelling terms using its adjoint. The same method applied to the radial centrifugal parameter yields $\langle r^{-2}\rangle = 1/[a^2n^3(l + 1/2)]$ at fixed radial node count. Treat l as a continuously varied radial parameter during differentiation, then evaluate at its physical integer value.

For $l > 0$, the stationary radial force identity $\langle dV_{\mathrm{eff}}/dr \rangle = 0$ with vanishing endpoint term gives

$$\langle r^{-3} \rangle = 1/[a^3 n^3 l(l+1/2)(l+1)].$$

Here V_{eff} is the potential in the radial equation. The step uses sufficient behaviour of u, u' at the origin. For $l = 0$, the integral of r^{-3} diverges in an s state and the neglected endpoint term need not vanish. Substituting $l = 0$ formally into this expression would therefore be invalid. The contact density of an s state needed below is $|\psi_{n00}(0)|^2 = 1/(\pi a^3 n^3)$, while states with $l > 0$ vanish at the origin.

Track the kinetic, spin–orbit and contact terms separately

The small parameter is $Z\alpha = k/(\hbar c)$, with α the fine-structure constant for $Z = 1$. Expand the relativistic dispersion about small momentum after subtracting rest energy: $p^2/(2m) - p^4/(8m^3c^2) + \cdots$. For an energy eigenfunction $p^2\psi = 2m(E_n + k/r)\psi$, so $\langle p^4 \rangle = 4m^2\langle (E_n + k/r)^2 \rangle$ follows by taking the squared norm of $p^2\psi$. Squaring the two operators as if p^2 and $1/r$ commute is unnecessary and would not be an operator identity. Inserting the first two radial moments gives

$$\Delta E_{\mathrm{kin}} = -C_n \left[\frac{1}{l+1/2} - \frac{3}{4n} \right],$$

$$C_n = \frac{mc^2(Z\alpha)^4}{2n^3}.$$

The Pauli expansion of the Dirac Hamiltonian adds $H_{\mathrm{so}} = (1/[2m^2c^2r])V'(r)\mathbf{L}\cdot\mathbf{S}$ and the Darwin contact $H_D = \hbar^2\nabla^2 V/(8m^2c^2)$. These are effective interactions through order $(Z\alpha)^4$; a purely nonrelativistic scalar equation does not generate the spin or contact term. For $V = -k/r$, $V' = k/r^2$ and $\nabla^2 V = 4\pi k\delta^3(\mathbf{r})$. Thus the contact shifts only s states by $+C_n$. For $l > 0$ insert the third inverse radial moment and the angular identity $\mathbf{L}\cdot\mathbf{S} = \hbar^2[j(j+1) - l(l+1) - 3/4]/2$. For the branch $j = l + 1/2$ the bracket is l; for $j = l - 1/2$ it is $-(l+1)$. Reducing fractions then gives

$$\Delta E_{\mathrm{so}} = C_n[1/(l+1/2) - 1/(j+1/2)].$$

For $l = 0$ the spin–orbit operator vanishes and the Darwin term supplies the required difference. The sum in either case is

$$\Delta E_{nj} = -C_n \left[\frac{1}{j+1/2} - \frac{3}{4n} \right].$$

At fixed n the answer depends on j but no longer separately on l. The cancellation cannot be inferred by merely attaching a phenomenological $\mathbf{L}\cdot\mathbf{S}$ splitting to a nonrelativistic p state. In particular it predicts identical energies for $2s_{1/2}$ and $2p_{1/2}$ in this approximation, while $2p_{3/2}$ lies higher. Radiative, recoil and finite-nuclear-size contributions can resolve some of these residual equalities. An experimentally resolved residual is evidence that the specified Hamiltonian omitted a physical term; it does not remove the cancellation inside that Hamiltonian.

Compare a small energy correction with a resolvable line

For hydrogen with $mc^2 \simeq 511\,000$ eV and $\alpha \simeq 1/137.04$, the $2p_{3/2}$–$2p_{1/2}$ interval is $C_2/2 \simeq 4.53 \times 10^{-5}$ eV or 10.95 GHz. Compare with the leading $n = 2$ binding energy 3.40 eV. A small correction to total binding can give a prominent splitting when a measurement subtracts nearly equal large energies. Resolving it in a Fourier-limited time-domain experiment requires a coherent observation time at least of order the inverse frequency difference, here around 0.09 ns. Actual linewidths, lifetimes and pulse shapes affect how two spectral components can be distinguished.

A useful numerical audit is to fit the radial spectrum with three successive physical models. First solve the nonrelativistic radial boundary problem with the correct near-origin power and check that 2s and 2p converge toward the same energy. Then evaluate expectation values of the three corrections on those numerical states. Finally combine terms. Converged binding energies alone do not guarantee a converged contact density, which samples one spatial endpoint. A coarse radial grid can imitate an anomalous splitting between states which the analytical correction predicts to be equal. Check the origin slope of u_{n0}, not only its norm or far tail.

Find where the electron is most likely to be detected

Confusion between spatial density and radial probability can lead to very different-looking descriptions of the same atom. For a hydrogenic ground state the normalised position-space wavefunction is $\psi_{100} = (\pi a^3)^{-1/2} e^{-r/a}$. Its density is largest at the centre, but a thin spherical shell at radius r contains probability $P(r)dr = 4r^2 e^{-2r/a} dr/a^3$. The shell volume tends to zero at the origin. Differentiating $\ln P$ gives $2/r - 2/a = 0$, so the most likely shell radius is a. The mean radius $\int rP(r)dr = 3a/2$ is different again because the shell distribution has a long tail. Neither number alone gives the probability that a finite spatial detector clicks.

Integrating the shell probability between zero and R gives

$$\Pr(r < R) = 1 - e^{-2R/a}\left(1 + \frac{2R}{a} + \frac{2R^2}{a^2}\right).$$

At the most likely shell radius $R = a$, the probability inside is $1 - 5e^{-2} = 0.3233$, substantially less than one half. At $R = 2a$ it is

$$1 - 13e^{-4} = 0.7619.$$

Taylor expansion at a small radius $R \ll a$ gives $4(R/a)^3/3$, equal to the ball volume times central density to leading order. This is the local scaling underlying finite-nucleus corrections to a contact-sensitive observable. Using the most likely radius as though the electron followed a thin circular orbit would give none of these cumulative probabilities, even though the same Coulomb length scale appears in the Bohr model.

For $2s$ and $2p$, both states have principal index two and the same leading energy. The $2s$ radial amplitude is proportional to $(2 - r/a)e^{-r/(2a)}$; its node at $2a$ separates regions of opposite amplitude sign. The $2p$ radial amplitude is proportional to $re^{-r/(2a)}$, with no positive-radius radial node. At short distance, the probability inside R scales as R^3 for a nonzero s amplitude and as R^5 for the p wave. A sufficiently localised weak perturbation near the nucleus can therefore split the nonrelativistic degeneracy even if it is rotationally symmetric. Rotational symmetry still protects equal shifts within the m multiplet. A radial perturbation and a field selecting a direction leave different patterns of protected degeneracy.

Diagonalise a degeneracy before expanding a weak electric field

The $n = 2$ Coulomb degeneracy creates a striking response to a weak uniform electric field along z. In the purely nonrelativistic model with spin ignored the relevant spatial states are $2s,\ 2p_0,\ 2p_{\pm1}$. The perturbation for an electron in electric field $\mathcal{E}\hat{z}$ can be written $e\mathcal{E}z$ up to an additive constant. Each unperturbed parity eigenstate has zero diagonal expectation of this odd operator. Applying ordinary nondegenerate first-order perturbation theory separately to all four states would therefore predict zero for every shift. But first-order perturbation theory in a degenerate manifold requires diagonalising the projected perturbation, including off-diagonal amplitudes.

The $z = r\cos\theta$ operator has $q = 0$ and changes parity, so within $n = 2$ it couples only $2s$ and $2p_0$. Its angular matrix element between Y_{00} and Y_{10} is $1/\sqrt{3}$. In a conventional phase convention the radial functions are $R_{20} = (2 - r/a)e^{-r/(2a)}/(2\sqrt{2}\,a^{3/2})$ and $R_{21} = (r/a)e^{-r/(2a)}/(2\sqrt{6}\,a^{3/2})$. The remaining radial integral is $\int r^3 R_{20}R_{21}\,dr$. Setting $s = r/a$ gives

$$a(2\cdot 4! - 5!)/(8\sqrt{3}) = -3\sqrt{3}a.$$

Multiplying the angular factor gives $-3a$. Rephasing one basis state would change this sign but leave all level shifts invariant.

The projected matrix has zero diagonal and off-diagonal $-3ea\mathcal{E}$. Its symmetric and antisymmetric combinations have linear shifts $\mp 3ea\mathcal{E}$, while $2p_{\pm1}$ remain unshifted to this order. The new states have definite first-order dipoles along opposite directions even though their zero-field basis states had zero dipoles. For $a = 5.29\times10^{-11}$ m and $\mathcal{E} = 1000$ V/m, an individual linear shift has magnitude 1.59×10^{-7} eV, corresponding to 38.4 MHz. This field is weak compared with the gross level separation, but whether the degenerate result is accurate in a real atom also depends on much smaller fine, hyperfine and radiative splittings. “Weak field” must specify the comparison energy.

A more precise two-state model retains a zero-field splitting Δ between the coupled states. After subtracting their mean the Hamiltonian is $(\Delta/2)\sigma_z + d\mathcal{E}\sigma_x$, with $d = 3ea$ in magnitude. The energies are $\pm\sqrt{(\Delta/2)^2 + d^2\mathcal{E}^2}$. At $d|\mathcal{E}| \ll |\Delta|$ the shift from each initial level is quadratic, $\pm d^2\mathcal{E}^2/|\Delta|$, while at $d|\mathcal{E}| \gg |\Delta|$ the slopes approach the linear-degenerate prediction. An observed crossover distinguishes a small unresolved internal splitting from a strictly zero projected dipole matrix element. Tracking energies over both positive and negative fields also tests for a stray dc field shifting the centre of the response.

Estimate a finite-size correction from the potential itself

The contact term derived from the Pauli expansion is not the same physical effect as giving the nucleus a finite charge radius. A simple electrostatic model separates the two scalings. Replace a point nucleus by a uniformly charged sphere of radius R_N. Inside it the electron potential becomes

$$V_{\mathrm{sph}}(r) = -k[3 - (r/R_N)^2]/(2R_N);$$

outside it is unchanged at $-k/r$. The perturbation $\delta V = k[1/r - 3/(2R_N) + r^2/(2R_N^3)]$ is positive for interior points and zero at the surface. The smoothed potential is less attractive than the point law near the centre.

For an s state and $R_N \ll a$, the unperturbed density varies little across the tiny sphere. First-order perturbation theory therefore gives

$$\delta E \simeq 4\pi k |\psi(0)|^2 \int_0^{R_N} \left(r - \frac{3r^2}{2R_N} + \frac{r^4}{2R_N^3} \right) dr$$

$$\frac{2\pi}{5}\, k |\psi(0)|^2 R_N^2 .$$

The first two radial integrals cancel and leave the $R_N^2/10$ contribution before multiplication by 4π. Equivalently write $\delta E = (2\pi/3) k |\psi(0)|^2 \langle r_N^2 \rangle$, since the uniform sphere has mean-square charge radius $3R_N^2/5$. The result is a positive shift, decreasing binding. Corrections to the constant-density approximation involve additional powers of R_N/a. A different microscopic charge distribution changes higher moments, while the leading small-size shift depends on its mean-square charge radius.

For a model $R_N = 1.0$ fm and the ordinary electronic hydrogen length $a = 5.29 \times 10^{-11}$ m, $R_N/a = 1.89 \times 10^{-5}$. For the ground state compare with $|E_1| = k/(2a)$ and $|\psi(0)|^2 = 1/(\pi a^3)$. The relative shift is $(4/5)(R_N/a)^2 = 2.86 \times 10^{-10}$, equivalent to roughly 3.9×10^{-9} eV. This illustrative uniform charge radius is input data of the model; do not equate it directly to a measured rms radius. For a heavier orbiting lepton a shorter Bohr radius increases the fractional sensitivity strongly. A complete precision spectrum would additionally include radiative and recoil effects and a realistic nuclear response. The present derivation isolates how one local perturbation scales and why s levels are especially sensitive.

Use dilation to audit stationary Coulomb energies numerically

A variational scaling argument gives a powerful independent check on a computed wavefunction. For any normalised trial state ψ, define the normalised rescaling $\psi_\lambda(\mathbf{r}) = \lambda^{3/2}\psi(\lambda \mathbf{r})$. The Coulomb potential is homogeneous of degree minus one, and the gradient acquires a factor λ. Its energy expectation is therefore

$$E(\lambda) = \lambda^2 \langle T \rangle + \lambda \langle V \rangle .$$

For an exact stationary bound state the energy functional is stationary with respect to norm-preserving variations, giving $2\langle T \rangle + \langle V \rangle = 0$ at $\lambda = 1$. Hence $\langle T \rangle = -E,\ \langle V \rangle = 2E$, consistent with the independently derived inverse-radius mean. The argument requires appropriate normalisation and boundary behaviour so the scaled trial function is allowed.

Suppose a numerical $1s$ reconstruction yields $\langle T \rangle = 13.2$ eV and $\langle V \rangle = -26.7$ eV. Its energy is -13.5 eV, yet its virial residual is -0.3 eV. Along the scale family the minimum occurs at $\lambda_* = -\langle V \rangle / (2\langle T \rangle) = 1.0114$, a slightly more concentrated state. The resulting energy reduction is only about 0.0017 eV, much smaller than the change in individual kinetic and potential terms. A small total-energy error can coexist with a noticeably incorrect radial scale because first-order energy errors cancel near a stationary solution. Monitoring separate expectation values, the virial residual and a contact-sensitive observable provides a more informative test of a numerical atomic calculation than reporting the total binding energy alone.

Distinguish orbital density from radial probability

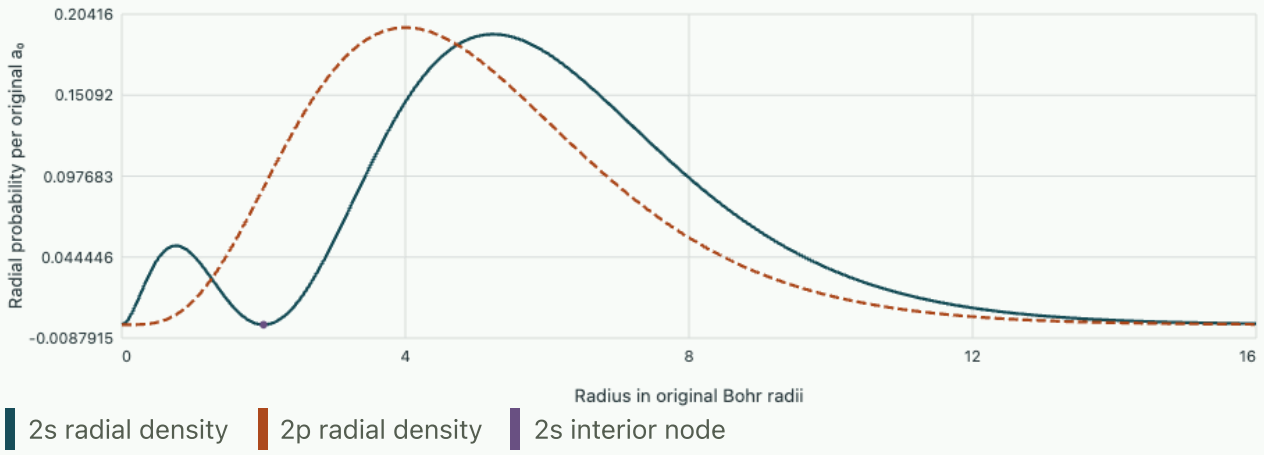
Compare radial states at the same principal quantum number. Inspect their nodes before considering which additional interactions can lift their degeneracy.

Open this experiment online

Try the calculation

Nuclear charge Z

1



The 2s node is at 2 original Bohr radii. The most probable 2p radius is 4 original Bohr radii.

Appraise a finite-grid Coulomb spectrum from convergence and degeneracy

To compute the radial Schrödinger eigenvalues directly, work in dimensionless radius $s = r/a$, energy unit $\hbar^2/(2ma^2)$, and write $[-d^2/ds^2 + l(l+1)/s^2 - 2/s]u = \varepsilon u$. On a uniform grid $s_j = jh$, use $u_0 = 0$ and a far boundary $u_{N+1} = 0$. The diagonal approximation is $2/h^2 + l(l+1)/s_j^2 - 2/s_j$ and its neighbours are $-1/h^2$. All potential terms are evaluated at positive interior grid points. Inserting an arbitrary finite value for $1/s$ at the origin and treating it as an ordinary interior point changes the boundary approximation. A tridiagonal symmetric eigensolver returns orthogonal numerical vectors; physical radial norm is $h\sum_j |u_j|^2$, so normalise appropriately before reconstructing spatial densities.

For $l = 0$ on an infinite grid the lowest mode permits an unusually informative exact lattice check. Try $u_j = jq^j$ for $0 < q < 1$. The finite-difference kinetic row divided by this trial value is $[2 - q - q^{-1}]/h^2 - (q - q^{-1})/(jh^2)$. Adding potential $-2/(jh)$, the $1/j$ coefficient vanishes when $q^{-1} - q = 2h$, or $q = \sqrt{1+h^2} - h$. The eigenvalue is then

$$\varepsilon_h = [2 - 2\sqrt{1+h^2}]/h^2 = -2/[1 + \sqrt{1+h^2}].$$

It tends to the exact continuum ground value -1 as $-1 + h^2/4 + O(h^4)$. This analytic discrete answer separates algebraic solver correctness from discretisation error for the exact same potential and boundary treatment.

At $h = 0.20$ the infinite-grid ground value is approximately -0.99020; at $h = 0.10$ it is -0.99751. Their errors differ by nearly a factor of four as predicted. A finite far wall shifts both energies further; repeat first at fixed h and increasing boundary radius to isolate that effect. An excited $n = 2$ state has a more extended tail and requires a larger radius than the ground state for comparable truncation bias. Solving $l = 0$ and $l = 1$ on a small common box can yield a spurious nonrelativistic 2s–2p splitting. Check separately that both energies tend to $-1/4$ before interpreting a much smaller physical fine splitting. Subtracting independently computed energies amplifies absolute numerical biases even if each number appears visually close to its expected value.

The distinctive near-origin behaviour supplies a second check. Since $\psi_{100}(0)$ is proportional to the slope of the reduced radial function at zero, a first forward difference u_1/h typically incurs a first-order error even when the energy error is second order. For the lattice shape above $u_j \propto jq^j$, the first two positive grid values can be used to estimate the endpoint derivative by $(4u_1 - u_2)/(2h)$. Test its convergence under the physical radial normalisation. For a contact perturbation, squaring an endpoint derivative doubles its small relative error to leading order. This is why an atomic calculation should include an observable-specific refinement criterion in addition to an energy tolerance.

Use an eigenvalue benchmark to separate numerical and physical shifts

A report on the infinite-grid hydrogenic ground state quotes energy -0.99750 at $h = 0.10$ and attributes the difference from -1 to a short-range interaction. Predict the lattice-only change on refinement to $h = 0.05$, and propose a test that could reveal a real interaction independently.

▼ **Derive and check the result**

The lattice expression gives $-2/[1 + \sqrt{1.0025}] \simeq -0.999376$ at 0.05, so the discretisation alone accounts for the original difference at the stated accuracy. A local physical correction with fixed continuum strength should converge toward a fixed nonzero shift as $h \to 0$, while the lattice bias vanishes approximately as $h^2/4$. Compute control and perturbed energies on exactly the same grids and compare their difference under refinement, with consistent treatment of the perturbation's physical range. An unresolved delta perturbation represented as a fixed diagonal value on one grid point changes its effective continuum strength upon refinement and would produce another artificial shift. Cross-check with the first-order expectation of a resolved physical potential or with the independently converged contact density.

Use an isotope pair to cancel a common transition-energy reference

High-precision spectroscopy often obtains its most reliable insight from combinations of frequencies rather than absolute energies. Consider two hydrogenic model isotopes with the same nuclear charge, different reduced masses μ_1, μ_2 and different mean-square charge radii R_1^2, R_2^2. For a specified transition the leading point-Coulomb frequency can be written $C\mu$, since its n-dependent dimensionless numbers are fixed. A local nuclear-size perturbation shifts each participating s level by a factor proportional to $|\psi_{ns}(0)|^2 R_i^2 \propto \mu_i^3 R_i^2/n^3$, while a p level receives a much smaller finite-size correction in the same limit. The different powers of reduced mass and radial quantum number permit differences of transitions to cancel selected terms.

For illustration compare a 1s–2s optical frequency with a 1s–2p frequency within one model isotope, assuming the fine, radiative and differing upper-state structures have been independently accounted for in the desired order. Subtracting these frequencies cancels the entire common lower 1s energy and the gross equal 2s/2p Coulomb energy, leaving the upper 2s–2p differences. If instead one sought the large 1s contact contribution, subtracting these same two lines would remove precisely the effect of interest. An apparently convenient common reference can therefore eliminate physical signal as well as noise. Write the coefficient of each contributing level explicitly before selecting a frequency combination.

Suppose two independently fitted line frequencies ν_a, ν_b each have a 10 MHz common reference error and independent residual standard errors of 0.30 and 0.40 MHz. The covariance from the shared reference is $100\,\mathrm{MHz}^2$. The difference has variance $0.30^2 + 0.40^2 = 0.25\,\mathrm{MHz}^2$, hence 0.50 MHz standard error. Treating both total errors as independent instead would suggest roughly 14 MHz. Conversely, an error in a calibration scale proportional to frequency leaves a residual proportional to the frequency difference; its cancellation is only approximate. Reporting the provenance of uncertainties and their covariance can matter more than recording an extra digit of each absolute transition.

Recover a contact shift from two excited-state probes

In a diagnostic model a local perturbation gives an unknown positive 1s shift D, an ns shift D/n^3, and zero shifts of p levels. Relative to a matched reference, how do 1s–2s, 1s–2p and 1s–3s frequencies change? Which experimental difference removes the unknown common lower-state shift yet recovers D?

▼ Derive and check the result

The changes are $(-7D/8)/h,\ -D/h,\ (-26D/27)/h$, respectively. Subtracting the 1s–2p shift from the 1s–2s shift gives $D/(8h)$, since the common lower-state contribution cancels. For a measured difference of 0.90 ± 0.05 MHz the implied $D/h = 7.2 \pm 0.4$ MHz. The 1s–3s shift should then be -6.93 MHz in this stipulated model. If unavailable corrections also differ among the upper states, that value is not an absolute nuclear-radius extraction. The third line gives an independent test of the $1/n^3$ contact scaling before attributing all measured differences to the single parameter D.

Tutorial · measure degeneracy through independent calculations

Verify two inverse moments directly in the $2p$ state

Use $R_{21}(r) = re^{-r/(2a)}/(2\sqrt{6}\,a^{5/2})$ and normalised Y_{1m}. Evaluate $\langle r^{-2}\rangle$, $\langle r^{-3}\rangle$ without parameter differentiation.

▼ Work through the solution

The radial measure is r^2dr, so after inserting R the general moment is $(24a^5)^{-1}\int_0^\infty r^{4-q}e^{-r/a}dr$ for r^{-q}. For $q=2$ the integral is $2a^3$, giving $1/(12a^2)$. For $q=3$ it is a^2, giving $1/(24a^3)$. Both agree with the formulas for $n=2, l=1$. Dropping the radial Jacobian would change both powers and could falsely suggest singular behaviour. The result is independent of m because the operator is rotationally scalar.

Calculate the complete $n = 2$ shifts in units of C_2

Resolve the kinetic, spin–orbit and Darwin contributions for $2s_{1/2}$, $2p_{1/2}$ and $2p_{3/2}$. Which comparison isolates the effect of the spin–orbit term cleanly at this order?

▼ **Work through the solution**

For s, kinetic gives $-[2 - 3/8] = -13/8$ and Darwin $+1$, summing to $-5/8$. For both p states the kinetic value is

$$-2/3 + 3/8 = -7/24.$$

The spin–orbit corrections are $2/3 - 1 = -1/3$ for $j = 1/2$ and $2/3 - 1/2 = 1/6$ for $j = 3/2$, giving $-5/8$ and $-1/8$. Subtracting the two p levels removes their shared kinetic term and zero contact term. Their interval is $C_2/2$. Comparing 2s with either p instead involves two different radial wavefunctions and does not isolate the same correction.

Separate a reduced-mass shift from fine structure

Consider two otherwise identical hydrogenic nuclei with $M/m = 1836$ and 3672. Predict the ratio of gross transition frequencies and compare its fractional change with the order of a fine-structure correction. Which common interpretation would conflate them?

▼ **Work through the solution**

Gross transition frequencies scale as reduced mass $\mu = m/(1 + m/M)$. The heavier-to-lighter ratio is $(1 + 1/1836)/(1 + 1/3672) = 1.000272$ approximately. The order of a relative fine-structure correction for $Z = 1$ is $\alpha^2 \simeq 5.3 \times 10^{-5}$ with state-dependent coefficients. A change of isotope can shift a gross line by more than a particular resolved fine splitting, even with identical nuclear charge. Centroid measurements across isotopes and intervals within one multiplet are distinct observables. Recoil and nuclear magnetism require further inputs for precision predictions.

Further reading

- Fließbach · Dreidimensionale Probleme
- Cambridge · hydrogen, helium and fine structure
- Course investigation · perturbations and level mixing

Quantum states, dynamics and measurement · 6. When a magnetic field changes the quantum numbers of an atom

Weak-field Zeeman slopes label total-angular-momentum multiplets. At stronger fields those slopes curve and intensities migrate. Solve an entire orbital-plus-spin manifold and infer coupling constants from measurable line positions and polarisation.

Choose the Hamiltonian appropriate to a resolved orbital manifold

Suppose an isolated atomic p manifold with $l = 1, s = 1/2$ is sufficiently far from other orbital or principal levels to treat only its six substates. Take z along a uniform external magnetic field B. Work to first order in the electronic Zeeman operator and model spin–orbit coupling by the constant $A > 0$. With $b = \mu_B B$ and electron spin factor approximated by two,

$$H = \frac{A}{\hbar^2}\mathbf{L}\cdot\mathbf{S} + \frac{b}{\hbar}(L_z + 2S_z).$$

Both A and b are energies. The sign of the second term is positive for the electron because magnetic moment is opposite to angular momentum and field energy is minus moment dot field. Here $\mu_B = e\hbar/(2m_e) > 0$. The orbital manifold approximation requires magnetic splittings small compared with gaps to omitted levels. Neglected terms can include the difference of the actual spin factor from two, hyperfine interactions and the diamagnetic B^2 term. An “intermediate field” in this discussion means b comparable to A; it need not exceed any other electronic binding scale.

At zero field the coupled levels $j = 1/2, 3/2$ have energies $-A, +A/2$. At nonzero field the projection $m = m_l + m_s$ is still conserved because $[H, J_z] = 0$. For intermediate fields J^2 need not commute with the Zeeman term. Consequently the six-state problem reduces to two one-dimensional and two two-dimensional invariant blocks, even when the label j loses its exact meaning. Following a state by magnetic quantum number and overlap with a neighbouring field value is generally more reliable than sorting all computed energies from low to high. Crossings of different m can reorder a sorted list without exchanging the underlying states.

Derive the Landé slope from angular momentum projection

In a state with definite j, l, s, m, expectation of any vector operator proportional in direction to $\mathbf{J}$ within its irreducible multiplet can be obtained from its scalar projection on $\mathbf{J}$. For spin,

$$\frac{\langle S_z\rangle}{\hbar} = m\,\frac{j(j+1) + s(s+1) - l(l+1)}{2j(j+1)}.$$

One way to obtain the projection numerator is $2\mathbf{S}\cdot\mathbf{J} = J^2 + S^2 - L^2$. Since $L_z + 2S_z = J_z + S_z$, the energy slope for weak fields is $dE/db = g_j m$ with $g_j = 1 + [j(j+1) + s(s+1) - l(l+1)]/[2j(j+1)]$. A state $j = 0$ has vanishing linear vector moment and should be treated separately instead of dividing by zero. Within the p manifold the $j = 1/2$ factor is $2/3$ and the $j = 3/2$ factor $4/3$. For $m = +1/2$ these correspond to slopes $1/3$ and $2/3$ in energy units of b. Their sum is exactly one, a trace constraint that remains valid for the sum of the two eigenvalues in that block at every field.

If $A/h = 8.00$ GHz as in the previous angular exercise, the zero-field interval is 12.00 GHz. At $B = 20.0$ mT, $b/h \simeq 0.280$ GHz using $\mu_B/h = 13.996$ GHz/T. The two positive-m shifts to linear order are $+0.0933$ and $+0.1866$ GHz. Actual optical frequencies measure final minus initial energies; an initial $s_{1/2}$ level has its own Zeeman slope. Omitting it is a common reason a slope inferred from a line scan seems inconsistent with the expected Landé factor.

Diagonalise the mixed levels across the entire crossover

In the $m = +1/2$ product basis $(|0,\uparrow\rangle, |1,\downarrow\rangle)$, expand $\mathbf{L}\cdot\mathbf{S} = L_zS_z + (L_+S_- + L_-S_+)/2$. The diagonal spin–orbit elements are $0, -A/2$; the off-diagonal element is $A/\sqrt{2}$. The Zeeman term is diagonal with entries $b, 0$. Hence

$$H_+(b) = \begin{pmatrix} b & A/\sqrt{2} \\ A/\sqrt{2} & -A/2 \end{pmatrix}, \qquad E_\pm(b) = \frac{b - A/2}{2} \pm \frac{1}{2}\sqrt{(b + A/2)^2 + 2A^2}.$$

At $b = 0$ the square root is $3A/2$, recovering the coupled levels. For the $m = -1/2$ basis $(|0,\downarrow\rangle, |-1,\uparrow\rangle)$, replace b by $-b$. The stretched levels $|1,\uparrow\rangle$ and $|{-1},\downarrow\rangle$ remain product states at every field with energies $A/2 \pm 2b$. Counting all levels and their traces provides an independent check: spin–orbit and Zeeman each have zero trace in the full six-dimensional space. At zero field both slopes in the $+$ block are finite and positive. At large positive b the upper slope tends to one and the lower to zero, approaching their uncoupled product labels.

In the negative-m block the two uncoupled energies would cross at $b = A/2$. The coupling opens a minimum gap $\sqrt{2}A$. Within the model, levels of the same m avoid one another whenever this matrix element is nonzero. Crossings between different m can remain exact because the uniform z-directed Hamiltonian does not mix them. A tilted perturbation could turn some of these into avoided crossings. Such symmetry dependence matters when trying to infer a coupling from the smallest visible distance between any two lines.

Obtain an eigenvector weight from an energy derivative

Suppose an initial s state has spin up. A weak $q = 0$ electric-dipole drive prepares the product basis state $|0,\uparrow\rangle$ in the $m = +1/2$ block. Its squared overlap with an exact eigenstate determines the angular part of that optical line's strength. Rather than computing a mixing angle with a branch ambiguity, differentiate the exact energies. Since $\partial H_+/\partial b = |0,\uparrow\rangle\langle 0,\uparrow|$, the eigenvalue derivative equals precisely that population:

$$w_\pm = \frac{dE_\pm}{db} = \frac{1}{2}\left[1 \pm \frac{b + A/2}{\sqrt{(b + A/2)^2 + 2A^2}}\right].$$

The weights sum to one as required by completeness. At zero field they are $2/3$ and $1/3$. At large positive field the upper line takes almost all this polarisation strength. In the negative block an analogous derivative with respect to $-b$ gives the population of $|0,\downarrow\rangle$. At its avoided crossing each eigenstate has equal weights and the two corresponding $q = 0$ intensities are equal for a selected initial spin down. The same experiment can test slopes measured from frequencies and overlaps measured through intensities, provided detection and radial coupling are common to both lines.

Set $b = A$ in the positive block. The level separation becomes $A\sqrt{4.25} = 2.06155A$, while the upper product weight is 0.8638. A naive extrapolation of the weak-field $g_j m$ slopes would give an interval $1.5A + A/3 = 1.833A$. The discrepancy is governed by the spin–orbit mixing scale rather than failure of the magnetic Hamiltonian itself. If the frequency analyser resolves only a single intensity-weighted centroid, completeness still constrains the first moment:

$$\sum_{\pm} w_{\pm} E_{\pm} = \langle 0, \uparrow | H_{+} | 0, \uparrow \rangle = b.$$

Thus the centroid of unresolved lines in this ideal selected excitation can move linearly even while each constituent bends.

Resolve a second angular-momentum hierarchy with the same algebra

The p-manifold example coupled orbital and electronic spin. In an s-state atom the dominant remaining weak angular coupling may be between an electronic $J = 1/2$ and a nuclear $I = 1/2$. This is a different scale and a different physical pair of degrees of freedom. To illustrate how a state label changes with field, take

$$H = \frac{A_h}{\hbar^2} \mathbf{I} \cdot \mathbf{J} + \frac{B}{\hbar} (g_J \mu_B J_z - g_I \mu_N I_z)$$

with positive hyperfine constant A_h and a positive model nuclear g_I. The minus before the nuclear-magneton term reflects the assumed positive nuclear magnetic moment. Actual sign and g-factor depend on the isotope. Here both A_h and the products of magnetic moments and field have energy units. At zero field the electronic and nuclear angular momenta combine to $F = 0, 1$. Their scalar-product shifts are $-3A_h/4$ and $+A_h/4$, respectively. A rotation of the entire coupled system leaves this zero-field Hamiltonian invariant, but independent rotations of just one constituent generally do not.

Within $m_F = 0$ order the product basis by electronic magnetic sign as $|\uparrow_J, \downarrow_I\rangle, |\downarrow_J, \uparrow_I\rangle$. Both diagonal hyperfine matrix elements are $-A_h/4$, off-diagonal exchange is $A_h/2$, and field changes the diagonal difference by $\delta = (g_J \mu_B + g_I \mu_N) B$. Hence the central pair of energies is

$$E_{\pm} = -A_h/4 \pm \tfrac{1}{2} \sqrt{A_h^2 + \delta^2}.$$

The two stretched $m_F = \pm 1$ levels sit at $+A_h/4 \pm (g_J \mu_B - g_I \mu_N) B/2$. Their slopes contain a difference of electronic and nuclear moments, while the central splitting depends on their sum. This sign distinction can be determined directly by comparing the relevant product states: in the anti-aligned pair the sign change reverses one angular momentum along with its opposite magnetic sign. A sign convention imported from electron spin alone would give an erroneous nuclear contribution.

The transition between the two central states has gap $\sqrt{A_h^2 + \delta^2}$ and zero linear slope at $B = 0$. Its quadratic shift is $\delta^2/(2A_h)$ for $|\delta| \ll A_h$. Measuring at a point with zero first derivative reduces sensitivity to slow field fluctuations without eliminating it. Suppose $A_h/h = 1.00$ GHz and $(g_J \mu_B + g_I \mu_N)/h = 28.0$ GHz/T in an illustrative species model. At a 1.0 mT bias the central gap rises by about 0.392 MHz. A 1 µT field error at that bias gives a first-order frequency error of about 784 Hz using the derivative of the quadratic

expansion. At zero mean bias, fluctuations with rms 1 μT instead give an average quadratic shift about 0.392 Hz. Stabilising the field mean and reducing its variance address different terms in the measured spectral position.

The magnetic drive operator for a small oscillating field along z is itself proportional in this block to σ_z. At zero bias the hyperfine eigenstates are the symmetric and antisymmetric superpositions, so this drive couples them off-diagonally despite the central transition frequency being stationary against a small static bias. The diagonal derivative and the off-diagonal transition matrix element are distinct quantities. At large bias the eigenstates approach product states and the same longitudinal drive becomes mostly diagonal, reducing its ability to flip between them. Thus a transition can have both a vanishing first-order shift and a nonzero resonant driving strength, consistent with the same Hamiltonian. Measuring both properties probes the field dependence of eigenvectors as well as eigenvalues.

Infer a field distribution from widths and centres

Spectra of spatially extended samples often contain a distribution of static magnetic fields. Consider a single weak-field transition with frequency $\nu(B) = \nu_0 + sB$, an intrinsic Gaussian line standard deviation w_0, and a sample field distributed approximately Gaussian with mean B_0 and standard deviation σ_B. A sum over independent source regions convolves the intrinsic line with the frequency distribution generated by sB. The observed centre is $\nu_0 + sB_0$, and variance is $w_0^2 + s^2\sigma_B^2$. A single linewidth cannot determine both an intrinsic width and a field inhomogeneity. Two lines with different known magnetic slopes or one calibrated zero-slope reference can separate the contributions.

For example two transitions with slopes 7.0 and 14.0 GHz/T have measured standard deviations 0.250 and 0.400 MHz. Subtract the squared widths to eliminate w_0^2:

$$\sigma_B^2 = \frac{(0.400)^2 - (0.250)^2}{(14000)^2 - (7000)^2}\ \mathrm{T}^2,$$

using MHz/T in the denominator. The result is $\sigma_B = 25.8\,\mu\mathrm{T}$, and the inferred intrinsic width is

$$\sqrt{0.250^2 - (7000\sigma_B)^2} = 0.173\,\mathrm{MHz}.$$

A third line with slope near zero supplies an out-of-sample check. If lines have significantly different lifetimes or power broadening, the assumption of a common w_0 should be relaxed; otherwise one can spuriously infer a magnetic gradient or even a negative intrinsic variance.

For a curved avoided-crossing line expand $\nu(B) \simeq \nu(B_0) + s(B - B_0) + q(B - B_0)^2/2$. A symmetric distribution shifts the measured mean by $q\sigma_B^2/2$ even when the mean field is known exactly. Near a stationary point the leading field broadening can be strongly asymmetric because a squared Gaussian variable has a one-sided distribution around its minimum. Fitting a symmetric line at such a point can shift its apparent peak or centre according to the fitting convention. This effect is especially relevant when locating a minimum gap from spectra at several nominal fields. A model integrating intensities over a measured spatial field distribution can be better constrained than independent fits of Gaussian centres, because all lines share the same underlying field profile.

An independent geometric test tilts the weak sensing light relative to the magnetic axis. For equal populations, a truly scalar average over all polarisations and emitted directions is insensitive to this coordinate change, but a selected q transition changes strength according to the decomposition of the laboratory polarisation. If a peak attributed to frequency splitting mainly changes its fitted centre while unresolved component intensities redistribute, some of its apparent shift may be an intensity-weighted centroid effect. Record spectra at two orthogonal polarisations, fit the same physical energy parameters and allow the predicted angular strengths to vary. A common energy correction that survives the intensity change carries a different interpretation from a change in the mixture of unresolved substates.

Predict state transfer during a field sweep

The negative-m avoided crossing of the p manifold also poses a time-dependent question. Does a changing field keep the atom in the instantaneous energy eigenstate, or in approximately the same product state? In the local two-state description subtract the trace and write $H = (\Delta(t)/2)\sigma_z + g\sigma_x$, where the difference of diabatic diagonal energies is Δ and the minimal adiabatic gap is $2|g|$. Introduce a mixing angle $\tan(2\vartheta) = 2g/\Delta$, chosen continuously through the crossing. Differentiating at fixed g gives

$$|\dot{\vartheta}| = |g\dot{\Delta}|/(\Delta^2 + 4g^2).$$

The moving eigenbasis itself couples the two instantaneous energy states with an energy scale $\hbar|\dot{\vartheta}|$.

At closest approach the order-of-magnitude adiabatic criterion becomes $\hbar|\dot{\Delta}|/(8g^2) \ll 1$. A slow sweep keeps occupation on an energy branch, which changes its product character across the avoided crossing. A fast sweep can leave the original product state approximately unchanged, moving population from one instantaneous energy branch to the other. Both descriptions refer to actual state transfer; the basis in which “remaining in the same state” is assessed is part of the observable. The criterion here follows directly by comparing the nonadiabatic derivative coupling with the instantaneous level separation. It estimates a regime but does not by itself give a transition probability.

For a strictly linear detuning passing from large negative to large positive values with constant g, the Landau–Zener result gives the diabatic survival probability $P_D = \exp[-2\pi g^2/(\hbar|\dot{\Delta}|)]$. Its applicability requires asymptotic start and end detunings well outside the coupling region, coherent passage and the indicated linearity over the crossing. In ordinary-frequency units take $g/h = 20$ kHz and $|d(\Delta/h)/dt| = 1.0 \times 10^{10}\ \mathrm{Hz/s}$. The exponent is $4\pi^2(2.0 \times 10^4)^2/10^{10} = 1.58$, giving $P_D \simeq 0.206$. Doubling the sweep rate halves the exponent and raises survival to about 0.454. Confusing angular with ordinary frequency in this conversion loses a factor 2π, large enough to change the predicted population qualitatively.

A double sweep forms a useful control. On entering and later leaving the avoided crossing, the two amplitudes propagated along different energy branches can accumulate different phases and interfere. Treating the two passages as independent classical jumps would miss oscillations versus waiting time between them. Strong dephasing or averaging over a broad field distribution can remove the oscillations while retaining the one-pass populations. Distinguish these mechanisms by calibrating single-passage transfer first and then varying the waiting time over several periods at multiple sweep speeds. This extends a static magnetospectroscopy model to a specified dynamical experiment without inferring the full time dependence from a static level diagram alone.

Resolve the crossover from coupled to uncoupled angular momenta

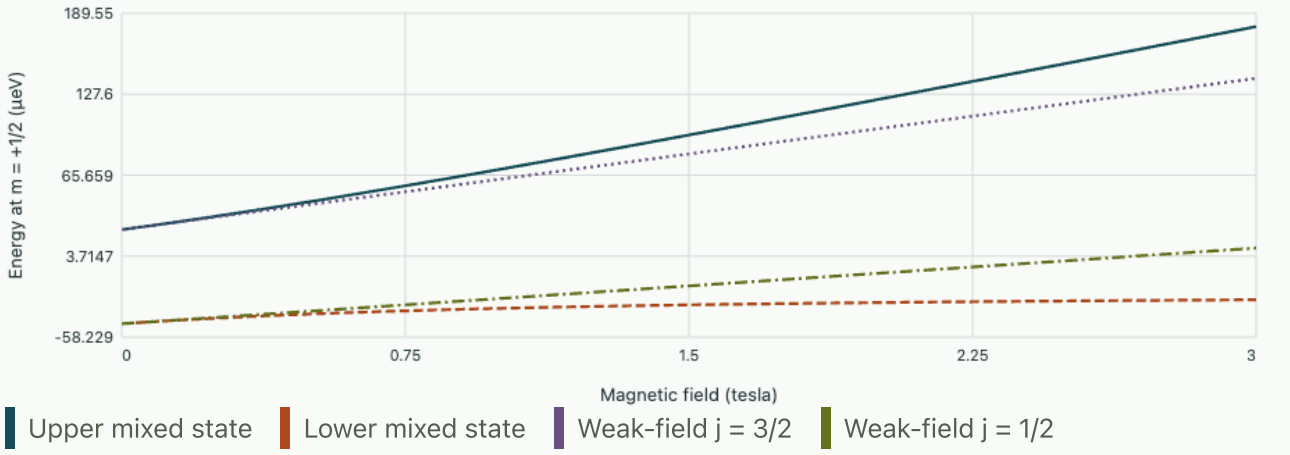
Scan the magnetic field across the spin–orbit scale. Compare the exact two-state spectrum at fixed magnetic quantum number with the weak-field shifts.

Open this experiment online

Try the calculation

Spin–orbit coefficient A (μeV) **48**

Selected magnetic field (T) **0.6**



Selected energies -39.516 and 50.246 μeV. The ratio μB B/A is 0.72355.

Test the orientation of a magnetic sensor from resolved spin populations

The scalar energy spectrum of an isotropic spin-$1/2$ Zeeman Hamiltonian measures field magnitude. A transition energy by itself cannot determine the signed orientation of that field. Let $H = \hbar\gamma\mathbf{B}\cdot\boldsymbol{\sigma}/2$, with signed angular gyromagnetic ratio γ defined in the experiment. Its eigenvalues are $\pm\hbar|\gamma||\mathbf{B}|/2$. If instead one prepares spin up along a known laboratory z direction and observes its population after evolution time t, the rotation axis appears in the dynamics. Exponentiating $U = \cos(\omega t/2)I - i\sin(\omega t/2)\hat{\mathbf{B}}\cdot\boldsymbol{\sigma}$ for a consistent choice of $\omega, \hat{\mathbf{B}}$ gives

$$P_{\downarrow z}(t) = (1 - \hat{B}_z^2)\sin^2(\gamma|\mathbf{B}|t/2).$$

The oscillation frequency gives magnitude and its contrast gives the squared transverse fraction. It is insensitive to whether the field points slightly above or below a perpendicular plane. Incomplete preparation or pulse contrast can also reduce the observed oscillation amplitude. A calibration with a known transverse field tests that ambiguity before assigning every missing contrast to geometric tilt.

Suppose a resolved precession has angular frequency corresponding to 0.50 mT and a calibrated flip contrast of 0.36 for initial $+z$. Then $\sqrt{B_x^2 + B_y^2} = 0.30$ mT and $|B_z| = 0.40$ mT. Repeating for an initial $+x$ state with

calibrated contrast 0.64 yields $|B_x| = 0.30$ mT and thus $B_y = 0$ for these numbers. Neither experiment identifies the signs of B_x and B_z. To resolve them one can measure an early-time transverse quadrature with a phase reference. In Bloch notation $\dot{\mathbf{r}} = \gamma \mathbf{B} \times \mathbf{r}$, so the initially zero slope $\dot{r}_y = -\gamma B_x$ for $+z$ is sign sensitive. This derivative is independent of B_z at the initial instant, giving a direct check complementary to the energy splitting.

A second strategy adds a calibrated bias $\mathbf{b}_0$ in opposite directions and examines squared frequencies. Since $|\mathbf{B} + \mathbf{b}_0|^2 - |\mathbf{B} - \mathbf{b}_0|^2 = 4\mathbf{B} \cdot \mathbf{b}_0$, the difference isolates a signed projection even when the zero-field splitting reveals only magnitude. For a 0.20 mT known bias along z and a 0.40 mT signed z component the squared-field difference should be $0.32\,\mathrm{mT}^2$. Alternating the two bias signs across the measurement reduces slow field drift. A quadratic diamagnetic response, anisotropic g tensor or an uncalibrated bias axis can break this simple inversion; repeating in three independent directions tests the vector model and reveals which assumptions are being used.

Separate an anisotropic magnetic response from an unknown field direction

A crystal-fixed effective spin has diagonal $g = \mathrm{diag}(2.0, 2.0, 2.4)$. Derive the transition energy for a field rotated in the x, z plane by angle θ from z, and explain what an isotropic fit would infer.

▼ **Derive and check the result**

The Hamiltonian is $\mu_B \boldsymbol{\sigma} \cdot (g\mathbf{B})/2$. The splitting is $\mu_B B \sqrt{2.0^2 \sin^2\theta + 2.4^2 \cos^2\theta}$. At 45° the effective g is $\sqrt{4.88} = 2.209$; interpreting the measured splitting with constant $g = 2$ would overestimate field magnitude by about 10.5%. The spin also precesses around the effective axis $g\mathbf{B}$, whose polar angle satisfies

$$\tan\theta_{\mathrm{eff}} = (2.0/2.4)\tan\theta.$$

Measuring contrast from a calibrated spin preparation and rotating a field of known magnitude can therefore distinguish material anisotropy from a simple error in magnet alignment. One scalar spectral line at an unknown orientation cannot separate these effects.

Tutorial · reconstruct a magnetically mixed spectrum

Infer the coupling from an anticrossing

The two negative-m lines exhibit a minimum frequency separation of 11.31 GHz at 0.286 T. Infer A/h from each measurement. What calibration would be needed for a comparison of absolute optical line frequencies?

▼ **Work through the solution**

Minimum gap divided by h equals $\sqrt{2}A/h$, giving $A/h = 8.00$ GHz. The crossing condition $b = A/2$ gives

$$A/h = 2(13.996)(0.286) = 8.01\,\mathrm{GHz}.$$

Their agreement checks field calibration independently of a common frequency reference. Both final states must be viewed from the same initial state when using their frequency difference. Comparing absolute optical

frequencies also requires the zero-field transition energy and the field-dependent initial-level shift. Two lines originating in different initial states would have a field-dependent separation even if their final levels had a fixed interval.

Extract the polarisation weight using a finite difference

Near $b = A$, estimate the slope of the upper positive-m level using its exact values at $b/A = 0.95, 1.05$. Compare with the exact weight and predict the second line's strength.

▼ **Work through the solution**

In units of A the upper level is $(t - 0.5 + \sqrt{(t+0.5)^2 + 2})/2$ with $t = b/A$. Subtracting the values and dividing by 0.10 gives about 0.864. The analytical derivative is

$$[1 + 1.5/\sqrt{4.25}]/2 = 0.8638.$$

The second line carries 0.1362 of the total angular strength. Halving the centred step should reduce the derivative's truncation error by about four for this smooth curve. In an experiment frequency noise per point is instead amplified as inverse step. Compare several field steps to establish a practical slope uncertainty.

Use an unresolved centroid to detect a calibration problem

At $b = A$ a weak $q = 0$ experiment driven from a selected spin-up preparation records both positive-m final states. Its excitation-weighted centroid after restoring the initial-state energy is $0.78A$. Could the exact two-level mixing alone produce that centroid?

▼ **Work through the solution**

The sum rule requires $b = A$. Direct calculation gives energies approximately $1.2808A$ and $-0.7808A$; weights 0.8638 and 0.1362 give $1.000A$ within rounding. In this model mixing alone cannot explain $0.78A$. A missing weak line, saturation, polarisation contamination, different collected fluorescence efficiencies or a mistaken correction for the initial state can shift a measured centroid. Compare both individual integrated line areas at low intensity and reverse the field with the corresponding spin preparation. These tests use distinct symmetry and strength predictions rather than interpreting one centroid as a complete spectrum.

Further reading

- Cambridge · magnetic fields, Zeeman structures and optical transitions
- Course investigation · angular momentum and atoms
- Fließbach · Näherungsmethoden

Quantum states, dynamics and measurement · 7. Two electrons, exchange splitting and the cost of localisation

Build a two-electron state that respects exchange, derive its charge and spin correlations, and then solve a two-site model exactly. The two examples reveal when a triplet is favoured and when an apparently weak hopping lowers the singlet instead.

Construct states before introducing a force

A two-electron wavefunction has two spatial arguments and two spin labels. The labels 1 and 2 identify argument slots; they do not attach persistent tags to individual identical electrons. Exchanging all position and spin variables must multiply an electronic state by minus one. This is the fermionic exchange postulate. It constrains which vectors describe electrons even when their Hamiltonian contains no spin-dependent term. A measurement with no access to the ordering of slots is represented by an observable symmetric under the same exchange.

Let $a(\mathbf{r}), b(\mathbf{r})$ be normalised orthogonal spatial orbitals. The symmetric and antisymmetric spatial combinations are $\Phi_\pm = [a(1)b(2) \pm b(1)a(2)]/\sqrt{2}$. Combine Φ_+ with the spin singlet $(|\uparrow\downarrow\rangle - |\downarrow\uparrow\rangle)/\sqrt{2}$, and Φ_- with any of the three symmetric triplet spin states. For equal positions the antisymmetric spatial combination vanishes exactly. Its joint probability has an exchange hole at coincidence even for noninteracting same-spin fermions. When $a = b$, the antisymmetric combination vanishes identically and only the symmetric spatial state with opposite spins in a singlet is available. Occupation of the same spatial mode by two electrons is thus compatible with the exclusion principle if the full spin orbitals differ.

For two distinct orthogonal modes, both Φ_+ and Φ_- have the same one-particle number density $|a(\mathbf{r})|^2 + |b(\mathbf{r})|^2$, normalised to two electrons. To see this, integrate $|\Phi_\pm(\mathbf{r}_1, \mathbf{r}_2)|^2$ over $\mathbf{r}_2$ and multiply by two. Cross terms contain $\langle a|b\rangle = 0$. Coincidence and correlation measurements can therefore distinguish preparations that share their entire one-particle density. The spin-antisymmetric singlet can also give correlated opposite spin outcomes along any common measurement axis, while both individual spins are unpolarised. Position and spin comparisons probe different reduced descriptions of the same total state.

Separate the direct and exchange integrals

For an independent-orbital estimate take $H = h(1) + h(2) + v(1,2)$ with $ha = \epsilon_a a,\ hb = \epsilon_b b$, and a symmetric spin-independent repulsion. Expand the expectation of v in $\Phi_\pm$. Diagonal terms give the same direct integral and off-diagonal terms are conjugates:

$$J_{ab} = \iint |a(1)|^2 v(1,2) |b(2)|^2 \, d^3r_1 d^3r_2,$$

$$K_{ab} = \iint a^*(1) b(1) v(1,2) b^*(2) a(2) \, d^3r_1 d^3r_2.$$

For Coulomb repulsion K_{ab} is nonnegative: it is the positive Coulomb quadratic form of the transition density a^*b, seen for instance from its Fourier representation weighted by $4\pi/k^2$. Orthonormality only makes the spatial integral of the transition density vanish, not its weighted self-interaction. The expectation energies are $\epsilon_a + \epsilon_b + J_{ab} \pm K_{ab}$. In this fixed pair of spatial orbitals the triplet is lower by $2K_{ab}$. If the orbitals have

disjoint support the exchange integral vanishes, although the direct repulsion need not. A splitting caused by spatial symmetry does not require an extra microscopic spin–spin repulsive force.

Set $J_{ab} = 0.80$ eV and $K_{ab} = 0.070$ eV in an illustrative excited configuration. Its Coulomb shifts are 0.87 eV and 0.73 eV. A weighted average over all four spin states is

$$J - K/2 = 0.765\,\mathrm{eV}.$$

Optical line strengths generally do not populate those four spin states equally. The energy difference is a statement about this restricted configuration; another spatial occupation can place a singlet below the entire triplet manifold. Predicting a ground-state spin therefore requires admitting the competing occupations and the one-body and correlation energies they carry.

Allow hopping and double occupation

Now take two orthonormal localised orbitals L, R of equal one-body energy. A fermion hops between them at amplitude $-t$, and placing opposite spins on the same site costs $U > 0$. Define $H = -t\sum_\sigma (c^\dagger_{L\sigma}c_{R\sigma} + c^\dagger_{R\sigma}c_{L\sigma}) + U\sum_i n_{i\uparrow}n_{i\downarrow}$. This is a specified two-site Hubbard model, not a complete microscopic Coulomb Hamiltonian. Its direct intersite exchange integral is set to zero here, so its spin ordering need not follow the fixed-orbital calculation above. Position, spin and field units enter through the experimentally or computationally determined t, U.

In the two-electron sector a state with two up spins must occupy one orbital on each site. Hopping would create two up spins in one orbital and therefore annihilates this state. Rotational symmetry implies the same energy zero for all three triplets. Define the singly occupied singlet $|S\rangle$ and symmetric doubly occupied state $|D_+\rangle = (|\uparrow\downarrow, 0\rangle + |0, \uparrow\downarrow\rangle)/\sqrt{2}$. A consistent fermionic ordering gives an off-diagonal $-2t$ between them; each direction and spin contributes and the normalisations leave the factor two. Changing the phase of D_+ reverses that matrix element but leaves the eigenvalues unchanged. The orthogonal antisymmetric doublon remains at energy U. The relevant singlet block is

$$H_S = \begin{pmatrix} 0 & -2t \\ -2t & U \end{pmatrix}, \qquad E_\pm = \frac{U \pm \sqrt{U^2 + 16t^2}}{2}.$$

The ground energy $E_- < 0$ for $t \neq 0$. At $U \gg |t|$ expand the square root to obtain

$$E_- \simeq -4t^2/U + 16t^4/U^3 + \cdots.$$

The singlet–triplet splitting $J_{\mathrm{eff}} = E_T - E_- \simeq 4t^2/U$ can be represented in the singly occupied subspace by $J_{\mathrm{eff}}(\mathbf{S}_L \cdot \mathbf{S}_R/\hbar^2 - 1/4)$. The singlet can lower its energy by virtual double occupation while spin symmetry blocks the triplets. The inferred spin coupling scales as the square of hopping and inversely with the energy cost. This mechanism is commonly called antiferromagnetic superexchange.

Determine a correlation without reading an eigenvector

The fraction of probability with double occupation in the ground state is $\langle \partial H/\partial U \rangle$. Differentiating its energy gives

$$D = \tfrac{1}{2}[1 - U/\sqrt{U^2 + 16t^2}].$$

For positive large U, $D \simeq 4t^2/U^2$. Comparing the derivative with the explicit eigenvector provides a useful independent test of signs and normalisations. From $Es = -2td$ one obtains

$$d/s = -E/(2t).$$

Normalising gives $D = E^2/(4t^2 + E^2)$, identical to the derivative expression for either lower-branch parameter value.

For $t = 10$ meV and $U = 100$ meV, $\sqrt{U^2 + 16t^2} = 107.70$ meV and the exact splitting is 3.85 meV. The leading 4.00 meV expression is about 3.9% high. Double occupation is only 3.58%, yet forbidding it at the outset would predict exactly zero splitting. A virtually occupied state can matter appreciably in a low-energy Hamiltonian even when a projective charge measurement rarely finds it occupied. At $U = 0$ the ground energy is $-2|t|$, corresponding to two opposite spins in the bonding one-electron orbital; the double-occupation fraction is one half. The large-U expression diverges as $U \to 0$ because its perturbative premise disappears. The exact two-state matrix remains finite.

Derive an effective screening charge for a helium-like ground state

A two-electron atom provides a continuous-space counterpart to the two-site model. In atomic units set $\hbar = m_e = e^2/(4\pi\epsilon_0) = 1$ and take an infinitely heavy nucleus of charge Z. The nonrelativistic Hamiltonian is

$$H = \sum_{i=1}^{2}[-\nabla_i^2/2 - Z/r_i] + 1/r_{12}.$$

The two one-electron ground orbitals may be identical in space because opposite spins can form an antisymmetric singlet. Use a trial product of two normalised hydrogenic functions $u_\zeta(\mathbf{r}) = (\zeta^3/\pi)^{1/2}e^{-\zeta r}$ with a variable positive exponent ζ. This single parameter lets the spatial cloud expand in response to mutual repulsion. Choosing the exponent equal to Z without testing it would impose the noninteracting size on an interacting problem.

A single orbital gives $\langle -\nabla^2/2\rangle = \zeta^2/2$ and $\langle 1/r\rangle = \zeta$, either by direct integration or by hydrogenic scaling. Two electrons thus contribute $\zeta^2 - 2Z\zeta$ to the expectation. To derive the repulsion term, average $1/|\mathbf{r}_1 - \mathbf{r}_2|$ over two independent uniform angles at fixed radii. Gauss's shell result, or a direct change of variable in the angular integral, gives $1/\max(r_1, r_2)$. The radial probability is

$$P(r) = 4\zeta^3 r^2 e^{-2\zeta r}.$$

Symmetry between the two electron labels permits restricting one integral to $r_2 < r_1$, then doubling:

$$J = 2\int_0^\infty \frac{P(r)}{r}\,dr \int_0^r P(s)\,ds,$$

$$\int_0^r P(s)ds = 1 - e^{-2\zeta r}(1 + 2\zeta r + 2\zeta^2 r^2).$$

The first part of the resulting r integral gives 2ζ. The three exponential subtraction terms sum to $11\zeta/8$, leaving $J = 5\zeta/8$. Their evaluation uses $\int_0^\infty r^n e^{-ar}dr = n!/a^{n+1}$. Both the dependence linear in ζ and the positive sign follow from scaling an inverse-distance repulsion; only the numerical coefficient needed the angular and radial integration. Replacing the expectation of $1/r_{12}$ by $1/\langle r_{12}\rangle$ would generally give a different coefficient because inverse distance is nonlinear.

Consequently $E(\zeta) = \zeta^2 - 2(Z - 5/16)\zeta$ is an upper bound on the ground energy. It minimises at $\zeta_* = Z - 5/16$, with $E_{\mathrm{var}} = -(Z - 5/16)^2$ hartree for positive ζ_*. For helium $Z = 2$, $\zeta_* = 1.6875$, giving -2.84766 hartree, compared with -2.75 hartree at $\zeta = 2$. The one-electron ion has energy -2 hartree, so this variational value lies below the threshold for an electron plus the ion and demonstrates binding within the model. The trial ionisation energy 0.84766 hartree is a lower bound on the exact ionisation energy when that threshold is known exactly. An upper bound on the neutral energy gives a lower bound on the energy required to remove an electron.

The interpretation of $5/16$ as a screening correction is limited. At short radii each electron feels nearly the full nuclear singularity, while far outside it sees the remaining net charge. One constant exponent cannot reproduce both limits and cannot describe how the two electron positions avoid one another at fixed one-particle radius. The product trial permits nonzero joint weight at electron coincidence. Multiplying by a factor involving r_{12} introduces genuine correlation beyond independent orbitals. Optimising a broader variational family containing this product can only lower or retain the variational energy, provided its integrals and normalisation are computed consistently. Monitoring energy together with the pair-separation distribution tests whether the enlargement captures the physics of repulsion rather than merely adjusting a one-body radius.

Infer a local two-electron boundary condition from the Coulomb singularity

Near coincidence of two unlike-spin electrons, the Coulomb repulsion diverges like $1/r_{12}$. The wavefunction itself can remain finite at coincidence, but its derivative must cancel this singularity in the Schrödinger equation. Consider a fixed smooth centre coordinate and average the wavefunction over the direction of the interelectron separation r, away from simultaneous nuclear coincidence. Assume an expansion $\bar{\Psi}(r) = A + Br + \cdots$. In atomic units the reduced mass is one half, so the relative spherical kinetic operator is $-[d^2/dr^2 + (2/r)d/dr]$ for the locally s-wave part. Its leading singular term is $-2B/r$. Adding $\bar{\Psi}/r$ gives coefficient $A - 2B$ of $1/r$. A finite energy eigenvalue requires this coefficient to vanish:

$$\left.\frac{d\bar{\Psi}}{dr}\right|_0 = \frac{1}{2}\,\bar{\Psi}(0).$$

The positive cusp slope means the spatial amplitude rises as the electrons move apart from contact, consistent with repulsion. The corresponding electron–nucleus cusp has opposite sign and coefficient set by the nuclear charge and reduced mass. In a same-spin state the scalar contact amplitude vanishes by

antisymmetry; this s-wave formula becomes $0 = 0$ and a leading higher-partial-wave analysis is needed. Forgetting either angular averaging or exchange symmetry can turn an instructive local condition into a false statement about every directional derivative of every wavefunction.

A product of independent $1s$ orbitals is smooth in r_{12} at a generic fixed centre and has no required linear cusp in the spherical average. A trial factor $1 + r_{12}/2$ in atomic units can impose the first-order unlike-spin cusp while leaving additional variational freedom to model long-range behaviour. Merely enforcing the cusp does not solve the entire two-electron problem. It constrains a local ratio of derivative to value, while energy depends on a six-dimensional integral. In variational Monte Carlo one can diagnose this distinction through the local energy $H\Psi/\Psi$ near coincidence. A cusp-mismatched trial may have a singular local energy even though the volume element $r^2 dr$ keeps its integrated average finite. Imposing the cusp can reduce variance and improve short-distance pair observables more dramatically than it changes the energy expectation.

Use one-body occupation measurements to detect missing correlations

A single determinant of orthonormal spin orbitals χ_i has a one-particle reduced density matrix $\gamma = \sum_{\text{occupied}} |\chi_i\rangle\langle\chi_i|$, normalised to the electron number N_e. Thus $\gamma^2 = \gamma$ and its eigenvalues are zero or one. This is an algebraic signature of a single pure Slater determinant in the spin-orbital convention. For a correlated pure fermion state, natural occupations can become fractional while remaining between zero and one and summing to N_e. Ensemble mixing can produce fractional occupations too, so knowing whether the entire state is pure matters if one wants to interpret fractional one-particle populations as evidence of correlation.

Consider the normalised two-electron singlet $|\Psi\rangle = \sqrt{0.8}\,|a\uparrow, a\downarrow\rangle + \sqrt{0.2}\,|b\uparrow, b\downarrow\rangle$, with each ket a determinant. A one-body operator changes at most one occupied spin orbital, so its matrix element between these two doubly different determinants vanishes. The four natural spin-orbital occupations are $0.8, 0.8, 0.2, 0.2$. Their sum is two while $\operatorname{tr}\gamma^2 = 1.36$, smaller than the determinant value two. An incoherent mixture of the two determinants at the same weights has the same one-body matrix, although it no longer has their joint coherence. A two-body pair-transfer operator that converts both a electrons into b electrons, plus its adjoint, can reveal a relative phase between these branches. Thus a complete one-body spectrum still need not determine a two-body state.

The symmetric Hubbard dimer ground state has another direct relation between energy derivatives and its one-body coherence. Let $T = \sum_\sigma (c^\dagger_{L\sigma} c_{R\sigma} + c^\dagger_{R\sigma} c_{L\sigma})$. The energy derivative gives

$$\langle T\rangle = -\partial E_-/\partial t = 8t/\sqrt{U^2 + 16t^2}.$$

At $U = 0$ and $t > 0$, $\langle T\rangle = 2$ because both electrons occupy the bonding orbital. At large U/t this coherence approaches zero even though the exact finite-t ground state remains a total spin singlet. In the bonding/antibonding spatial basis, the sum of both populations is two and their difference is $\langle T\rangle$. For the example $U = 100,\ t = 10$ meV this gives spatial occupations roughly 1.371 and 0.629. Dividing by two gives the spin-orbital occupations for each spin in this singlet. Site populations alone are one on each site by symmetry at every U/t; their apparent constancy completely misses this changing form of correlation.

Break site symmetry and measure the onset of charge transfer

Add a static site-energy imbalance with energies $-\Delta/2$ on L and $+\Delta/2$ on R. The singly occupied configuration still has total site energy zero, while double occupations cost $U-\Delta$ and $U+\Delta$. For $|t| \ll U - |\Delta|$ the singly occupied singlet gains the second-order shift $-2t^2/(U-\Delta) - 2t^2/(U+\Delta)$, since its matrix element to either double occupation has magnitude $\sqrt{2}|t|$. The triplets remain blocked. The effective exchange splitting is $4t^2U/(U^2-\Delta^2)$. At zero imbalance it reduces to the earlier $4t^2/U$; small imbalance changes it quadratically, consistent with exchanging left and right sites.

For $U = 100,\ t = 5,\ \Delta = 40$ meV, the estimate gives 1.19 meV compared with 1.00 meV at zero bias. Increasing imbalance can make one virtual double occupation especially inexpensive, changing the gap before the mean site charge substantially relocates. Near $\Delta = U$ the denominator vanishes and the perturbative model predicts a divergence. The true three-state singlet matrix instead has an avoided crossing of singly and doubly occupied configurations. A sweep through that region should retain both double occupations and compute site charge from $-2\,\partial E/\partial\Delta$, with the sign matched to the specified imbalance. Here an apparent runaway effective spin coupling marks the failure of eliminating charge degrees of freedom, rather than an arbitrarily large spin energy in the actual finite Hamiltonian.

Measure singlet–triplet exchange without a spin force

Change the on-site repulsion in a two-electron dimer. Check whether exchange inferred from the spectrum follows the virtual-hopping estimate.

Open this experiment online

Try the calculation

On-site energy U (meV) **6**

Hopping t (meV) **1**



Triplet energy 0. Lower singlet energy -0.60555 meV. Estimated gap 4t²/U = 0.66667 meV.

See exchange interference directly in a two-port experiment

A lossless balanced beam splitter for two orthonormal single-particle modes can be chosen to act on creation operators as $a^\dagger \to (c^\dagger + d^\dagger)/\sqrt{2},\ b^\dagger \to (c^\dagger - d^\dagger)/\sqrt{2}$. Bring two identical particles to the device, one per input, with wave-packet timing and internal states controlled. The input $a^\dagger b^\dagger|0\rangle$ contains no explicit interaction. Nevertheless the coincidence statistics after the device depend on exchange because two paths can lead to the same unordered output configuration. This provides a way to test exchange far from the Coulomb energy calculations of the previous sections.

For identical spinless bosons multiply the two sums and use commuting creation operators. The cross terms cancel, leaving $[(c^\dagger)^2 - (d^\dagger)^2]|0\rangle/2 = (|2,0\rangle - |0,2\rangle)/\sqrt{2}$. Both particles leave the same port and coincidence probability vanishes. The $\sqrt{2}$ in a normalised doubly occupied Fock state is essential. For identical fermions in the same internal state the repeated creation terms vanish and the cross terms add because $d^\dagger c^\dagger = -c^\dagger d^\dagger$. The outgoing state has one particle in each port with unit probability. Neither result requires an attractive or repulsive force at the splitter. Their interpretation turns on whether the alternatives remain indistinguishable and on the symmetry of the total input.

Now give the two particles internal wave packets $|u\rangle, |v\rangle$, which may encode time, frequency or spin, and suppose the detectors report output ports but do not resolve internal labels. One coincidence alternative puts u in c and v in d; the other interchanges them. The interference cross term contains the product $\langle u|v\rangle\langle v|u\rangle = |\langle u|v\rangle|^2$. At a balanced splitter the coincidence probability is $[1 - |\langle u|v\rangle|^2]/2$ for initially independently prepared bosons and $[1 + |\langle u|v\rangle|^2]/2$ for corresponding fermions. At zero overlap both reduce to one half, as expected for two distinguishable independent particles each taking a random output.

Take transform-limited Gaussian wavepacket intensities of common time variance σ_t^2 with delay τ between their centres and no carrier mismatch. Integrating their two normalised amplitude envelopes gives

$$|\langle u|v\rangle|^2 = \exp[-\tau^2/(4\sigma_t^2)].$$

For $\sigma_t = 0.50$ ps and delay 1.00 ps this is

$$e^{-1} = 0.368.$$

The predicted bosonic coincidence fraction is 0.316 and the fermionic value 0.684. A narrow time gate can itself identify the particles differently at different delays and must be included in the counting model. Measuring the single-output rates together with coincidences tests splitter balance and detection bias before converting dip or peak contrast into an overlap estimate.

Infer distinguishability with an unbalanced splitter

A calibrated splitter has intensity transmittance $T = 0.60$, reflectance $R = 0.40$ and negligible loss. Two photons from separate inputs give coincidence probability 0.184 at equal central arrival time. Infer their internal squared overlap. Would equal-time arrival alone have guaranteed perfect bunching?

▼ Derive and check the result

For indistinguishable paths the two coincidence amplitudes have opposite signs with magnitudes T, R. A nonresolving detector gives

$$P_c = T^2 + R^2 - 2TR|\langle u|v\rangle|^2.$$

Substitution yields squared overlap $(0.52 - 0.184)/0.48 = 0.70$. Even perfect internal overlap at this unbalanced splitter would leave $(T - R)^2 = 0.040$ coincidences. Equal arrival time controls only one possible distinguishing label; orthogonal polarisation or spectral mismatch can still reduce overlap. A far-delay reference should give $T^2 + R^2 = 0.52$ for distinguishable, otherwise comparable photons. This independent control helps separate exchange interference from lost counts or a miscalibrated splitter.

Tutorial · discriminate spatial exchange from virtual hopping

Normalise two nonorthogonal orbitals before predicting coincidences

Let a, b each have norm one but overlap $s = 0.30$. Find the normalisations of their symmetric and antisymmetric products. Does the antisymmetric state still vanish at common position?

▼ **Work through the solution**

The inner product $\langle ab|ba\rangle = |s|^2 = 0.09$. The normalisation denominators are

$$\sqrt{2(1 + 0.09)} = 1.476,$$

$$\sqrt{2(1 - 0.09)} = 1.349.$$

At identical positions the antisymmetric numerator cancels pointwise for every s. When the orbitals become identical its norm tends to zero and there is no independent antisymmetric state of that pair. For nonzero overlap the one-body cross terms in the earlier density calculation no longer integrate away, so those equal-density formulas must be rederived. Orthonormalising local orbitals changes the parameters of a corresponding Hubbard model as well.

Infer a hopping amplitude from a measured singlet gap

A calibrated two-site sample has $U = 120$ meV and a singlet–triplet gap 5.0 meV. In the model above find t exactly, predict the double-occupation probability and compare with a large-U inference.

▼ **Work through the solution**

Writing $J = (\sqrt{U^2 + 16t^2} - U)/2$ gives $4t^2 = J(U + J)$, hence $|t| = 12.50$ meV. The large-U estimate $\sqrt{JU}/2 = 12.25$ meV is close but measurably different. The double-occupation fraction is

$$\tfrac{1}{2}[1 - U/(U + 2J)] = J/(U + 2J) = 0.03846.$$

Gap alone cannot distinguish signs of t in a two-site model because rephasing one orbital reverses the sign. Measuring charge fluctuations independently tests whether the observed spin gap can be explained by this same virtual process.

Predict coherent double-occupation oscillations

Start suddenly in the singly occupied singlet of the symmetric two-site model. Find the probability of observing either doubly occupied site after time τ and its maximum at $U = 100,\ t = 10$ meV. Predict the triplet control.

▼ **Work through the solution**

Subtract $U/2$ times identity from the two-dimensional Hamiltonian. The traceless matrix squares to $(U^2 + 16t^2)I/4$. Exponentiating gives

$$P_D(\tau) = 16t^2 \sin^2[\sqrt{U^2 + 16t^2}\,\tau/(2\hbar)]/(U^2 + 16t^2).$$

Its maximum is

$$1600/11600 = 0.138.$$

This is larger than the ground-state admixture because the sudden preparation is a coherent superposition of both energy eigenstates. A triplet evolves with no doubly occupied component in this ideal Hamiltonian. Observing double occupation after triplet preparation would test spin mixing, state-preparation fidelity or additional orbitals.

Further reading

- Fließbach · Mehrteilchensysteme
- Cambridge · electron exchange, helium and determinants
- Course investigation · exchange of identical particles

Quantum states, dynamics and measurement · 8. From a finite pulse to a continuum transition rate

Switch a weak perturbation on for a measured duration. Its Fourier transform determines the amplitude of a discrete transition. Summing over a dense set of final states reveals where a time-independent transition rate comes from and where it fails.

Remove the known free evolution before approximating

Let $H_0|n\rangle = E_n|n\rangle$ and $H(t) = H_0 + V(t)$. Expand $|\psi(t)\rangle = \sum_n c_n(t) e^{-iE_n t/\hbar}|n\rangle$. Substituting into the time-dependent Schrödinger equation cancels the free phase derivatives and leaves an exact equation $i\hbar \dot{c}_f = \sum_n e^{i(E_f - E_n)t/\hbar} V_{fn}(t) c_n(t)$. Suppose the initial state is $|i\rangle$ and the perturbation is appreciable only between 0 and T. Iterating the integral equation once, replacing $c_n(t)$ on the right by δ_{ni}, yields

$$c_f^{(1)}(T) = -\frac{i}{\hbar}\int_0^T e^{i\omega_{fi}t} V_{fi}(t)\, dt,$$

$$\omega_{fi} = (E_f - E_i)/\hbar.$$

For $f \neq i$ the leading transition probability is $|c_f^{(1)}|^2$. It is second order in the perturbation even though the amplitude is first order. Conservation of total probability to this order requires a second-order correction to the initial amplitude. Simply appending all positive final probabilities while keeping the initial probability exactly one would fail that test. The approximation is controlled when total probability removed from the initial state is small over the observation duration and higher-order pathways are negligible.

Let the resonant component of a drive have matrix element $V_{fi}(t) = v e^{-i\omega t}$ for $0 < t < T$. For a real cosine perturbation the two exponentials each carry half the real peak amplitude, so v refers to just the near-resonant part. Define $\Delta = \omega_{fi} - \omega$. Direct integration gives

$$P_f^{(1)} = \frac{|v|^2 T^2}{\hbar^2}\operatorname{sinc}^2(\Delta T/2),$$

$$\operatorname{sinc} x = \sin x / x.$$

At resonance the amplitude grows linearly in time while its phase remains coherent. A detuned contribution winds around in the complex plane and largely cancels. The first zeros occur at ordinary detuning $\pm 1/T$ in hertz. The full width at half height is approximately $0.886/T$ in ordinary frequency since $\sin x/x = 1/\sqrt{2}$ at $x \simeq 1.3916$. Doubling duration quadruples the line-centre probability for one final state but halves the linewidth, a distinction central to interpreting a continuum rate.

Sum over final states before taking a long-time limit

A large box provides a discrete set of final levels with spacing δE; at fixed finite time many can lie inside the pulse's energy bandwidth. Let $\rho(E)$ be the density of the accessible final states per joule, including degeneracy exactly once. Replace the sum by an integral with $E_* = E_i + \hbar\omega$:

$$P_{\text{out}} \simeq \frac{T^2}{\hbar^2}\int dE\, \rho(E)|v(E)|^2 \operatorname{sinc}^2\left[\frac{(E - E_*)T}{2\hbar}\right].$$

If $\rho|v|^2$ changes little across the dominant width and the line is well away from thresholds, take it outside the integral. Substitute $u = (E - E_*)T/(2\hbar)$, and use $\int_{-\infty}^{\infty} (\sin u/u)^2 du = \pi$. The area of the squared Fourier transform grows linearly, giving

$$\Gamma = \frac{P_{\mathrm{out}}}{T} \simeq \frac{2\pi}{\hbar} |v(E_*)|^2 \rho(E_*).$$

The identity for the sinc area also follows by Parseval from the energy in the rectangular time window. This is Fermi's golden rule with ρ per energy. If a supplied density is per unit angular frequency,

$$\rho_\omega = \hbar \rho_E;$$

failing to change that measure introduces a factor of $\hbar$. The units are a strong check: energy squared times states per energy divided by action is inverse seconds.

Several limits have been taken in a definite order. The perturbation lasts long enough to resolve the scale on which $\rho|v|^2$ varies but short enough that many levels still fit in its bandwidth. A window of times must exist between a reservoir correlation time and a recurrence time of order $2\pi\hbar/\delta E$. In addition $\Gamma T \ll 1$ for the first-order depletion argument. Taking $T \to \infty$ at fixed finite box instead resolves individual levels and can produce coherent oscillations or recurrences. Extending the constant rate to a full exponential decay uses a further memoryless approximation and renewed weak transitions of the remaining population. A linear short-time fit by itself does not establish exponential dynamics at every time.

Keep matrix elements and density normalisation consistent

For illustration choose $|v| = 5.00 \times 10^{-6}$ eV and $\rho = 20.0\ \mathrm{eV}^{-1}$ for box-normalised accessible modes dense enough on the pulse scale, giving $\Gamma \simeq 4.77 \times 10^{6}\ \mathrm{s}^{-1}$ as a formal product. But the implied mean level spacing $1/\rho = 0.050$ eV corresponds to a recurrence scale of only 8.27×10^{-14} s. Using a nanosecond pulse with this literal finite density violates the continuum criterion, irrespective of how small ΓT looks. This numerical mismatch is a useful trap: reproducing a golden-rule number to many digits does not ensure the system supports irreversible decay in the chosen time range.

Now enlarge the quantisation volume by 10^6 for continuum-normalised physical coupling. The number of accessible states per energy grows by 10^6, while each squared matrix element shrinks by 10^6 for a localised initial state and individually unit-normalised extended final states. The same product gives the same Γ, but spacing is now 5.0×10^{-8} eV and the recurrence scale 82.7 ns. At $T = 2.0$ ns, $\Gamma T = 0.00954$ and roughly $h/(T\delta E) \simeq 41$ spacings fit up to the first positive zero. Whether density and coupling are locally smooth on that bandwidth remains an additional condition. The scaling removes explicit box dependence from a physical rate while clarifying why direct sums at finite volume can require larger spaces.

Use phase space to predict the shape of a continuum edge

For free relative motion in three dimensions, count single scalar internal channels in a cubic periodic volume $\mathcal{V}$. One state occupies volume $(2\pi)^3/\mathcal{V}$ in wave-vector space. The shell between $k, k + dk$ thus contains $\mathcal{V} 4\pi k^2 dk/(2\pi)^3$. From $E = \hbar^2 k^2/(2m)$ it follows that $\rho(E) = \mathcal{V} m k/(2\pi^2\hbar^2)$, which vanishes like $\sqrt{E}$ at threshold. In one dimension the corresponding free density diverges like $1/\sqrt{E}$; the geometrical shell

measure is different. A threshold suppression observed in one spectrum could come from available states, the coupling matrix element, or both.

If a local transition couples chiefly to a final orbital partial wave l, its regular low-k free radial factor near the source scales as k^l when the potential is sufficiently short ranged and no threshold resonance changes the law. Squaring and multiplying by the three-dimensional density gives

$$\Gamma_l \propto k^{2l+1} \propto E^{l+1/2}.$$

For a p-wave channel doubling the excess energy increases this ideal rate by $2^{3/2} = 2.83$. Long-range Coulomb fields alter the final-state radial behaviour and can invalidate the short-range threshold power. Very close to any edge a finite pulse straddles energies where the density changes rapidly or vanishes. Replace the local golden-rule product by the finite-window integral to model the measured onset.

Compare pulse shapes at equal area and equal energy

The rectangular pulse is useful because its Fourier transform is elementary. Its abrupt start and end also generate sidelobes that can excite nearby unwanted transitions. For a general narrowband drive write its resonant matrix element $v(t)e^{-i\omega t}$. First order gives

$$P_f = |\int v(t)e^{i\Delta t}dt|^2/\hbar^2.$$

At zero detuning only the complex pulse area $\int v(t)dt$ matters. After summing over a flat continuum, Parseval gives $\int P_f(\Delta)d\Delta = (2\pi/\hbar^2)\int |v(t)|^2 dt$, so it is the temporal integral of squared coupling that controls total spectral weight. Two pulses with the same area can have different continuum probabilities; two with the same integrated intensity can have different resonant peak heights.

For a Gaussian envelope $v(t) = v_0 e^{-t^2/(2\tau^2)}$ on the full line, complete the square in its Fourier integral. The amplitude is $v_0\sqrt{2\pi}\tau e^{-\Delta^2\tau^2/2}$, so the transition profile has no sidelobes and has full half-height angular width $2\sqrt{\ln 2}/\tau$. The time intensity is $|v_0|^2 e^{-t^2/\tau^2}$, with temporal full half-height width $2\sqrt{\ln 2}\tau$. Multiplying this by the ordinary-frequency full width gives

$$2\ln 2/\pi = 0.441.$$

Replacing an amplitude width by an intensity width changes that product by $\sqrt{2}$; specifying the plotted quantity is necessary when comparing a spectrum with temporal photodetector data.

Take a Gaussian with $\tau = 0.50$ ms. Its spectral intensity full width is 530 Hz and pulse intensity full temporal width 0.833 ms. An unwanted line 1.0 kHz away receives a relative first-order probability $e^{-(2\pi 1000\tau)^2} \simeq 5.17 \times 10^{-5}$. A nominally same-duration rectangular pulse may place an ideal zero near some precisely chosen detuning, but neighbouring frequencies generally see sidelobes. Which pulse gives smaller unwanted excitation depends on what quantity is fixed, where the extra lines lie and how much uncertainty there is in their positions. A shaped envelope can suppress spectral leakage without improving every possible resolution metric.

A pair of pulses illustrates how coherently adding amplitudes differs from broadening a single envelope. Let identical, short pulses of area A be separated by start-time difference T_s, and let the second have a

controlled drive phase ϕ. At a detuning small compared with each pulse bandwidth, the amplitude is proportional to $A[1 + e^{i(\Delta T_s + \phi)}]$. Its squared magnitude has fringes $2|A|^2[1 + \cos(\Delta T_s + \phi)]$ inside the broader single-pulse line. Their ordinary-frequency spacing $1/T_s$ can be much smaller than the inverse individual pulse duration. Randomising the relative phase removes fringes while keeping the two single-pulse energies unchanged. The observed fine spectral structure is therefore a measurement of coherent time separation as well as energy difference.

Derive depletion and the energy shift from the same kernel

The first-order rate gives initial population loss in a useful time window. To see which extra assumptions allow exponential decay, retain a single initial discrete level coupled to many initially empty final levels with time-independent couplings v_f in a rotating frame. Let $c_i(0) = 1,\ c_f(0) = 0$. In the interaction picture $\dot{c}_f = -(i/\hbar) v_f e^{i\omega_{fi} t} c_i(t)$. Integrate this equation exactly in terms of the unknown c_i and insert the result in its partner equation for $\dot{c}_i$. Assuming final levels do not couple directly to one another gives

$$\dot{c}_i(t) = -\int_0^t K(t - t') c_i(t')\, dt',$$

$$K(\tau) = \hbar^{-2} \sum_f |v_f|^2 e^{-i\omega_{fi}\tau}.$$

No irreversibility has been assumed in this elimination. The previous discrete amplitudes are encoded in a memory kernel and can feed back into the initial level. At very short times $c_i(t) \simeq 1 - K(0)t^2/2$ when the second moment is finite, yielding a quadratic survival loss. At long times a sharply structured or bounded continuum can produce nonexponential decay. A finite number of exactly known final levels evolves unitarily under the full Hamiltonian and can show recurrences; treating the memory as identically zero after any arbitrarily short interval would discard this possibility.

When the spectral coupling varies slowly over the line and extends across a sufficiently broad band, phase cancellation makes $K(\tau)$ decay over a correlation time τ_c. For τ_c short relative to changes in c_i, write $c_i(t - \tau) \approx c_i(t)$ inside its memory integral after the initial transient, and extend its upper limit to infinity. The regulated integral $\int_0^\infty e^{-i\omega\tau - \eta\tau} d\tau = (\eta + i\omega)^{-1}$ tends to $\pi\delta(\omega) - i\,\mathcal{P}(1/\omega)$ as a distribution. Its real part gives

$$\dot{c}_i = -\Gamma c_i/2 + \cdots,$$

with the same golden-rule population rate Γ. The imaginary part gives a coherent energy shift proportional to $\mathcal{P}\sum_f |v_f|^2/(E_i - E_f)$, requiring the physical bandwidth and a consistent bare energy. This shows how an absorptive linewidth and a dispersive shift can emerge from different parts of the same elimination, without claiming a perfectly flat infinite continuum supplies a physically meaningful absolute shift.

For a symmetric model with constant spectral strength inside $-W < \omega_{fi} < W$, the kernel is proportional to $\sin(W\tau)/\tau$. Narrowing the band increases its memory time and can delay the onset of an approximately constant rate. Moving the discrete level close to a band edge also removes the cancellation between positive and negative detunings responsible for a vanishing symmetric shift. An experiment that varies the carrier across such an edge should fit the full finite-window spectrum before inferring a time-independent linewidth or level shift. A numerically cheap sum over known discrete final energies provides a check: double the

spectral cutoff, halve level spacing and track the early quadratic regime separately from any intermediate exponential segment.

Ask whether frequent projective tests inhibit a transition

For an initial pure state with finite energy variance under a time-independent H, expand the survival amplitude $A(t) = \langle i|e^{-iHt/\hbar}|i\rangle$ to second order. The linear term $-it\langle H\rangle/\hbar$ is a phase. Squaring gives

$$P_i(t) = 1 - (\Delta H)^2 t^2/\hbar^2 + O(t^3),$$

with still higher-order control depending on available moments. Define $t_Z = \hbar/\Delta H$. In the model with one initial level coupled only off-diagonally to the final levels, $(\Delta H)^2 = \sum_f |v_f|^2$, agreeing with the memory-kernel expansion. If the needed moments diverge in an idealised continuum, this short-time expansion requires a physical high-frequency regularisation.

Now make ideal instantaneous projective tests of whether the system is still in $|i\rangle$ every $\tau = T/N$, selecting only histories that have passed every test. Conditional on survival, each projection prepares exactly the same initial state. The joint survival probability is $P_i(\tau)^N \simeq [1 - (T/Nt_Z)^2]^N \to 1$ as $N \to \infty$ for fixed total duration T. This is a mathematically precise limiting model of the quantum Zeno effect. It is not obtained by simply looking at a stored record more often after a single final measurement; the successive physical interventions reset the conditional state.

With a resonantly coupled two-state Hamiltonian $H = v\sigma_x$, the survival against a single interval is $\cos^2(v\tau/\hbar)$. Choose $vT/\hbar = \pi/2$; unobserved survival at T is zero. For ten equally spaced perfect tests the joint survival is

$$\cos^{20}(\pi/20) = 0.7805.$$

If the instrument has 2% independent loss per successful test, the recorded joint fraction falls to

$$0.7805(0.98)^{10} = 0.638.$$

A finite-duration detector may also change H or broaden spectral coupling rather than implement an instantaneous projection. The ideal repeated-measurement result gives a comparison baseline, while predicted observed counts must include the physical instrument and conditioning.

Derive the sweep-rate scale for a transition through resonance

For a chirped weak drive let its instantaneous detuning from one discrete transition change linearly, $\Delta(t) = \dot{\Delta}\, t$, crossing zero at the middle of a long pulse. The phase accumulated in the first-order integral is $\int^t \Delta(t')dt' = \dot{\Delta}\, t^2/2$, not $\Delta(t)t$. For approximately constant coupling v around the crossing and sufficiently far endpoints the oscillatory Gaussian integral gives $|c_f^{(1)}|^2 \simeq 2\pi|v|^2/(\hbar^2|\dot{\Delta}|)$. A slower passage accumulates a larger resonant amplitude, but this weak-coupling formula cannot exceed probability one. At large transfer the full two-level avoided-crossing dynamics replaces it.

For $|v|/\hbar = 2\pi \times 200$ Hz and an ordinary-frequency sweep $d(\Delta/2\pi)/dt = 10^8$ Hz/s, the estimate is 0.0158. Changing only the sign of the sweep gives the same first-order probability in this symmetric idealisation, while the phase of the transition amplitude changes. Coherently driving a second passage can convert that phase difference into an observable interference pattern. Missing endpoints, asymmetric pulse shaping and additional nearby lines can spoil the simple symmetry. Comparing both sweep directions and checking that the result scales as inverse speed over a low-transfer range are concrete tests of the stationary-phase approximation instead of assuming every apparent line crossing signifies complete adiabatic transfer.

Separate a transition frequency from coherence loss

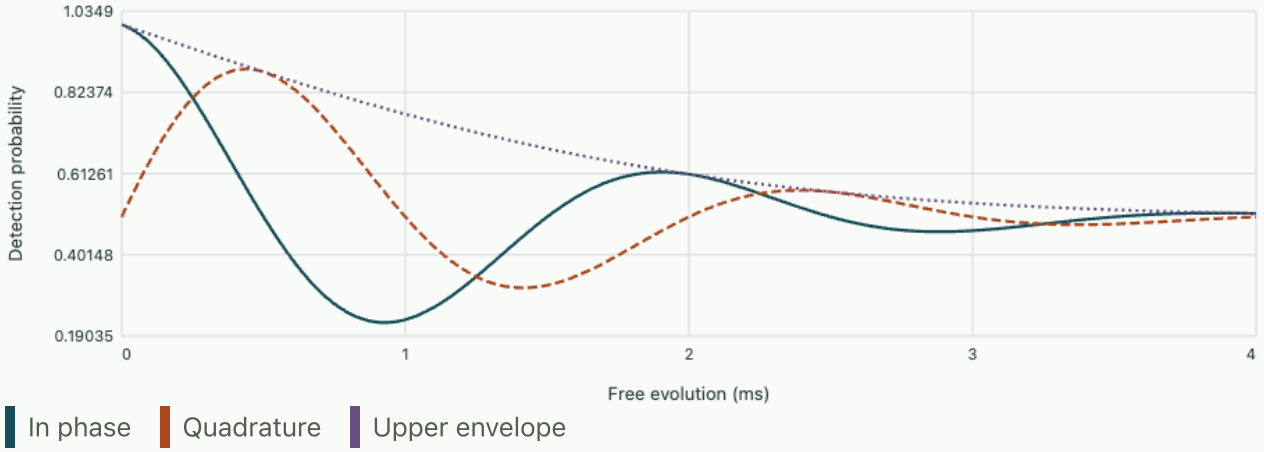
Vary detuning and shot-to-shot spread while reading both pulse quadratures. Determine whether a change of population comes from a shifted carrier or a fading phase.

Open this experiment online

Try the calculation

Mean cyclic detuning (Hz) **500**

Shot-to-shot rms spread (Hz) **80**



Contrast after 1 ms = 0.53455. The two probabilities at 0.50 ms are 0.5 and 0.87729.

Derive the spectral distinction between a phase-coherent pulse and stationary noise

A fluctuating perturbation is often characterised by a power spectral density rather than a prescribed pulse phase. Suppose $V_{fi}(t) = d_{fi}F(t)$ with F a real classical, zero-mean stationary random process and the coupling weak enough for first-order amplitudes in each realisation. Averaging the modulus squared produces a double time integral involving the autocorrelation $C_F(\tau) = \langle F(t+\tau)F(t)\rangle$:

$$\langle P_f(T)\rangle = \frac{|d_{fi}|^2}{\hbar^2}\int_{-T}^{T}(T-|\tau|)C_F(\tau)e^{i\omega_{fi}\tau}\,d\tau.$$

The factor $T - |\tau|$ counts the length of pairs of times in $[0, T]$ separated by τ. If T is long compared with the correlation time and depletion remains weak, divide by T to find rate $|d_{fi}|^2 S_F(\omega_{fi})/\hbar^2$, where $S_F(\omega) = \int_{-\infty}^{\infty} C_F(\tau) e^{i\omega\tau} d\tau$ is the two-sided angular-frequency spectrum. No sum over a continuum of final quantum states was involved here. A continuum of drive frequencies supplies a different physical route to an approximately linear transition probability of one resolved final state.

For exponentially correlated noise $C_F(\tau) = F_{\mathrm{rms}}^2 e^{-|\tau|/\tau_c}$, integration gives

$$S_F(\omega) = 2F_{\mathrm{rms}}^2 \tau_c / [1 + \omega^2 \tau_c^2].$$

Fix F_{rms} and vary correlation time. At a nonzero fixed transition frequency, extremely rapid fluctuations have little integrated spectral weight there because their fixed variance is spread over a very broad band. Very slow fluctuations concentrate their weight near zero frequency. Differentiating the spectral expression gives a maximum excitation rate at $\tau_c = 1/|\omega_{fi}|$. This nonmonotonic dependence cannot be inferred just by quoting the field's total rms amplitude. Unit conventions are also critical: changing to ordinary-frequency spectral densities and a one-sided instrument display requires the corresponding Jacobian and factor of two.

A real classical stationary process has an even spectrum $S_F(-\omega) = S_F(\omega)$, so this model drives upward and downward transitions equally per available source population when matrix elements are conjugate. A quantum environment at thermal equilibrium can have unequal positive and negative frequency unsymmetrised spectra. Its absorption and emission probabilities encode detailed balance. Thus an observed difference between calibrated upward and downward rates cannot generally be explained by merely drawing samples from a real classical noise spectrum of the same symmetrised power. Distinguishing a driven classical source from an equilibrium quantum bath requires precise statements about which correlations enter the transition probability.

Infer a fluctuation timescale from a rate ratio

Two transitions with equal coupling strengths see the same exponentially correlated classical field at ordinary frequencies f and $2f$. Their measured weak transition rates obey $\Gamma(2f)/\Gamma(f) = 0.40$. Infer the dimensionless correlation frequency and, for $f = 50.0$ kHz, the correlation time. What feature of the acquisition would invalidate this inference?

▼ **Derive and check the result**

Let $x = (2\pi f \tau_c)^2$. The ratio is $(1 + x)/(1 + 4x) = 0.40$, giving $0.60 = 0.60x$ and $x = 1$. The correlation time is

$$1/(2\pi f) = 3.18\,\mu\mathrm{s}.$$

At the lower frequency the noise spectrum lies at half its zero-frequency value; the higher line samples one fifth of that value. If the exposure time is comparable to or shorter than τ_c, the triangular window in the double integral still influences both rates and the infinite-time Lorentzian ratio is inadequate. Likewise unequal matrix elements or a finite observation band must be corrected separately. Measuring a third transition at another frequency supplies an independent test of the exponential-correlation model rather than simply determining its fitted timescale.

Tutorial · choose a pulse duration and check the perturbation

Measure a frequency width without confusing two line shapes

A rectangular pulse lasts 4.00 ms with resonant coupling $|v|/\hbar = 25.0\,\mathrm{s}^{-1}$. Find the line-centre probability, separation of the first zeros and full half-height width in hertz.

▼ **Work through the solution**

At resonance first-order probability is

$$(25 \times 0.004)^2 = 0.0100.$$

The first zeros are 250 Hz on either side, giving a 500 Hz separation. The full half-height width is

$$0.886/0.004 = 221.5\,\mathrm{Hz}.$$

A Lorentzian fit with its width interpreted as a spontaneous lifetime would mistake pulse broadening for decay. Doubling T while keeping coupling fixed is a diagnostic: the first-order peak would rise fourfold and the width halve. At large peak probability use the full two-level dynamics rather than extrapolating the quadratic indefinitely.

Verify the breakdown against exact two-level dynamics

Assume an isolated resonantly driven two-state system with rotating-frame Hamiltonian off-diagonal v and zero detuning. What replaces the first-order expression when $T = \pi\hbar/(2|v|)$? At which small pulse area is the fractional error approximately one percent?

▼ **Work through the solution**

The resonant Hamiltonian squares to $|v|^2 I$, so the exact probability is $\sin^2(|v|T/\hbar)$. At the stated pulse time it is unity while the first-order result is $(\pi/2)^2 = 2.47$, impossible as a probability. For pulse area $a = |v|T/\hbar$,

$$\sin^2 a = a^2 - a^4/3 + \cdots.$$

The relative discrepancy is approximately $a^2/3$, reaching 1% at $a \simeq 0.173$. The pulse can already make a measurable few-percent transition while first-order theory remains reasonably accurate. A dense continuum requires checking the total across all levels as well.

Infer an accessible density from the observed time dependence

At long-enough but weak-depletion times an ensemble loses 2.0% population in 5.0 ns. The squared box matrix element is calibrated as $2.5 \times 10^{-17}\,\mathrm{eV}^2$. Infer ρ, estimate the recurrence scale and test whether this interpretation is internally consistent.

▼ **Work through the solution**

The slope estimate is $4.0 \times 10^{6}\ \mathrm{s}^{-1}$. With $\hbar = 6.5821 \times 10^{-16}\,\mathrm{eV\,s}$ the inferred $\rho = \Gamma\hbar/(2\pi|v|^{2}) = 1.68 \times 10^{7}\,\mathrm{eV}^{-1}$. The corresponding spacing is 5.97×10^{-8} eV and recurrence scale $h/\delta E \simeq 69$ ns. A 5 ns observation fits within that scale, with about 14 spacings to the first zero. Two percent is compatible with weak depletion. Smoothness of the density and a single accessible channel still require independent spectral checks. Repeating the measurement at several durations reveals whether the inferred slope is stable.

Further reading

- Fließbach · Näherungsmethoden
- MIT 8.322 · time-dependent perturbation theory and scattering
- Course investigation · driven transitions and finite pulse spectra

Quantum states, dynamics and measurement · 9. Inferring a short-range interaction from elastic scattering

A beam of neutral particles encounters a weak, localised static potential. Derive differential cross section from current, extract phase shifts by radial matching and compare exact low-energy scattering with the Born approximation and its failure near a bound state.

Define an observable from incident and outgoing current

Consider elastic scattering from a real, short-range, spherically symmetric potential in three dimensions. In a two-body problem use the relative coordinate and reduced mass m; here the target may simply be a prescribed static potential. At a large distance the stationary solution for a plane wave incident along z has the form $\psi \simeq e^{ikz} + f(\theta)e^{ikr}/r$. The amplitude f has dimensions of length in this convention. Incident current density is $\hbar k/m$ for unit plane-wave amplitude. The outgoing spherical component has radial current density $\hbar k|f(\theta)|^2/(mr^2)$ to leading order. Multiplying by detector area $r^2 d\Omega$ and dividing by incident flux gives

$$d\sigma/d\Omega = |f(\theta)|^2.$$

Normalised wave packets and finite detectors supply a physical limiting interpretation for the plane waves.

The incident and scattered components also interfere. Away from a vanishingly narrow forward region the far-field detector resolves the outgoing scattered beam in this derivation. Integrated forward interference accounts for removed incident flux and leads to the optical theorem. Dropping the cross term everywhere and then demanding total current conservation would incorrectly add a stream of scattered particles without depleting the forward beam. For different outgoing and incident wave numbers an additional ratio of group velocities enters the differential flux; the simple squared amplitude here assumes elastic kinematics.

Match a regular radial solution to free waves

Expand a plane wave in Legendre polynomials as $e^{ikz} = \sum_l (2l+1) i^l j_l(kr) P_l(\cos\theta)$. Outside a short-range potential the reduced radial function in each partial wave is a combination of spherical Bessel and Neumann solutions, with large-distance behaviour proportional to $\sin(kr - l\pi/2 + \delta_l)$. Fix the incoming part equal to that in the incident plane wave. Then the ratio by which the outgoing coefficient is changed is $S_l = e^{2i\delta_l}$. For a real one-channel Hamiltonian conservation of each partial wave's radial current gives $|S_l| = 1$, so δ_l is real modulo π. It is the change in radial phase at the same energy, not a separate potential-dependent energy shift of the free particles far from the target.

Separating the excess outgoing part gives

$$f(\theta) = \sum_{l=0}^{\infty} \frac{2l+1}{k} e^{i\delta_l} \sin\delta_l \, P_l(\cos\theta),$$

$$\sigma_{\mathrm{el}} = \frac{4\pi}{k^2} \sum_l (2l+1) \sin^2\delta_l.$$

The second formula follows from orthogonality of Legendre polynomials in the angular integral. At $\theta = 0$, $P_l(1) = 1$ and $\mathrm{Im}(e^{i\delta_l}\sin\delta_l) = \sin^2\delta_l$, so $\sigma_{\mathrm{el}} = 4\pi\,\mathrm{Im}\,f(0)/k$ in this purely elastic model. The differential intensity at some other angle can result from cancellations between waves, even though their contributions to the integrated cross section add separately. A narrow angular detector cannot replace full angular integration without a model of the partial waves.

Derive and interpret a scattering length

Take an attractive spherical well $V = -V_0$ for $r < R$, zero outside. At zero incident energy the regular s-wave reduced solution inside is $u = A\sin(\kappa r)$,

$$\kappa = \sqrt{2mV_0}/\hbar.$$

Outside $u = B(r - a)$; extrapolating this line to zero defines the scattering length a. Matching the logarithmic derivative at R gives $\kappa\cot(\kappa R) = 1/(R - a)$, or

$$a = R\left[1 - \frac{\tan u}{u}\right],$$

$$u = \kappa R.$$

A regular zero-energy extrapolation node can lie outside the range of the potential. It is an intercept characterising the exterior solution and need not mark an actual hard surface. For weak attraction $u \ll 1$ one finds $a/R = -u^2/3 - 2u^4/15 + \cdots$, so a is negative. As u crosses $\pi/2$ the first s-wave bound state appears at threshold and a diverges and changes sign. A large positive scattering length can indicate a shallow bound state for a short-range attraction, whereas a hard repulsive sphere also has positive length. Its sign alone cannot reconstruct an arbitrary potential.

At nonzero k, regular interior solution has wave number $q = \sqrt{k^2 + \kappa^2}$. Match $q\cot(qR) = k\cot(kR + \delta_0)$ to compute an exact phase modulo π. For $kR \ll 1$ and away from singular length scales, the effective range expansion $k\cot\delta_0 = -1/a + r_e k^2/2 + \cdots$ describes the first energy dependence. Writing $f_0 = 1/(k\cot\delta_0 - ik)$ retains unitarity automatically. Neglecting the effective range gives

$$\sigma_0 = 4\pi a^2/(1 + k^2a^2).$$

The zero-energy result $4\pi a^2$ is justified only if $k|a| \ll 1$ as well as range effects being small. Taking a to infinity at fixed k gives the finite bound $4\pi/k^2$ for one partial wave. The apparent infinite cross section at the threshold arose from interchanging limits.

Turn a potential into a first-order Fourier amplitude

The outgoing free Green function obeys $(\nabla^2 + k^2)e^{ikr}/r = -4\pi\delta^3(\mathbf{r})$. Rearrange Schrödinger's equation into a free wave plus an integral of this kernel times $V\psi$. At large observation distance $|\mathbf{r} - \mathbf{r}'| \simeq r - \hat{\mathbf{r}}\cdot\mathbf{r}'$. Replacing the wave inside the integral by the incident plane wave gives the first Born amplitude

$$f_B(\mathbf{k}', \mathbf{k}) = -\frac{m}{2\pi\hbar^2} \int e^{-i(\mathbf{k}'-\mathbf{k})\cdot\mathbf{r}'} V(\mathbf{r}')\, d^3r',$$

$$|\mathbf{k}' - \mathbf{k}| = 2k\sin(\theta/2).$$

For the square well the angular integral is $4\pi\sin(Qr)/(Qr)$,

$$Q = |\mathbf{k}' - \mathbf{k}|.$$

Integrating $r^2 dr$ gives

$$f_B = (2mV_0/\hbar^2)[\sin(QR) - QR\cos(QR)]/Q^3.$$

At $Q \to 0$ the bracket is $(QR)^3/3 + \cdots$, so $a_B = -f_B(0) = -u^2R/3$. This reproduces the first weak-well term but misses the bound-state pole entirely. For a real central potential $f_B(0)$ is real. Its first-order imaginary part is zero, while the integrated Born cross section is already second order in V. The forward imaginary contribution needed by the optical theorem first appears at that same second order. Applying the theorem as though a first-order amplitude were exact would mix orders inconsistently.

Extract a phase numerically without fitting an arbitrary sinusoid

For a finite-range real potential, one of the most useful laboratory calculations integrates each radial equation from its regular origin to a matching radius r_m outside the interaction. Use the reduced radial functions $\hat{j}_l(z) = zj_l(z)$ and $\hat{n}_l(z) = zn_l(z)$; their large-z limits are $\sin(z - l\pi/2)$ and $-\cos(z - l\pi/2)$. The exterior solution can be written $u = A[\hat{j}_l(kr)\cos\delta_l - \hat{n}_l(kr)\sin\delta_l]$. The interior ODE supplies u_m, u'_m up to an arbitrary common normalisation. Form the matching determinants rather than estimating a phase by reading one oscillation maximum from a plot.

Taking the radial derivative and eliminating A gives

$$\tan\delta_l = \frac{k\hat{j}'_l(kr_m)u_m - \hat{j}_l(kr_m)u'_m}{k\hat{n}'_l(kr_m)u_m - \hat{n}_l(kr_m)u'_m},$$

where primes on the hatted functions differentiate their dimensionless argument. Both numerator and denominator remain finite if u_m happens to lie close to a node; a direct logarithmic derivative u'_m/u_m can instead amplify roundoff severely. Use the two-argument arctangent before reducing the result modulo π. A reported phase can jump by π under a continuously varying energy while $\sin^2\delta_l$ and S_l remain continuous. Unwrap branches by checking neighbouring energies together with the desired physical reference, especially when estimating an energy derivative of the phase.

For $l = 0, \hat{j}_0 = \sin z, \hat{n}_0 = -\cos z$, choose a simple controlled test: a hard sphere of radius R imposes $u(R) = 0$. With $u_m = 0$ at $r_m = R$, the ratio reduces to $-\tan kR$, giving $\delta_0 = -kR \pmod{\pi}$. At $kR = 0.40$, the exact contribution is $4\pi R^2[\sin(0.40)/0.40]^2 = 0.9478(4\pi R^2)$, while the zero-energy length estimate gives $4\pi R^2$. The finite-k effective-range expansion of the hard sphere follows from $k\cot\delta_0 = -k\cot kR = -1/R + k^2R/3 + \cdots$, so

$$a = R,\ r_e = 2R/3.$$

Comparing this term with the previous denominator retaining a alone explains why their leading corrections at finite k need not agree.

A general radial solver should separately vary the first finite radius, step size, matching radius and maximum partial wave $l_{\max}$. Near a nonsingular origin the regular solution behaves up to normalisation as r^{l+1}; initialize both value and derivative with this local solution or a more accurate series. For Coulomb or more singular long-range interactions the exterior wavefunctions must be changed rather than matching to free Bessel functions at an arbitrary finite radius. Relative error near a zero of differential intensity can be meaningless as a convergence measure. Report absolute angular error there along with integrated current, compare several scattering directions and retain the exact free result $V = 0$ as a phase-zero test.

Relate a rapidly varying phase to a wave-packet time delay

A narrow incident energy packet accumulates an extra phase from an elastic partial wave relative to free propagation. The S-matrix phase is $2\delta_l(E)$. In a stationary-phase arrival-time calculation the derivative of phase with respect to energy shifts the envelope peak, giving the Wigner time delay $\tau_l = 2\hbar\, d\delta_l/dE$ when the potential varies slowly across the packet bandwidth and the outgoing branch is well resolved. A derivative of the observable scattering intensity is not enough; $\sin^2\delta$ loses the branch and sign information required for a delay. Causality and reference distances must be treated with care, particularly when a finite detector counts a sum of waves or a long-range potential changes even the asymptotic reference.

A narrow isolated resonance can be represented approximately by a slowly varying background plus a phase with $\cot\delta_{\mathrm{res}} = (E_r - E)/(\Gamma/2)$. Choose the continuous branch increasing through $\pi/2$. Then

$$\sin^2\delta_{\mathrm{res}} = (\Gamma/2)^2/[(E-E_r)^2 + (\Gamma/2)^2],$$
$$d\delta_{\mathrm{res}}/dE = (\Gamma/2)/[(E-E_r)^2 + (\Gamma/2)^2].$$

With nearly constant k and zero background the partial cross section has full energy width Γ and its peak reaches the unitarity limit. The associated peak delay in this convention is $4\hbar/\Gamma$, whereas the population lifetime inferred from an isolated pole with amplitude $e^{-\Gamma t/(2\hbar)}$ is $\hbar/\Gamma$. Both involve the same width, but comparing them as if they were identical measurements would introduce a factor of four.

For $\Gamma = 0.10$ meV and $\hbar = 0.6582\ \mathrm{meV\,ps}$, the pole lifetime is 6.58 ps and the peak partial-wave delay is 26.3 ps in this model. A finite incoming energy spread comparable to 0.10 meV samples a changing phase derivative; it can distort the shape of the outgoing packet and invalidate the simple peak-delay interpretation. A background phase also causes interference: $\sin^2(\delta_{\mathrm{bg}} + \delta_{\mathrm{res}})$ may exhibit an asymmetric feature or a dip while the resonant phase still evolves by almost π. Observing the peak position of a single angular intensity curve is therefore a poor standalone estimator of the resonance energy when background amplitudes are appreciable.

Symmetrise the scattering amplitude for identical particles

If two identical particles emerge into opposite directions in their centre-of-mass frame, detecting one at θ and the other at $\pi - \theta$ does not assign unique incoming particle labels. For a definite spatial symmetry the indistinguishable alternatives interfere. For spinless identical bosons the amplitude is $f(\theta) + f(\pi - \theta)$; for a spatially antisymmetric channel it is $f(\theta) - f(\pi - \theta)$. A differential cross section defined as the number of unordered final pairs per incident flux can be integrated over one hemisphere, or over the whole sphere with a

factor $1/2$. If an instrument instead records the count of individual outgoing particles over all angles it uses a different event convention. State the convention before quoting integrated enhancement or suppression factors.

Since $P_l(-\cos\theta) = (-1)^l P_l(\cos\theta)$, the symmetric combination retains only even l and the antisymmetric one only odd l. At very low energy short-range s-wave scattering is typically dominant. For spinless identical bosons with $f \simeq -a$, the unordered-pair total becomes

$$2\pi|2a|^2 = 8\pi a^2;$$

for distinguishable particles it is $4\pi a^2$. Fully spin-polarised identical fermions instead have antisymmetric spatial motion and no s-wave channel. Low-energy collisions can be suppressed without a repulsive force. If internal spin states differ or are mixed, the allowed symmetric and antisymmetric spin fractions must be tracked before assigning a measured cross section.

For two unpolarised spin-$1/2$ identical fermions with equal independent spin populations and a spin-independent potential, the spin singlet fraction is $1/4$ and permits symmetric spatial motion; the triplet fraction $3/4$ requires antisymmetric spatial motion. Under the stated unordered-pair convention the low-energy total from the s-wave singlet is $2\pi a^2$ after spin averaging. Preparing a particular unlike-spin product and tagging the two final spin species changes the counting experiment, and one should compute its spin-resolved amplitudes rather than reusing the unpolarised factor. A detector that can label internal states can distinguish alternatives that a spin-insensitive detector combines.

See which potential features low-energy data can determine

At low momentum a finite set of parameters such as a, r_e summarises scattering over a narrow energy band. This does not usually identify a complete potential $V(r)$. An illustrative degeneracy is already visible within spherical square wells: $\tan u/u$ has poles and multiple branches, so different well strengths at the same range can give the same scattering length while supporting different numbers of bound states. A single very-low-energy total cross section loses even the sign of that length. Including a measured bound-state count, phase-sensitive interference or higher partial waves can remove some of these ambiguities. The intended parameterisation and the measured energy interval define the inverse problem.

To extract a, r_e from phase-sensitive s-wave data, plot $Y = k\cot\delta_0$ against $X = k^2$. In the effective-range window a straight-line fit has intercept $-1/a$ and slope $r_e/2$. Suppose values in nm units are $(X, Y) = (0.010, -0.190), (0.040, -0.160), (0.090, -0.110)$. They lie on $Y = -0.200 + 1.00X$, giving $a = 5.00$ nm and $r_e = 2.00$ nm. Repeat at a fourth moderately larger k to test curvature from higher terms, then repeat the fit omitting that point. A near-zero intercept makes the extracted a highly sensitive to measurement noise even if individual phase points are accurate. Reporting the intercept and its uncertainty directly can be more informative than a huge indistinct scattering length with asymmetric error bars.

Infer low-energy scattering from a model well

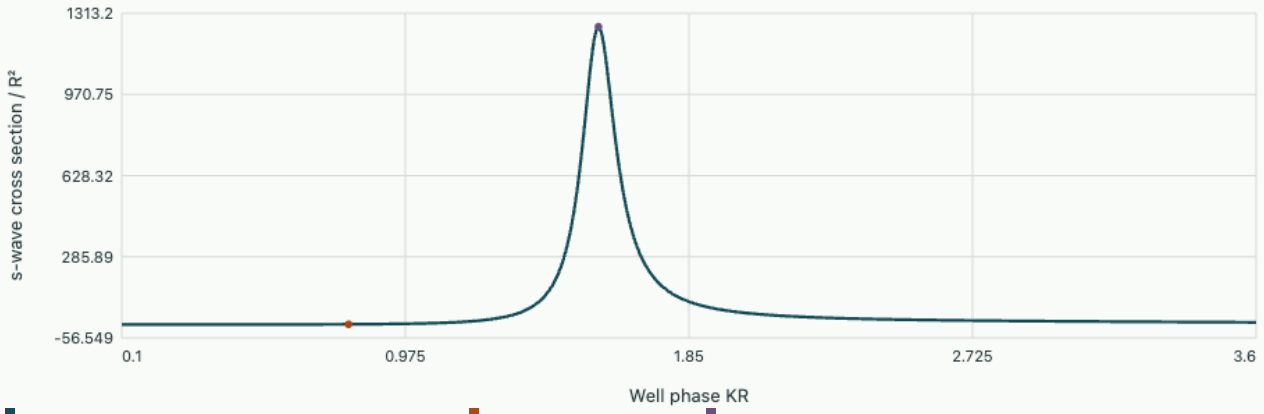
Vary the well strength through a near-threshold state. Compare the measured scattering length with the geometrical range of the potential.

Open this experiment online

Try the calculation

Well phase KR **0.8**

Incoming wave number kR **0.1**



Leading low-energy cross section | Selected depth | First threshold

At KR = 0.8 the cross section is 1.035 R². The finite-k limit at resonance is 1257 R².

Derive an effective range from a zero-energy solution

The scattering length captures the intercept of a zero-energy exterior s-wave. A second coefficient can be related to how the interior wave differs from that extrapolated straight line. For a finite-range real potential choose the dimensionless zero-energy radial solution $u_0(r) \to 1 - r/a$ outside the range. A convenient finite-k exterior normalisation is $u_k = \cos kr + \cot\delta_0 \, \sin kr$; its zero-energy limit gives the same straight line when $k\cot\delta_0 \to -1/a$. Two regular radial equations at energies $0, \hbar^2k^2/(2m)$ give a Wronskian derivative $d(u_0u_k' - u_0'u_k)/dr = -k^2u_0u_k$. Integrate to a radius beyond the potential. The origin contribution vanishes for regular solutions.

Expand the exterior wave using $k\cot\delta_0 = -1/a + r_ek^2/2 + \cdots$. To order k^2 it is $u_k = v + k^2w$, with $v = 1 - r/a$ and $w = -r^2/2 + r^3/(6a) + r_er/2$. In the exterior Wronskian $vw' - v'w$ simplifies to $r_e/2 - \int_0^r (1 - s/a)^2 ds$. Equating to the integrated differential equation gives Bethe's effective range identity

$$r_e = 2\int_0^\infty \left[\left(1 - \frac{r}{a}\right)^2 - u_0(r)^2\right] dr.$$

The integrand vanishes identically outside the true range, so the formal infinite limit is harmless. Both solutions must use the specified equal exterior normalisation; rescaling one independently would leave a divergent difference rather than a material coefficient. The proof also shows why a single scattering length cannot fix an effective range: the former fixes only the exterior line, while r_e measures an integral of the true interior probability relative to its extrapolation.

For a hard sphere of radius $R = a$, set $u_0 = 0$ inside. The integral gives $2\int_0^R (1 - r/R)^2 dr = 2R/3$, agreeing with the direct expansion of $-k\cot kR$. For the attractive square well inside radius R, write $u_0 = (1 - R/a)\sin(\kappa r)/\sin(\kappa R)$. The integral of its square uses

$\int_0^R \sin^2(\kappa r)dr = R/2 - \sin(2\kappa R)/(4\kappa)$. Combining with the scattering-length matching condition reduces the result to $r_e = R - R^3/(3a^2) - 1/(\kappa^2 a)$. This expression should not be evaluated at exactly zero scattering length using naive division; the adopted expansion and exterior normalisation then have to be reconsidered. Close to a diverging length in this finite well one instead finds $r_e \to R$, a natural range scale even while $|a|$ is much larger.

Distinguish two short-range interactions from their energy-dependent phases

A hard sphere and a different finite-range well happen to have equal scattering length $a = 5.0$ nm but effective ranges 3.33 and 5.00 nm. Predict the difference of $k\cot\delta_0$ at $k = 0.10\ \mathrm{nm}^{-1}$. Which measured uncertainty would resolve it at about three standard deviations?

▼ **Derive and check the result**

The shift between the two predictions is

$$\Delta(k\cot\delta) = \tfrac{1}{2}(5.00 - 3.33)(0.10)^2 = 0.00835\,\mathrm{nm}^{-1}.$$

Their values are approximately -0.18335 and $-0.1750\,\mathrm{nm}^{-1}$. If the theoretical curves and common length are accurately specified, a measurement uncertainty below roughly $0.0028\,\mathrm{nm}^{-1}$ would distinguish their difference at three standard deviations. If comparing two independent equally uncertain experimental values, require each to be below $0.00835/(3\sqrt{2}) = 0.00197\,\mathrm{nm}^{-1}$. The expansion error from fourth and higher powers of k must also be smaller than the target difference. Repeating at multiple wave numbers tests that the observed difference scales as k^2 before treating it as evidence for a distinct effective range.

Read a spatial length scale from an angular diffraction envelope

For a weak smooth isotropic potential $V(r) = V_g \exp[-r^2/(2R^2)]$, the first Born amplitude follows from three one-dimensional Gaussian Fourier integrals. In the convention used above,

$$f_B(Q) = -\sqrt{2\pi}\frac{mV_gR^3}{\hbar^2}\exp(-Q^2R^2/2).$$

Its differential intensity relative to the forward value is $\exp(-Q^2R^2)$, with $Q = 2k\sin(\theta/2)$. Forming this ratio cancels the unknown scalar prefactor and fixes the product kR from the angular width. In contrast, a single absolute forward intensity measures $|V_g|^2R^6$ and cannot separate radius and strength. Neither intensity-only measurement fixes the sign of V_g at this order. Thus even in an exactly specified two-parameter family, different angular data have different inverse information.

Suppose $k = 0.40\ \mathrm{nm}^{-1}$ and the intensity at 60° is half that at zero angle. Then $Q = k$ at 60° and $R = \sqrt{\ln 2}/k = 2.08$ nm. At 90°, $Q = \sqrt{2}k$, so the predicted ratio is $1/4$. A third angle tests the Gaussian shape rather than merely refitting its radius. An unmodelled isotropic background would lift the ratio at large angle and bias the inferred radius low if one took logarithms of raw intensity without fitting that background. Use counts divided by incident flux, detector solid angle and efficiency before fitting. Differences of

measurements at several wave numbers can check whether the same spatial R accounts for all angular envelopes.

The integrated cross section can also be evaluated without numerical quadrature. Since $Q^2R^2 = 2(kR)^2(1-\cos\theta)$, integrate over $u = \cos\theta$ to obtain

$$\sigma_B = 2\pi|f_B(0)|^2[1 - e^{-4(kR)^2}]/[2(kR)^2].$$

At $kR \to 0$ the ratio of the exponential difference to $2(kR)^2$ tends to two, yielding the isotropic $4\pi|f_B(0)|^2$. At $kR \gg 1$ the angular envelope narrows and the integrated cross section falls roughly as $1/(kR)^2$ relative to forward intensity. This is a geometrical focusing of the weak-scattering distribution and does not imply that the physical range of the potential changes with incident energy.

Test first Born consistency after fitting a length

For the Gaussian model a fitted low-energy length magnitude is $0.15R$. Infer the dimensionless strength $\eta = m|V_g|R^2/\hbar^2$ predicted by the Born formula. How would a comparison at a second field preparation test whether the amplitude fit is still perturbative?

▼ **Derive and check the result**

The model gives $|a_B|/R = \sqrt{2\pi}\eta$, hence $\eta = 0.0598$. This is small compared with unity, a useful first consistency check for weak low-energy scattering by a smooth single-scale potential. It does not rule out other interactions or state-dependent channels absent from this parametric model. If a controlled preparation doubles the potential amplitude without changing range, first Born predicts four times the differential intensity at every angle and the same normalised angular envelope. Failure of either scaling after calibration can reveal higher-order scattering or a changing spatial form. The test also illustrates why fitting an angular width alone is insufficient to establish that the Born approximation is controlled.

Tutorial · decide which approximation the data support

Compare exact and perturbative lengths at two well strengths

For $R = 2.00$ nm, compute a and a_B for $u = 0.50$ and 1.40. At $k = 0.020\ \mathrm{nm}^{-1}$, determine whether $4\pi a^2$ is a good low-energy cross-section estimate.

▼ **Work through the solution**

At $u = 0.50$, $a/R = 1 - \tan(0.50)/0.50 = -0.0926$, giving -0.185 nm versus -0.167 nm in Born approximation. Here $kR = 0.040$ and $k|a| \simeq 0.0037$. At $u = 1.40$, $\tan 1.40 \simeq 5.798$, giving $a = -6.28$ nm against $a_B = -1.31$ nm. Now $k|a| \simeq 0.126$; the leading unitarity denominator alone reduces $4\pi a^2$ by about 1.6%, before effective-range effects. Weak range resolution and weak scattering are separate criteria. A particle can have wavelength much larger than the target while Born approximation performs poorly.

Reconstruct interference between two partial waves

Only $l = 0, 1$ contribute, with $\delta_0 = \pi/4, \delta_1 = -\pi/6$. Find $k^2 d\sigma/d\Omega$ forward and backward and $k^2\sigma_{\mathrm{el}}$. Verify the optical theorem with the forward value.

▼ **Work through the solution**

In units of $1/k$, the s coefficient is $(1 + i)/2$, and the p coefficient multiplying $\cos\theta$ is $-3\sqrt{3}/4 + 3i/4$. Forward amplitude is roughly $-0.799 + 1.25i$, giving dimensionless intensity 2.20. Backward it is $1.799 - 0.25i$, giving 3.30. The integrated cross section is

$$4\pi[1/2 + 3(1/4)] = 5\pi.$$

The same value follows from the forward imaginary part $4\pi(1.25) = 5\pi$, whereas the forward intensity 2.20 cannot itself be substituted in the optical theorem. Phase-sensitive information survives in angular asymmetry.

Determine what a single low-energy cross section cannot tell you

An elastic isotropic sample gives $\sigma = 400\pi\ \mathrm{nm}^2$ at sufficiently low k. Infer the scattering length magnitude and propose a sign-sensitive check. What changes at $k = 0.1\ \mathrm{nm}^{-1}$?

▼ **Work through the solution**

The zero-energy relation gives $|a| = 10$ nm. The integrated cross section alone admits both signs, and the finite-k expression with zero effective range still depends only on a^2. Interference with a known reference scattering amplitude, a measured phase shift, or independent evidence for a shallow bound state together with range constraints can supply additional information. At the specified finite wave number $k|a| = 1$ the predicted cross section is $200\pi\ \mathrm{nm}^2$ when the effective range remains negligible. Fitting it with the zero-energy relation would return 7.07 nm and obscure the energy dependence.

Further reading

- Fließbach · Dreidimensionale Probleme and scattering
- Cambridge · partial waves, optical theorem and the Born expansion
- MIT 8.322 · scattering lectures 17–22

Quantum states, dynamics and measurement · 10. Distinguishing entanglement from ordinary shared randomness

Two distant analysers sometimes agree even when individual outcomes look random. Derive which correlations shared classical information can produce, compute the quantum prediction and identify what a finite table of coincidence counts can establish.

Build the full probability table for two quantum systems

Each of two separated laboratories receives one two-state system from a joint preparation. For orthonormal local bases the joint basis vectors are $|00\rangle, |01\rangle, |10\rangle, |11\rangle$. A pure state is a complex matrix of coefficients C_{ij} with $\sum_{ij} |C_{ij}|^2 = 1$. If $C_{ij} = a_i b_j$ the state is a product, and all local measurements have independent probabilities. A sum of product terms is always possible but may not factorise into one product. Singular-value decomposition $C = UDV^\dagger$ gives the Schmidt form $\sum_k s_k |u_k\rangle |v_k\rangle$, with orthonormal local bases and $s_k \geq 0,\ \sum s_k^2 = 1$. For two qubits two nonzero Schmidt numbers imply entanglement of the pure state.

Measure only the first system and sum over a complete set of results on the second. Its state is $\rho_A = CC^\dagger$, with eigenvalues s_k^2. For a globally pure state the local purity is therefore

$$\operatorname{tr} \rho_A^2 = \sum s_k^4;$$

it is one only for a product. If the global state is mixed, reduced-state impurity alone does not certify entanglement. A fifty-fifty classical mixture of $|01\rangle$ and $|10\rangle$ already has completely random local measurement results along z and perfect opposition along that axis. A second incompatible measurement arrangement is needed.

Take the singlet $|\Psi^-\rangle = (|01\rangle - |10\rangle)/\sqrt{2}$. The reduced state of either system is $I/2$. Both local means vanish for any analyser direction. Direct calculation gives $\langle \sigma_i \otimes \sigma_j \rangle = -\delta_{ij}$, or equivalently use rotational invariance and the action of each equal Pauli pair on the singlet. Measuring eigenvalues $s, t = \pm 1$ along $\mathbf{a}, \mathbf{b}$ uses product projector $(I + s\mathbf{a}\cdot\boldsymbol{\sigma}) \otimes (I + t\mathbf{b}\cdot\boldsymbol{\sigma})/4$, giving

$$P(s,t \mid \mathbf{a}, \mathbf{b}) = \frac{1 - st\,\mathbf{a}\cdot\mathbf{b}}{4},$$

$$E(\mathbf{a}, \mathbf{b}) = \sum_{s,t} stP = -\mathbf{a}\cdot\mathbf{b}.$$

Aligned analysers give complete anticorrelation; orthogonal axes give independent equiprobable results; opposite axes give complete agreement. The marginal $\sum_t P(s,t) = 1/2$ is independent of the remote axis. Conditioning on its outcome can sharpen predictions for the other system, but that conditional dataset requires the remote recorded information. For linear photon polarisation analysers the corresponding Bloch angle is twice the polariser angle, a detail that changes physical dial settings even though the probability algebra is the same.

Derive a four-setting inequality from local response functions

Suppose each emitted pair carries information λ drawn from a common distribution independent of the experimenters' analyser choices. A local shared-randomness model supplies outcomes $A, A' \in \{\pm 1\}$ at the

first location and $B, B' \in \{\pm 1\}$ at the second, depending on the local choice and on λ. Local probabilistic response can be treated by including additional random variables in this construction or by bounding their means between minus and plus one. Only one setting is actually selected at each location per run. The model nevertheless assigns responses that can be averaged under the same λ distribution for all four possible pairs.

For each assignment $A(B + B') + A'(B - B') = \pm 2$, since exactly one bracket vanishes and the other is ± 2. Averaging and using the triangle inequality yields the CHSH bound

$$|S| = |E(a, b) + E(a, b') + E(a', b) - E(a', b')| \leq 2.$$

This algebra does not assert that arbitrary measured quantum observables have pre-existing joint outcomes for incompatible settings. It specifies what a particular class of local shared-variable descriptions predicts. It also relies on comparing the same underlying source ensemble in all four settings. Outcome-dependent selection, untracked setting-dependent losses or a changing preparation can invalidate the link between the measured correlations and the inequality. Randomising settings and recording the acquisition and treatment of every event are physical parts of a meaningful experiment.

For the singlet choose $\mathbf{a} = z,\ \mathbf{a}' = x,\ \mathbf{b} = (z + x)/\sqrt{2},\ \mathbf{b}' = (z - x)/\sqrt{2}$. The first three correlations are $-1/\sqrt{2}$, the last $+1/\sqrt{2}$, giving $S = -2\sqrt{2}$. Neither local outcome becomes predictable. What exceeds the bound is a weighted combination of correlations observed in four independently chosen arrangements. A product state will never exceed it, nor will a classical probabilistic mixture of product states, since the correlations of separable preparations admit such local models.

Derive a quantum upper bound and a visibility threshold

Let A, A', B, B' now denote Hermitian operators with squared value identity at their respective locations. Construct $\mathcal{B} = A \otimes (B + B') + A' \otimes (B - B')$. Multiplying out, using the squared identities and retaining cross terms gives

$$\mathcal{B}^2 = 4I - [A, A'] \otimes [B, B'].$$

Each commutator has operator norm at most two, so $\|\mathcal{B}\| \leq 2\sqrt{2}$. The singlet settings above reach this bound. If the two candidate observables commute at either end the cross term vanishes and this construction allows no violation. Thus the upper bound and the need for local incompatibility follow from the same operator product.

Mix the singlet with uniformly random pairs,

$$\rho_v = v|\Psi^-\rangle\langle\Psi^-| + (1 - v)I/4.$$

Every product correlation becomes $-v\,\mathbf{a} \cdot \mathbf{b}$; the tested CHSH settings violate only for $v > 1/\sqrt{2}$. Entanglement itself persists farther into the noise. Transposing just the second subsystem of the singlet projector gives eigenvalues $+1/2, +1/2, +1/2, -1/2$. The smallest partial-transpose eigenvalue of the mixture is therefore $(1 - 3v)/4$. Every separable state's partial transpose is positive, since ordinary transposition preserves positivity on each product factor. Thus $v > 1/3$ certifies entanglement even where this CHSH experiment no longer violates. This argument establishes a sufficient witness from the negative eigenvalue without assuming failure of one witness proves separability.

Report correlation uncertainty using the counted events

For one arrangement write $N_{++}, N_{+-}, N_{-+}, N_{--}$ and N their sum. Estimate $E = (N_{\text{same}} - N_{\text{opposite}})/N$. Each recorded product outcome is ± 1 with variance $1 - E^2$; for independent trials a plug-in standard error is $\sqrt{(1 - \hat{E}^2)/N}$. Separate correctly randomised runs can produce independent estimation errors in the four setting groups. The variance of their signed sum then adds. Marginal balance and full tables offer checks hidden by reporting only one aggregate number. Two tables with the same E can have quite different marginal responses or efficiency problems.

Suppose each setting has 400 accepted pairs and same-result counts are $60, 64, 56, 340$, respectively. The correlations are $-0.70, -0.68, -0.72, +0.70$. Thus $S = -2.80$ and the independent-count plug-in deviation is about 0.071. That comparison is conditional on the sample construction and the independent-trial model. A full experimental Bell test also treats losses, timing, source memory and randomness of settings. A simulation drawing directly from the four Born distributions verifies the arithmetic of the prediction; agreement of its simulated S is not an independent laboratory test of the assumptions.

Use a product-basis measurement to estimate a two-qubit witness

A witness is an observable whose expectation is constrained for every separable preparation but can cross that limit for some entangled states. Consider $W = I/2 - |\Psi^-\rangle\langle\Psi^-|$. To understand the half, maximise squared singlet overlap over a product input $|a\rangle|b\rangle$. Contracting the first spin leaves an unnormalised vector on the second of norm $1/\sqrt{2}$, because the singlet's reduced state is $I/2$. Cauchy–Schwarz then bounds squared product overlap by $1/2$, with equality for appropriately opposite spinors. Any mixture of product states obeys the same bound by linearity. A measured negative $\langle W\rangle$ therefore certifies entanglement without requiring the whole state to be pure or exactly a white-noise mixture.

The singlet projector equals $[I - \sum_i \sigma_i \otimes \sigma_i]/4$, so only three equal-axis correlation settings are needed to measure this witness. Suppose independent experiments yield

$$E_{xx} = -0.55,\ E_{yy} = -0.63,\ E_{zz} = -0.74.$$

The singlet fraction is $F_s = (1 + 1.92)/4 = 0.730$ and $\langle W\rangle = -0.230$. If each correlation has standard uncertainty 0.04, independent random errors give a singlet-fraction uncertainty $\sqrt{3}(0.04)/4 = 0.0173$. Misoriented axes can bias multiple settings together, so independent statistical errors alone are not a calibration error budget. This test does not require verifying an exact isotropic visibility parameter; its bound holds across the entire separable set provided the measurements implement the stated Pauli observables.

A witness is tailored to a target. The maximally entangled $(|00\rangle + |11\rangle)/\sqrt{2}$ has zero singlet overlap, giving positive $\langle W\rangle$ rather than a violation. A known local rotation converts that state to the singlet and would make the same physical analyser scheme sensitive. Without such preparation knowledge, one can measure the full three-by-three correlation tensor and independently choose optimal axes for a separate validation run. Choosing axes to maximise a noisy estimate and then quoting naïve significance on the same data biases the result upward. Calibration, model selection and independent validation serve different roles even in an elementary two-qubit experiment.

Find the best CHSH settings from a measured correlation tensor

For a general two-qubit state define the real 3×3 matrix $T_{ij} = \mathrm{tr}[\rho(\sigma_i \otimes \sigma_j)]$. Its product correlation along unit directions is $\mathbf{a}^T T \mathbf{b}$, irrespective of the local Bloch vectors. The CHSH expression becomes

$$S = \mathbf{a}^T T(\mathbf{b} + \mathbf{b}') + \mathbf{a}'^T T(\mathbf{b} - \mathbf{b}').$$

The sum and difference of two unit vectors are perpendicular. Write them as $2\cos\theta\,\mathbf{u}$ and $2\sin\theta\,\mathbf{v}$ for orthonormal $\mathbf{u}, \mathbf{v}$ and $0 \le \theta \le \pi/2$. For fixed $\mathbf{u}, \mathbf{v}$, choose $\mathbf{a}$ parallel to $T\mathbf{u}$ and $\mathbf{a}'$ parallel to $T\mathbf{v}$ when these are nonzero. The remaining scalar maximisation gives $2\sqrt{\|T\mathbf{u}\|^2 + \|T\mathbf{v}\|^2}$.

The maximum of this sum of quadratic forms over orthonormal $\mathbf{u}, \mathbf{v}$ is the sum of the two largest eigenvalues of $T^T T$. One can see it by expanding both unit vectors in the eigenbasis: each squared projection weight summed over $\mathbf{u}, \mathbf{v}$ lies in $[0, 1]$, their sum is two, and the largest possible weighted sum fills the two largest eigenvalues. Thus $S_{\max} = 2\sqrt{s_1^2 + s_2^2}$ with s_i the singular values of T. A specific state permits a violation by projective spin measurements exactly when $s_1^2 + s_2^2 > 1$. If the singular values are near-degenerate, optimal axes may vary markedly under noise even though the best attainable S changes little.

For a concrete physical Bell-diagonal mixture take $\rho = 0.75|\Psi^-\rangle\langle\Psi^-| + 0.15|\Psi^+\rangle\langle\Psi^+| + 0.10|\Phi^+\rangle\langle\Phi^+|$, where $\Psi^\pm = (01 \pm 10)/\sqrt{2}$, $\Phi^+ = (00 + 11)/\sqrt{2}$ in ket shorthand. The respective correlation triples are $(-1,-1,-1), (1,1,-1), (1,-1,1)$. Their weighted sum is $(-0.50, -0.70, -0.80)$, giving best CHSH magnitude $2\sqrt{0.8^2 + 0.7^2} = 2.126$. If a particular apparatus sampled only the x, y plane its best value would be $2\sqrt{0.5^2 + 0.7^2} = 1.720$. The state and source are identical in both calculations; changing which axes are accessible changes what the experiment can demonstrate. A fixed set of settings optimised for an isotropic singlet might similarly underestimate an anisotropic source.

Derive the noise threshold for separability in a symmetric family

The negative partial-transpose eigenvalue proved entanglement for $v > 1/3$ in the white-noise singlet family. For this special family one can also construct a separable preparation exactly at that boundary. Average product states whose Bloch vectors point in opposite directions:

$$\rho_{\mathrm{avg}} = \int (I + \mathbf{n}\cdot\boldsymbol{\sigma}) \otimes (I - \mathbf{n}\cdot\boldsymbol{\sigma})\, d\Omega/(16\pi).$$

Symmetry gives $\langle n_i \rangle = 0$ and $\langle n_i n_j \rangle = \delta_{ij}/3$. Expanding yields $\rho_{\mathrm{avg}} = [I \otimes I - \sum_i \sigma_i \otimes \sigma_i/3]/4$, precisely the Werner singlet mixture with $v = 1/3$. Even a discrete uniform selection of the six signed Cartesian axes has the same first and second moments here. Mixture with $I/4$, itself separable, then constructs every $0 \le v \le 1/3$.

The full picture of this specific preparation family is therefore quantitative. Below and including one third it has a separable construction. Above one third it is entangled. Up to the CHSH threshold $1/\sqrt{2}$, its correlations still fail to exceed 2 in the test optimised over two spin directions per side. The gain from demanding a stronger operational certificate is a stricter threshold and potentially more demanding statistics. Failing a CHSH test in that intermediate interval does not erase the entanglement witness already derived. Conversely witnessing entanglement with trusted calibrated Pauli devices is a different experimental claim from testing a class of local causal models with explicitly addressed device and sampling assumptions.

For $v = 0.50$, the singlet fraction is $(1 + 3v)/4 = 0.625$ and the smallest partial-transpose eigenvalue is -0.125. The maximal CHSH value is $2\sqrt{2}v = 1.414$. No improvement in count precision can move these ideal mean correlations across 2 without changing the state or measurement scenario. At $v = 0.72$ the maximal value is about 2.036, technically above the threshold but small enough that repeat count and systematic uncertainties matter substantially. This comparison distinguishes identifiability from statistical power: one experiment cannot average its way through an exact theoretical bound, while a narrow permitted violation can become detectable with better data and calibration.

Compute remote conditional states while preserving no signalling

After a local measurement with operators M_a on system A, the unnormalised conditional state of B is $\tilde{\rho}_{B|a} = \mathrm{tr}_A[(M_a \otimes I)\rho_{AB}(M_a^\dagger \otimes I)]$. Its trace is the probability of the local outcome; dividing by that trace gives the conditional state. Summing over all outcomes and using $\sum_a M_a^\dagger M_a = I$ under the partial trace returns ρ_B. The result holds for any complete local instrument, including a nonprojective measurement with forgotten outcomes. A remote observer lacking the classical label sees exactly the same state as before. Conditioning becomes operational only when the two records can be compared.

For the singlet, if A measures direction $\mathbf{a}$ sharply and obtains $+1$, B's conditional Bloch vector is $-\mathbf{a}$; outcome -1 gives $+\mathbf{a}$. In the white-noise mixture those vectors shrink to $\mp v\mathbf{a}$, while each outcome remains equally probable. If the remote partner groups trials by A's announced result and measures along a fixed $\mathbf{b}$, it recovers the same conditional probabilities as the original correlation formula. Without that grouping the two opposite vectors average to zero for every $\mathbf{a}$. This calculation distinguishes a physical method for remotely preparing an ensemble conditional on communication from a method for sending a chosen bit by merely varying the local measurement angle.

A delayed readout changes none of these predicted coincidences because local operators $M_a \otimes I$ and $I \otimes M_b$ commute at the level of this separated systems model. The order in which a data analyst applies conditional probability does change which denominator appears in a finite table. In a test with imperfect detectors, report whether a conditional rate divides by all local triggers, all heralds or only coincidences. Setting-dependent missing events can make a conditional table look no-signalling or strongly correlated for purely sampling reasons. A transparent acquisition protocol preserves the correspondence between the Born joint probabilities being predicted and the ensemble included in their statistical test.

Test which preparations and settings exceed a CHSH bound

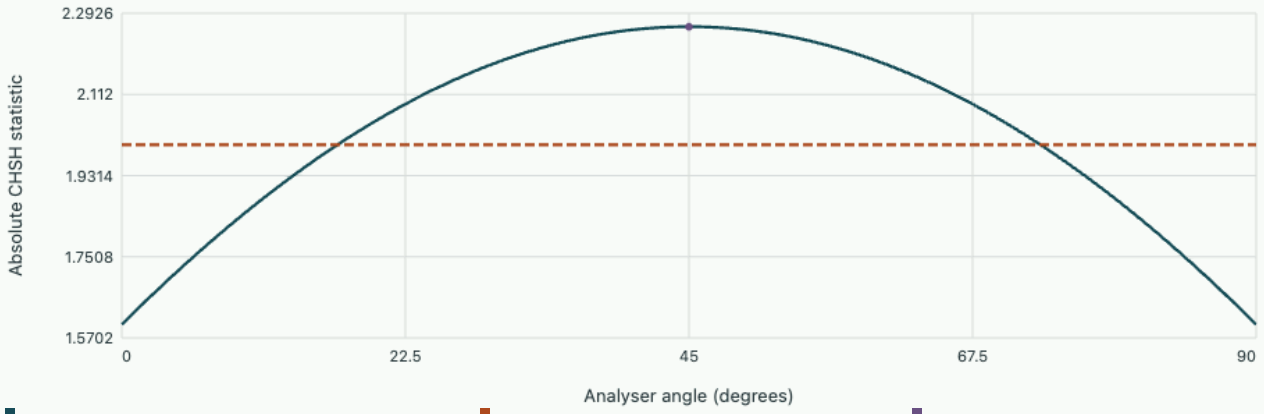
Vary analyser angle and visibility independently. Compare the expected joint statistic with the fluctuation scale of a finite counting experiment.

Open this experiment online

Try the calculation

Preparation visibility **0.8**

Symmetric analyser angle (degrees) **45**



Singlet with unpolarised admixture | Local binary assignment bound | Selected angles

Predicted |S| = 2.2627. With these angles the visibility required to reach two is 0.70711.

Build an entangled pair by conditioning two independent sources

Entanglement is a property of a joint preparation, not a permanent label attached to an individual particle. A four-qubit example illustrates how changing which outcomes are retained can create new conditional pair correlations. Prepare A, B in $|\Phi^+\rangle = (|00\rangle + |11\rangle)/\sqrt{2}$ and independently prepare C, D in the same Bell state. Before any further measurement the reduced preparation of A, D is $I/4$ because the two sources are independent and each outer qubit is individually maximally mixed. A separate central apparatus receives B, C and measures in the Bell basis. The correct prediction after this operation depends on whether its recorded result is available.

Expand the initial state in the order $A, D; B, C$, then use the identity expressing products $|00\rangle, |11\rangle$ as sums and differences of $\Phi^\pm$ and $|01\rangle, |10\rangle$ as sums and differences of $\Psi^\pm$. Regrouping gives

$$|\Phi^+\rangle_{AB}|\Phi^+\rangle_{CD} = \frac{1}{2}\sum_{Q\in\{\Phi^+,\Phi^-,\Psi^+,\Psi^-\}} |Q\rangle_{AD}|Q\rangle_{BC}$$

for the consistent real Bell basis used here. The norm stays one because the four central labels are orthogonal. Each central result occurs with probability one quarter. Given a particular result Q, the two outer systems are jointly in Q, even though they came from independent sources and did not directly interact. Ignoring the central result leaves an equally weighted Bell mixture $I/4$, the same outer reduced state as before. Conditioning, or applying a known local Pauli correction using the central label, is necessary to expose a consistent set of Bell correlations in the outer records.

For example, central outcomes Φ^+ and Φ^- both predict equal outer z outcomes, whereas Ψ^+ and Ψ^- predict opposite. In the x basis their signs follow a different pattern. A central device reporting only the parity of its z outcomes distinguishes the Φ from the Ψ subspace but cannot distinguish their relative phases. Conditioned on even parity alone the outer state is $(|\Phi^+\rangle\langle\Phi^+| + |\Phi^-\rangle\langle\Phi^-|)/2$, identical to the classical

mixture of $|00\rangle$ and $|11\rangle$. The very same perfect z correlation therefore has different implications for a resolved Bell label and a mere parity label. What the central device physically measures is essential background for interpreting the outer data.

Quantify how central-label mistakes change outer Bell contrast

Suppose the central Bell outcome is reported correctly with probability q, and otherwise is replaced by each of the three wrong labels with equal probability. The outer parties apply Pauli corrections based on the reported label to target Φ^+. Derive the effective visibility and threshold for a two-setting Bell violation.

▼ **Derive and check the result**

Because every correct label yields the target and wrong Pauli corrections map it to the other three orthogonal Bell states, the corrected outer ensemble is Bell diagonal with target weight q and equal wrong weights $(1-q)/3$. Comparing with $v|\Phi^+\rangle\langle\Phi^+| + (1-v)I/4$ gives $q = (1+3v)/4$, so $v = (4q-1)/3$. In the useful regime $q \geq 1/4$ the maximal CHSH value is $2\sqrt{2}(4q-1)/3$, above two when $q > (1+3/\sqrt{2})/4 = 0.7803$. At $q = 0.85$ the visibility is 0.80 and the best value is about 2.263. Central efficiency and central label fidelity affect different things: if losses are independent, lower efficiency reduces the number of heralded events, while wrong labels reduce conditional contrast. In a realistic inference, setting dependence of losses or an imperfect outer measurement must also be checked before assigning all observed contrast loss to central reporting errors.

Compare local entropy, global entropy and shared classical information

For a density matrix ρ with eigenvalues p_i, define von Neumann entropy in bits by $S(\rho) = -\sum_i p_i \log_2 p_i$, interpreting the zero-eigenvalue term by continuity. For a pure bipartite state the two reduced spectra agree by Schmidt decomposition, so both reduced entropies equal the binary or multi-outcome entropy of the squared Schmidt coefficients. This is an operationally meaningful measure of entanglement for a pure bipartite preparation. For a mixed state, local entropy also contains ordinary uncertainty due to forgotten preparation records and cannot by itself quantify entanglement.

A singlet has $S(AB) = 0,\ S(A) = S(B) = 1$. The equally weighted unentangled anticorrelation mixture $[|01\rangle\langle 01| + |10\rangle\langle 10|]/2$ has $S(AB) = 1$ and the same local entropies. Completely uncorrelated white noise $I/4$ gives $S(AB) = 2$ and still the same local values. Their quantum mutual informations $S(A) + S(B) - S(AB)$ are respectively 2, 1 and 0 bits. The two bits for a singlet do not mean each party receives two freely readable classical bits in a single spin measurement. With aligned local measurements the observed binary records share one bit, while the full quantum mutual information is a property of the joint density operator across all possible probes.

Infer entanglement entropy and contrast for a pure pair

A calibrated pure source has squared Schmidt coefficients $0.90, 0.10$. Find local entropy and compare the strongest CHSH value in its Schmidt basis with that of an incoherent mixture of its two Schmidt product states. Which part of the global description changes after completely dephasing one subsystem in the Schmidt basis?

▼ **Derive and check the result**

The pure-pair entanglement entropy is the binary value $-0.9\log_2(0.9) - 0.1\log_2(0.1) = 0.469$ bits. Write $\cos^2\theta = 0.9$, giving $\sin 2\theta = 2\sqrt{0.09} = 0.60$, and the best CHSH value $2\sqrt{1+0.60^2} = 2.332$. Complete dephasing removes off-diagonal coherence between the two global Schmidt products and leaves their same classical weights. The marginals and local entropies stay exactly the same. The global entropy rises from zero to 0.469 bits; the correlation tensor has only its longitudinal component of unit magnitude and hence best CHSH value two. Comparing these examples shows precisely which physical information is lost when a preparation record or coherent relative phase becomes inaccessible, and why an unchanged local entropy can coexist with a changed experimentally accessible joint correlation.

Tutorial · determine exactly what correlations identify

Distinguish a singlet from classical anticorrelation

Compare the singlet with an equally weighted mixture of $|01\rangle, |10\rangle$. Compute $E(z,z), E(x,x)$ and $E(z,x)$ for both. Which measurement distinguishes them?

▼ **Work through the solution**

The singlet gives $-1, -1, 0$ respectively. In the mixture each prepared product has perfect z opposition, but individual states measured along x have zero mean. Product outcomes factor on each component, so $E(x,x) = 0$ and $E(z,x) = 0$. Measuring just $E(z,z)$ cannot distinguish the two; $E(x,x)$ does. Distinguishing two named hypotheses with one extra setting does not establish a CHSH violation against all local shared-randomness models. The hypotheses and tested claim determine the required data.

Determine a partially entangled state's best planar settings

Let $|\psi\rangle = \cos\theta|00\rangle + \sin\theta|11\rangle$. Use first-side settings z, x and second-side $\mathbf{b}, \mathbf{b}' = (\pm\sin\alpha, 0, \cos\alpha)$, with the plus sign assigned to $\mathbf{b}$. Optimise S.

▼ **Work through the solution**

The correlation tensor in the x, z plane has entries $T_{zz} = 1,\ T_{xx} = \sin 2\theta$ and vanishing cross terms. Therefore $S = 2[\cos\alpha + \sin 2\theta\ \sin\alpha]$. Maximisation gives $\tan\alpha = \sin 2\theta$ and $S_{\max} = 2\sqrt{1+\sin^2 2\theta}$ for these directions. At $\theta = \pi/12$ it is $\sqrt{5} = 2.236$, at a product endpoint it is 2, and at the maximally entangled midpoint $2\sqrt{2}$. The optimising dial settings depend on the state; a poorly chosen apparatus can miss an available violation.

Estimate the needed pair count for a visibility-limited test

Take $v = 0.80$ at the ideal singlet CHSH settings and assume equal independent counts per setting. Estimate the number per setting for a nominal five-standard-error separation from 2. What limits this calculation?

▼ **Work through the solution**

The predicted excess is $2\sqrt{2}v - 2 = 0.2627$. Each product mean has magnitude $v/\sqrt{2}$, so

$$\operatorname{sd} S = 2\sqrt{(1 - v^2/2)/N} = 1.649/\sqrt{N}.$$

Requiring the excess to exceed five such deviations gives $N \gtrsim 986$ pairs per setting. This is a planning estimate using Gaussian independent-sample errors and known visibility. It is not a complete finite-sample hypothesis test and gives no protection against systematic errors or outcome-dependent postselection. Report the four realised counts along with acquisition, losses and uncertainty rather than presenting the planned count as guaranteed evidence.

Further reading

- Cambridge · quantum foundations, Bell inequalities and density matrices
- Course investigation · spin correlations in composite states
- Fließbach · Mehrteilchensysteme

Quantum states, dynamics and measurement · 11. How an unobserved environment changes a quantum state

Model a qubit and a two-state environment by a joint unitary. Derive channels, the continuous-time master equation and the relation between longitudinal and transverse relaxation. A recorded event and an unread detector produce different conditional predictions.

Derive loss of coherence from a larger unitary system

A qubit prepared in $\alpha|0\rangle + \beta|1\rangle$ interacts with an environment initially in $|e\rangle$. A joint unitary correlates $|0, e\rangle \to |0, e_0\rangle,\ |1, e\rangle \to |1, e_1\rangle$, with both environmental states normalised. The joint output is a pure state. Its qubit density matrix follows by tracing over a complete environment basis. Populations stay $|\alpha|^2, |\beta|^2$. The off-diagonal entry is $\alpha\beta^*\langle e_1|e_0\rangle$. Orthogonal environment records remove coherence from all local qubit observations; identical records leave its magnitude intact. Partial distinguishability gives a continuous range in between. Energy need not flow in this controlled dephasing model. An observed reduction in fringe contrast can arise from entanglement with unobserved degrees of freedom even when total evolution is unitary.

Consider instead amplitude loss from an excited qubit to an initially empty environment mode:

$$|0, 0_e\rangle \mapsto |0, 0_e\rangle, \qquad |1, 0_e\rangle \mapsto \sqrt{1-p}|1, 0_e\rangle + \sqrt{p}|0, 1_e\rangle.$$

The two output states remain orthogonal and unit-normalised, so this map on the prepared environment subspace can be extended to a unitary on the full joint space. If environment state k is unobserved, sum the associated unnormalised alternatives in density-matrix form:

$$\rho' = \sum_k K_k \rho K_k^\dagger.$$

Here $K_0 = |0\rangle\langle 0| + \sqrt{1-p}|1\rangle\langle 1|$ and $K_1 = \sqrt{p}|0\rangle\langle 1|$. Since $\sum K_k^\dagger K_k = I$, trace is preserved. The excited population obeys $\rho'_{11} = (1-p)\rho_{11}$ and the coherence $\rho'_{01} = \sqrt{1-p}\rho_{01}$. Averaging state vectors before forming outer products would introduce interference between orthogonal environmental records that have already been traced out.

Take a controlled infinitesimal limit

In a memoryless approximation each small interval dt meets a fresh environment record with vanishing probability of a previously lost excitation returning. Let jump operators L_j have units $1/\sqrt{\mathrm{s}}$, set $K_j = \sqrt{dt}\, L_j$ for events and $K_0 = I - dt(iH/\hbar + \sum L_j^\dagger L_j/2)$. Expanding the completeness relation shows trace preservation through first order in dt. Expand $\sum K_k \rho K_k^\dagger - \rho$, divide by dt and keep the finite terms:

$$\frac{d\rho}{dt} = -\frac{i}{\hbar}[H, \rho] + \sum_j \left(L_j \rho L_j^\dagger - \tfrac{1}{2} L_j^\dagger L_j \rho - \tfrac{1}{2} \rho L_j^\dagger L_j \right).$$

The first term of each dissipative bracket adds probability after an event and the anticommutator subtracts probability from the no-event branch. Their traces cancel. This construction is completely positive, meaning that the same local channel remains positive even when tensored with identity on an unused entangled

ancilla. Positivity only on isolated input states would be too weak: transposition maps density matrices to density matrices on a single system, yet partial transposition can produce a negative eigenvalue when applied to half an entangled pair. The Lindblad form embodies the relevant stronger constraint for the assumed Markovian dynamics.

Independent loss and pure dephasing can be represented by $L_1 = \sqrt{\Gamma_1}|0\rangle\langle 1|$,

$$L_\phi = \sqrt{\Gamma_\phi/2}\,\sigma_z.$$

The factor one half in the dephasing operator fixes our convention for Γ_ϕ. Direct substitution gives $\dot\rho_{11} = -\Gamma_1\rho_{11}$, while $\dot\rho_{01}$ acquires $-(\Gamma_1/2 + \Gamma_\phi)\rho_{01}$ in addition to its Hamiltonian phase. Thus

$$T_1 = \Gamma_1^{-1},$$

$$T_2^{-1} = (2T_1)^{-1} + \Gamma_\phi.$$

At zero temperature with these mechanisms, $T_2 \le 2T_1$. This upper bound is tied to definitions and assumptions. A broad ensemble with static detuning spread, a driven nonequilibrium sample or a refocused pulse sequence may yield an observed envelope with a different shape and timescale. Fitting every contrast decay with one exponential and interpreting that number as the homogeneous T_2 can assign an unphysical dephasing rate.

Update a state when an individual event is recorded

If an ideal detector reports branch j, the probability is $p_j = \operatorname{tr} K_j\rho K_j^\dagger$, and the normalised conditional output is $K_j\rho K_j^\dagger/p_j$. The conditional evolution depends on which environment observable is measured; summing outcomes gives the same physical unconditioned channel. In the loss model, detecting one emission places the qubit in its ground state. Absence of an emission also carries information. At finite duration t, no emission acts by $K_0 = |0\rangle\langle 0| + e^{-\Gamma_1 t/2}|1\rangle\langle 1|$ for the simple undriven zero-temperature case.

From initial $(|0\rangle + |1\rangle)/\sqrt{2}$, at $t = T_1 \ln 2$ the no-event probability is

$$(1 + 1/2)/2 = 3/4.$$

Conditional excited probability is

$$(1/2)/(1 + 1/2) = 1/3.$$

With the event branch in the ground state, the unconditioned excited probability is $(3/4)(1/3) = 1/4$, agreeing with exponential decay of its initial one half. Repeatedly renormalising only no-event trajectories and calling their mean the ensemble population would overestimate survival. If the event detector misses photons, “no click” groups genuine no-emission with undetected emissions and its conditional state is generally mixed.

Use heating and cooling to infer the reservoir

Allow upward and downward transitions at rates $\Gamma_\uparrow, \Gamma_\downarrow$. Rate equations give

$$\dot{p}_1 = \Gamma_\uparrow(1 - p_1) - \Gamma_\downarrow p_1,$$

$$p_{1,\infty} = \frac{\Gamma_\uparrow}{\Gamma_\uparrow + \Gamma_\downarrow},$$

$$p_1(t) = p_{1,\infty} + [p_1(0) - p_{1,\infty}]e^{-(\Gamma_\uparrow + \Gamma_\downarrow)t}.$$

Both upward and downward rates contribute half their sum to coherence decay. If the reservoir is in thermal equilibrium, detailed balance gives

$$\Gamma_\uparrow/\Gamma_\downarrow = e^{-\hbar\omega/(k_B T)}.$$

The population relaxation time measures their sum and equilibrium population measures their ratio, allowing a substantive check of a proposed bath temperature. The relation is a thermodynamic assumption in addition to the two-state rate model. A pumped bath can have the same measured relaxation time with an entirely different stationary population.

For a 5.00 GHz transition, $\hbar\omega/k_B = h(5\,\mathrm{GHz})/k_B \simeq 0.240$ K. A stationary excited fraction 0.10 would imply $T = 0.240/\ln 9 = 0.109$ K under equilibrium. With population relaxation 20 µs the sum of rates is $5.0 \times 10^4\,\mathrm{s}^{-1}$, giving 5000 upward and $45\,000$ downward transitions per second for the respective source populations. Verified independent upward and downward preparations test more than fitting the decay of an initially excited state alone.

Discriminate static detuning, Markovian dephasing and coherent error

A Ramsey experiment prepares an equal superposition, allows free evolution for time t, then converts relative phase to a population by a final analysis pulse. If the detuning δ is fixed in each run but varies randomly between runs, then the ensemble coherence is multiplied by the characteristic function $C(t) = \int p(\delta)e^{-i\delta t}d\delta$. Here δ is an angular frequency. For a Gaussian detuning of mean δ_0 and standard deviation σ,

$$C = e^{-i\delta_0 t}e^{-\sigma^2 t^2/2}.$$

A uniform detuning offset shifts fringe phase without reducing the contrast of a fully coherent, identically repeated preparation. A Lorentzian distribution yields an exponential envelope which can resemble homogeneous Markovian dephasing in a simple time scan. The fitted functional form alone may therefore fail to identify the physical cause of lost contrast.

An ideal instantaneous π pulse about x halfway through free evolution reverses the effect of a static z-detuning on relative phase: $e^{-i\delta t\sigma_z/4}\sigma_x e^{-i\delta t\sigma_z/4} = \sigma_x$, since σ_x anticommutes with σ_z. All static offsets refocus at the echo. Independent white Markovian dephasing accumulated in each half is uncorrelated and cannot be undone in this way. The deterministic Hamiltonian error and a rapidly fluctuating environment can share a short Ramsey contrast while giving different echo contrasts. If the pulse itself has finite duration or an angle error, the algebraic cancellation is no longer exact; repeating at two pulse powers tests that particular assumption.

Take $\sigma/2\pi = 20.0$ kHz and negligible damping. At $t = 10.0\,\mu$s the free Ramsey contrast from Gaussian detuning alone is

$$e^{-(1.257)^2/2} = 0.454.$$

An ideal echo returns unity. Add independent $T_1 = 80\,\mu$s, $T_\phi = 50\,\mu$s. The homogeneous coherence time is

$$[1/(160\,\mu\text{s}) + 1/(50\,\mu\text{s})]^{-1} = 38.1\,\mu\text{s}.$$

The expected echo contrast is now $e^{-10/38.1} = 0.769$ and the ordinary Ramsey contrast 0.349. A single fitted T_2^* cannot display these three separate timescales. Measuring populations, Ramsey fringes and echoes on consistent ensembles gives three complementary observables with independently interpretable limits.

For a time-dependent classical detuning $\delta(t)$, pulse sequences choose a modulation $y(t) = \pm 1$ multiplying the noise phase. The phase error is

$$\phi = \int y(t)\delta(t)dt.$$

For stationary zero-mean Gaussian noise, $\langle e^{-i\phi}\rangle = e^{-\langle\phi^2\rangle/2}$ and the variance is a double integral of the noise correlation weighted by $y(t)y(t')$. Equivalently it is the spectral integral of the power density weighted by $|\int y(t)e^{i\omega t}dt|^2$, with the normalisation set by the chosen two-sided Fourier convention. A single echo has zero weight at $\omega = 0$ because its two half integrals cancel, while keeping finite-frequency sensitivity. Families of pulse spacings can therefore probe noise timescales rather than simply fitting larger and larger numbers to a nominal coherence time.

Find the damped saturation curve from optical Bloch equations

A continuously driven qubit has an additional route to separate population and coherence relaxation. In a rotating frame let $H = \hbar(\Omega\sigma_x + \Delta\sigma_z)/2$, with $z = p_e - p_g$, equilibrium $z_{\text{eq}} = -1$ at zero temperature, and transverse damping $1/T_2$. Choose a consistent Bloch basis so the commutator gives the cross product of $(\Omega, 0, \Delta)$ with (x, y, z). The equations are

$$\dot{x} = -\Delta y - x/T_2,$$
$$\dot{y} = \Delta x - \Omega z - y/T_2,$$
$$\dot{z} = \Omega y - (z - z_{\text{eq}})/T_1.$$

At steady state the first equation gives

$$x = -\Delta T_2 y.$$

The second then gives

$$y = -\Omega T_2 z/(1 + \Delta^2 T_2^2).$$

Inserting into the third gives

$$z = z_{\mathrm{eq}}/[1 + \Omega^2 T_1 T_2/(1 + \Delta^2 T_2^2)].$$

Thus the excited fraction for $z_{\mathrm{eq}} = -1$ is

$$p_{e,\infty} = \frac{\Omega^2 T_1 T_2}{2[1 + \Delta^2 T_2^2 + \Omega^2 T_1 T_2]}.$$

A weak resonant drive gives a population proportional to its power, and a strong continuous drive saturates toward one half rather than preparing a permanently inverted state. Coherent π-pulse inversion is a transient unitary process; continuous steady balance with relaxation gives a different preparation. The full angular-frequency width at half of the on-resonance excitation is $2\sqrt{1 + \Omega^2 T_1 T_2}/T_2$, so increasing power broadens the line even at unchanged intrinsic T_2.

Choose $T_1 = 20$ µs, $T_2 = 16$ µs and resonant $\Omega/2\pi = 10$ kHz. The saturation parameter is

$$s = \Omega^2 T_1 T_2 = 1.26.$$

The stationary excited fraction is $s/[2(1 + s)] = 0.279$, and the ordinary-frequency full width is

$$\sqrt{1 + s}/(\pi T_2) = 29.9\,\mathrm{kHz}.$$

At very low drive it would be 19.9 kHz. A measured linewidth that increases approximately as the square root of power at high drive can have this coherent saturation origin without any increase in the environment's pure-dephasing rate. Comparing the zero-power linewidth extrapolation with an independent time-domain T_2 is a stronger test than fitting a single apparent line broadening.

Connect an individual event stream to an ensemble lifetime

The lifetime T_1 of one excited qubit is a distribution of observed emission times across many trials. With perfect detection, no drive and initially excited state, survival $S(t) = e^{-\Gamma t}$ implies waiting-time density $w(t) = -dS/dt = \Gamma e^{-\Gamma t}$. The mean waiting time and standard deviation are both $1/\Gamma$. A no-click trajectory stays in the excited state conditionally until its first emission when the initial preparation is certainly excited. Its unnormalised weight decays exponentially, but assigning every no-click trajectory a continuously decreasing normalised excitation would confuse conditional and unconditioned statements. For an initial superposition the absence record instead changes the normalised state as derived earlier.

Real acquisitions may stop each trial at a fixed deadline T_{stop}. Treating all no-click trials as though they emitted exactly at the deadline biases lifetime inference. For n observed emissions at times t_j and m censored trials with no emission through T_{stop}, the likelihood is proportional to $\prod_{j=1}^{n} \Gamma e^{-\Gamma t_j} \prod_{k=1}^{m} e^{-\Gamma T_{\mathrm{stop}}}$. Optimising gives

$$\hat{\Gamma} = n/(\sum_j t_j + m T_{\mathrm{stop}}).$$

The numerator is actual events and the denominator all time observed at risk. For 40 detections totalling 480 µs and 10 additional censored runs each observed 30 µs, the estimate is $40/780 = 0.0513\,\mu\mathrm{s}^{-1}$, or

$T_1 \simeq 19.5\,\mu s$. Discarding the censored runs instead would report 12 µs from the mean detected delay. This statistical correction follows directly from the same physical survival law used for the quantum channel.

Detection inefficiency can cause a different data problem. In a single-excitation undriven trial, a missed decay leaves a qubit in its ground state and unable to emit again. The probability of no registered event up to t is $1 - \eta[1 - e^{-\Gamma t}]$ at constant efficiency η, with a nonzero late plateau $1 - \eta$. It is not $e^{-\eta\Gamma t}$, which would describe thinning a renewable stationary Poisson event stream. Long-time survival of the recorded count and independent final-state readout can distinguish a missed emission from a genuinely long-lived excitation. This example shows why the detector model must specify whether events can repeat after one has been missed.

Audit a reconstructed Pauli noise channel

Suppose three independently prepared Bloch components appear to shrink by factors $\lambda_x, \lambda_y, \lambda_z$ after a calibrated waiting time, with no displacement of the centre. A diagonal unital qubit channel can be written $\mathcal{E}(\rho) = \sum_{\nu=0,x,y,z} p_\nu \sigma_\nu \rho \sigma_\nu$ for a physical Pauli mixture. Expanding its action on the three axes and inverting gives

$$p_0 = (1 + \lambda_x + \lambda_y + \lambda_z)/4,$$
$$p_x = (1 + \lambda_x - \lambda_y - \lambda_z)/4,$$

with cyclic partners for p_y, p_z. Complete positivity demands all four numbers be nonnegative. Checking each $|\lambda_i| \le 1$ only checks lengths along single Bloch axes and, for this diagonal map, positivity on a single qubit. It does not guarantee that the reconstructed operation is consistent on half of an entangled system.

For $\lambda = (0.9, 0.9, 0.5)$, every axis appears to shrink, yet $p_z = (1 - 0.9 - 0.9 + 0.5)/4 = -0.075$. Thus the exact diagonal unital channel inferred from those numbers is not completely positive. Finite measurement noise, neglected affine offsets or changing preparation could be responsible. Compare the fit with uncertainty regions and a constrained process model; simply forcing each measured contraction coefficient into $[-1, 1]$ cannot repair this violation. As a constructive control, $\lambda = (0.8, 0.7, 0.6)$ gives $p_0 = 0.775,\ p_x = 0.125,\ p_y = 0.075,\ p_z = 0.025$, all valid and summing to one. A simulator using these four random Pauli operations on entangled inputs then supplies a direct check of the estimated channel beyond single-qubit positivity.

Test how a coherence measurement depends on an ensemble

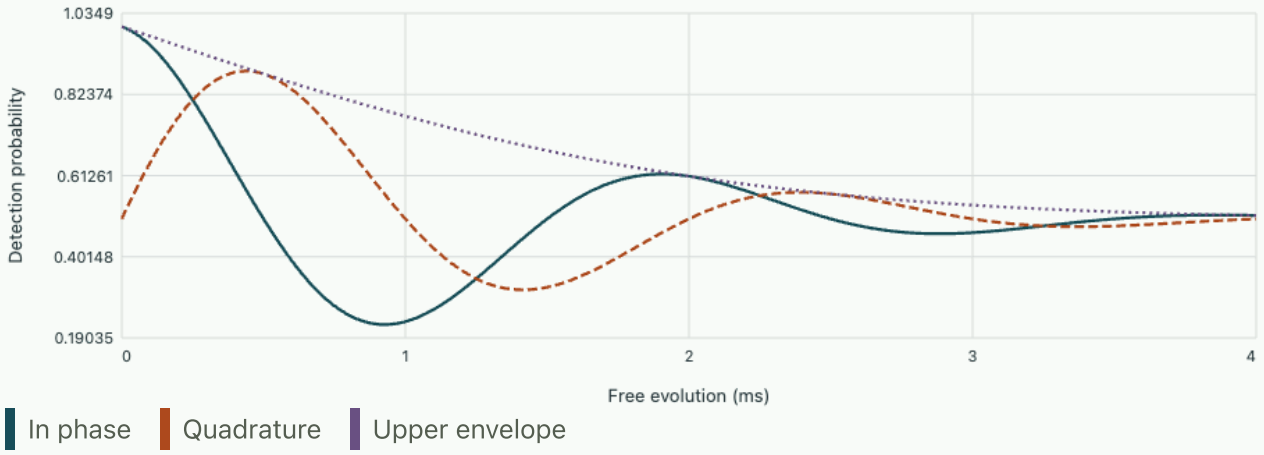
Compare quasistatic frequency spread with homogeneous decay in a Ramsey sequence. Identify which further measurement could distinguish the mechanisms.

Open this experiment online

Try the calculation

Mean cyclic detuning (Hz) **500**

Shot-to-shot rms spread (Hz) **80**



Contrast after 1 ms = 0.53455. The two probabilities at 0.50 ms are 0.5 and 0.87729.

Prove when two different event descriptions give the same channel

A given unconditioned quantum operation does not determine a unique set of environmental records. Suppose a set of Kraus operators K_j describes a channel. If an environment detector resolves an alternative orthonormal basis related by unitary $U = (u_{\alpha j})$, its new system operators are $\tilde{K}_\alpha = \sum_j u_{\alpha j} K_j$. Summing the unnormalised conditional outputs gives

$$\sum_{\alpha,j,k} u_{\alpha j} u^*_{\alpha k} K_j \rho K_k^\dagger = \sum_j K_j \rho K_j^\dagger .$$

This calculation explains why environment-dependent state trajectories can be quite different while every unconditioned prediction on the system agrees. A simulator's choice of individual jump records only describes a particular monitoring scheme when the environment observable actually corresponds to those records.

Consider complete dephasing in the z basis. One representation is $K_0 = |0\rangle\langle 0|,\ K_1 = |1\rangle\langle 1|$, an ideal path measurement with its result forgotten. Rotate the two environment labels by the Hadamard matrix to obtain

$$\tilde{K}_+ = (I/\sqrt{2}),\ \tilde{K}_- = (\sigma_z/\sqrt{2}).$$

These describe equally likely identity or phase-flip operations. For input $|+x\rangle$, the first recorded instrument conditionally gives $|0\rangle$ or $|1\rangle$; the second gives $|+x\rangle$ or $|-x\rangle$. Both produce $I/2$ if their outcome is ignored. For initial $|0\rangle$ the first record is deterministic, while the second remains equally random and leaves the state unchanged up to a phase. Measuring only the system after discarding the labels cannot tell which set was used, but correlations with a retained environmental measurement can immediately tell them apart.

The same distinction is useful for a partially dephasing environment. If $|0\rangle, |1\rangle$ become correlated with environment states of real overlap c, the qubit's transverse Bloch vector contracts by c. For $-1 \le c \le 1$ a random phase-flip representation has probabilities $p_I = (1+c)/2,\ p_Z = (1-c)/2$. For $c < 0$ a fringe phase reversal accompanies partial contraction; a reported positive “visibility” loses that sign. One can separate a deterministic phase rotation from the magnitude of random or entangling dephasing if the phase reference is maintained. Over independent identical intervals a real c multiplies repeatedly; the coherence after n steps is c^n. If the same randomly chosen phase flip is instead held fixed throughout all intervals, successive errors are correlated and the even-step coherence can return to one. A single-step channel tomography cannot identify the environmental memory shared across steps.

Tell apart a memoryless phase-flip channel and a fixed hidden phase

Both devices individually implement $p_Z = 0.20$ over a calibrated interval for freshly prepared qubits. In device A the phase-flip draws at successive intervals are independent. In device B one draw is held fixed for both consecutive intervals. Predict $+x$ readout after one and two intervals for an initial $|+x\rangle$.

▼ **Derive and check the result**

One interval leaves $x = 1 - 2p_Z = 0.60$, so both devices give

$$P(+x) = 0.80.$$

Independence in A gives $x = 0.60^2 = 0.36$ after two intervals, or $P(+x) = 0.68$. For B, two identical phase flips multiply to identity whether the hidden choice was identity or Z, hence $P(+x) = 1$. In both devices the one-step process applied to an independently prepared ensemble is consistent with the measured completely positive map. Composing that map twice implicitly assumed fresh, independent environment conditions; a memory experiment tests exactly that assumption. Observing a revival thus need not imply an energy input, a negative probability or a nonunitary failure in the larger coupled system.

Distinguish dipole coherence from an excited-state population lifetime

Consider a single initially excited emitter in a memoryless zero-temperature environment with radiative population decay Γ and no additional dephasing. The probability density of emitting at time $t \ge 0$ is $\Gamma e^{-\Gamma t}$. A normalised single-photon temporal mode consistent with this ideal undistinguished radiative channel is $g(t) = \sqrt{\Gamma}\, e^{-\Gamma t/2} e^{-i\omega_0 t}$ on $t \ge 0$. Its field amplitude decays twice as slowly as the population probability. Use the Fourier convention $\tilde{g}(\omega) = (2\pi)^{-1/2} \int g(t) e^{i\omega t} dt$. The half-line exponential integral gives

$$|\tilde{g}(\omega)|^2 = \frac{\Gamma}{2\pi[(\Gamma/2)^2 + (\omega - \omega_0)^2]}.$$

It integrates to one in angular frequency. At a detuning of $\Gamma/2$ the intensity has half its peak, so the full angular-frequency linewidth is Γ, or $\Gamma/(2\pi)$ in hertz. Using the population decay directly as a field amplitude would predict a linewidth twice too large and the wrong wave-packet envelope. The transform-limited result requires a single radiative mode in the sense of a pure emitted temporal state and absence of additional

phase randomisation. Extra pure dephasing broadens the spectrum while population decay may remain unchanged.

For $\Gamma^{-1} = 10.0$ ns the ideal linewidth is 15.9 MHz. Add independent homogeneous pure dephasing at $\Gamma_\phi = 2.0 \times 10^7\ \mathrm{s}^{-1}$. The first-order dipole correlation decays at $\Gamma/2 + \Gamma_\phi$, giving a full line width $(\Gamma/2 + \Gamma_\phi)/\pi = 22.3$ MHz. The photon detection time distribution can still have 10 ns decay. A measured line twice its nominal transform-limited width might indicate pure dephasing, but spatially varying frequencies, slow source drift or spectral resolution can also broaden the observed distribution. A lifetime measurement alone does not calibrate those effects.

The acquisition window has an independently calculable consequence. If only photons arriving before time T are retained, their normalised temporal mode is a truncated exponential divided by $\sqrt{1 - e^{-\Gamma T}}$ in this ideal pure-emission model. Its Fourier amplitude gains factor $1 - e^{-[\Gamma/2 - i(\omega - \omega_0)]T}$ in the numerator. At $T \ll 1/\Gamma$ the shape approaches the squared sinc of a short rectangular temporal window. Selecting only early photons can thus broaden the spectrum even though the emitter and its environment are unchanged. A time gate, an energy filter and unconditioned counting describe different optical preparations and different uncertainty budgets.

Infer the transform-limited fraction from a linewidth and test the model

A homogeneous line has measured weak-drive full width 25.0 MHz and population lifetime 10.0 ns. Compute T_2 and the implied pure dephasing rate assuming ideal Lorentzian broadening. Which second measurement would discriminate this inference from static sample inhomogeneity?

▼ **Derive and check the result**

With angular half width $1/T_2$, the frequency full width is $1/(\pi T_2)$, so $T_2 = 12.73$ ns. Subtracting $1/(2T_1) = 5.00 \times 10^7\ \mathrm{s}^{-1}$ from $1/T_2 = 7.85 \times 10^7\ \mathrm{s}^{-1}$ gives

$$\Gamma_\phi = 2.85 \times 10^7\ \mathrm{s}^{-1}.$$

The coherence relative to the radiative limit is

$$T_2/(2T_1) = 0.637.$$

Compare a time-domain echo, a single-emitter linewidth or spectra over short acquisition segments with the ensemble line. A recoverable component of contrast or slowly wandering line centres would indicate a static or slow contribution instead of assigning every megahertz to homogeneous phase damping.

Tutorial · distinguish different sources of coherence loss

Recover a pure-dephasing rate and assess a conflicting fit

A population measurement gives

$$T_1 = 30.0\,\mu\mathrm{s};$$

homogeneous Ramsey contrast gives

$$T_2 = 24.0\,\mu\mathrm{s}.$$

Find T_ϕ. What would a reported $T_2 = 80\,\mu$s imply in the same model?

▼ **Work through the solution**

Subtract $1/(60\,\mu\mathrm{s})$ from $1/(24\,\mu\mathrm{s})$ to get $\Gamma_\phi = 0.0250\,\mu\mathrm{s}^{-1}$, hence $T_\phi = 40.0\,\mu$s. Replacing 24 by 80 yields a negative pure dephasing rate, incompatible with the specified independent time-homogeneous channels. Check the fitted envelope, uncertainties, thermally shifted equilibrium population and whether the two times were measured under comparable conditions. A negative fitted number is evidence about the model or data interpretation, not a physically negative random-event rate.

Calculate an inefficient no-click update

The initial excited probability is one half, the decay probability for an initially excited qubit during the window is 0.40, and a true emitted excitation is detected with efficiency 0.75. Find the probability of no click, its conditional excited fraction and the unconditioned population.

▼ **Work through the solution**

A real emission occurs with probability $0.5 \times 0.40 = 0.20$; a click is seen with probability 0.15, so no click has probability 0.85. Remaining excited and no click occurs with probability $0.5(1 - 0.40) = 0.30$. Conditional excitation is $0.30/0.85 = 0.3529$; the unconditioned excitation is 0.30 since clicked branches are ground. For an initially coherent preparation the no-click off-diagonal term must also be updated by grouping the undetected-emission and true-no-emission Kraus outcomes. Simply replacing p by detector efficiency times p would predict the wrong physical excitation loss.

Diagnose a nonphysical time step and repair it

Apply one forward-Euler step to $\dot{p}_1 = -\Gamma p_1$ with initially excited state and $\Gamma\Delta t = 1.2$. Compute the prediction and an exact completely positive alternative. Would enforcing unit trace fix Euler's failure?

▼ **Work through the solution**

Euler gives $p_1 = 1 - 1.2 = -0.2,\ p_0 = 1.2$, already with exact trace one. The finite-time amplitude-damping channel has $p = 1 - e^{-1.2} = 0.6988$, giving $p_1 = 0.3012$. For this simple model the exact Kraus step can be applied repeatedly at arbitrary duration. In a driven model an operator-splitting scheme with unitary Hamiltonian substeps and completely positive damping substeps maintains positivity while introducing a controllable splitting error. Check convergence by halving the step and comparing with an independent observable. Renormalising trace or clipping a negative eigenvalue changes the numerical trajectory without diagnosing the original time-step error.

Further reading

- Cambridge · open systems, measurements and the Lindblad equation
- Course investigation · density matrices and dephasing
- Course investigation · driven coherent response

Quantum states, dynamics and measurement · 12. How a turning point supplies the missing semiclassical phase

Far from a turning point the wavelength follows the classical momentum. At the turning point that approximation becomes singular. Derive the Airy connection, quantise a smooth well, distinguish a hard wall and estimate a tunnelling exponent with a defensible error check.

Expand the action before interpreting a local wavelength

For a stationary one-dimensional state with smooth potential $V(x)$, write $\psi = e^{iS(x)/\hbar}$. Substitution into Schrödinger's equation gives

$$S'^2 - i\hbar S'' = 2m(E - V) = p^2(x).$$

Expand $S = S_0 + (\hbar/i)S_1 + \cdots$. The leading terms give $S_0' = \pm p$ and $S_1' = -p'/(2p)$ in an allowed region where $p > 0$. Thus travelling waves have form $Cp^{-1/2}\exp[\pm i\int^x p\,dx/\hbar]$. The amplitude factor is physically essential: for a single such branch the current to leading order is $\pm|C|^2/m$, independent of x, as required for steady flux in a real potential. A constant amplitude with variable wavenumber would predict current piling up in a stationary region.

A local condition for this expansion is $\hbar|p'|/p^2 \ll 1$ together with control over higher derivatives on the wavelength scale. Away from a barrier the phase can remain accurate even if absolute amplitude normalisation must be fixed globally. Where $E < V$, define $\kappa = \sqrt{2m(V - E)}$ with units of momentum. The local solutions become $\kappa^{-1/2}\exp[\pm\int \kappa\,dx/\hbar]$. A single real decaying branch carries zero probability current by itself. Stationary tunnelling flux through a finite barrier involves a complex combination satisfying both exterior matching conditions, even though the leading size of transmission can often be inferred from the decaying exponential.

Resolve the apparent divergence near a simple turning point

Let x_t satisfy

$$V(x_t) = E,$$

with slope $F = V'(x_t) > 0$. Linearise $V - E \simeq F(x - x_t)$. The local Schrödinger equation becomes

$$\psi'' = (2mF/\hbar^2)(x - x_t)\psi.$$

Introduce length $\ell = (\hbar^2/(2mF))^{1/3}$ and $\xi = (x - x_t)/\ell$, leaving $d^2\psi/d\xi^2 = \xi\psi$. Its two independent solutions are Ai and Bi. On the positive side $\mathrm{Ai}(\xi)$ decays, whereas $\mathrm{Bi}(\xi)$ grows. A bound state extending into a semi-infinite forbidden region selects the former. At $\xi = 0$ the Airy function is finite; the apparent divergence $p^{-1/2}$ came from extending the outer approximation beyond its range.

The asymptotic forms for $s > 0$ large are

$$\mathrm{Ai}(s) \sim \frac{e^{-2s^{3/2}/3}}{2\sqrt{\pi}\,s^{1/4}}, \qquad \mathrm{Ai}(-s) \sim \frac{\sin(2s^{3/2}/3 + \pi/4)}{\sqrt{\pi}\,s^{1/4}}.$$

For a linear slope, $2s^{3/2}/3$ equals $|\int_{x_t}^{x} p\,dx|/\hbar$ on the allowed side or $\int_{x_t}^{x} \kappa\,dx/\hbar$ on the forbidden side. Matching in an interval where $|x - x_t| \gg \ell$ but the potential remains effectively linear gives the connection from a decaying tail of coefficient C to $2C\,p^{-1/2}\sin[\hbar^{-1}\int_{x}^{x_t} p\,dx + \pi/4]$. The coefficient two and phase $\pi/4$ both come from the same local solution. A turning point with zero slope, a sharp step or two turning points closer than their Airy lengths requires a different local treatment.

Join two decaying tails to a standing wave

For a smooth well with two well-separated simple turning points x_1, x_2, the left tail matches to $\sin[\hbar^{-1}\int_{x_1}^{x} p\,dx + \pi/4]$. The right tail matches to $\sin[\hbar^{-1}\int_{x}^{x_2} p\,dx + \pi/4]$. Their zeros and logarithmic derivatives must coincide throughout the overlap, up to an overall sign. The sum of the two phase arguments is the full one-way action divided by $\hbar$ plus $\pi/2$, which must be an integer multiple of π. Taking $n \geq 0$ gives

$$\int_{x_1}^{x_2} p(x, E_n)\,dx = \pi\hbar(n + 1/2).$$

For a harmonic oscillator the turning point magnitude is $a = \sqrt{2E/(m\omega^2)}$ and $p = m\omega\sqrt{a^2 - x^2}$. The action is the area of a semicircle times $m\omega$, equal to $\pi E/\omega$. The rule reproduces $E_n = \hbar\omega(n + 1/2)$ exactly for this special spectrum, even though its outer WKB wavefunction is still inaccurate near each turning point and globally for low quantum number. Equality of a spectral result does not imply equality of spatial densities or agreement of all observables.

Different boundaries change the phase budget. Take a hard wall at $x = 0$ and a linearly rising potential Fx for $x > 0$. The solution decaying to the right is $\mathrm{Ai}[(x - E/F)/\ell]$. Its exact energies follow from $\mathrm{Ai}(-E/F\ell) = 0$. The wall imposes a node without an Airy phase at the left. Setting the right-matched standing wave to zero at the wall gives

$$\int_{0}^{E/F} p\,dx = \pi\hbar(n + 3/4).$$

Thus $E/(F\ell) \simeq [3\pi(n + 3/4)/2]^{2/3}$. For $n = 0$ this is about 2.320 versus the first exact zero 2.338; with $n = 4$ the approximation is about 7.94. Replacing the wall by a second smooth turning point would instead introduce an erroneous half offset.

Separate a credible exponential estimate from its prefactor

For a barrier with two simple turning points x_a, x_b, a large forbidden action $I = \int_{x_a}^{x_b} \kappa\,dx/\hbar$ suppresses the transmitted flux approximately as $T \simeq e^{-2I}$, up to prefactors and corrections that depend on geometry and matching. For a triangular forbidden region with height $V_0 - E = \Delta$ at $x = 0$ falling as $\Delta - Fx$ to zero at Δ/F, its action is $I = 2\sqrt{2m}\Delta^{3/2}/(3\hbar F)$. A discontinuous incident-side boundary may affect the prefactor substantially. It does not justify assigning a second smooth-turning-point phase to the discontinuity. For a rectangular barrier the exact thick-barrier prefactor is $16E(V_0 - E)/V_0^2$ times the decaying exponential at equal exterior potentials. It can exceed one while total transmission remains small.

Suppose two measurements change only the forbidden width of a flat barrier from d to $d + \Delta d$, keeping both interfaces and asymptotic energies the same. In the thick limit the ratio $T(d + \Delta d)/T(d) \simeq e^{-2\kappa\Delta d/\hbar}$

cancels the common prefactor. If $\kappa/\hbar = 2.0\,\mathrm{nm}^{-1}$ and $\Delta d = 0.50$ nm, this ratio is

$$e^{-2} = 0.1353.$$

An offset error in barrier width that leaves this ratio unchanged can still cause a large error in absolute transmission. Near the top two turning points can merge, I becomes small, and the raw exponential lacks a unitary connection to the over-barrier reflection regime. Use a suitable uniform approximation or a direct scattering solution there.

Predict a high-energy spectrum without a closed-form wavefunction

Consider a pure quartic trap $V(x) = \lambda x^4$ with $\lambda > 0$. Classical turning points lie at $x = \pm a,\ a = (E/\lambda)^{1/4}$. Unlike the harmonic oscillator its period changes with energy, so its levels cannot be equally spaced. The semiclassical action can be evaluated once in dimensionless coordinates and then rescaled to any m, λ, E:

$$A(E) = \int_{-a}^{a} \sqrt{2m(E - \lambda x^4)}\, dx = 2\sqrt{2m}\, \lambda^{-1/4} E^{3/4} I_4,$$

$$I_4 = \int_0^1 \sqrt{1 - y^4}\, dy.$$

With $s = y^4$,

$$I_4 = \frac{1}{4} B(1/4, 3/2) \simeq 0.8740.$$

Quantising $A(E_n) = \pi\hbar(n + 1/2)$ predicts $E_n \simeq [\pi\hbar(n + 1/2)\lambda^{1/4}/(2\sqrt{2m} I_4)]^{4/3}$. The dependence $E \propto n^{4/3}$ and the dimensional factor $\hbar^{4/3}\lambda^{1/3}m^{-2/3}$ can be checked independently from scaling the full Schrödinger equation. That dimensional argument does not supply the coefficient or the half-integer offset. The action and boundary phases supply the additional physics.

Choose units such that $H = -d^2/dx^2 + x^4$. Then $2m = \hbar = 1$ in the scaled equation, and the leading energies are $[\pi(n + 1/2)/(2I_4)]^{4/3}$. For $n = 0$ this gives about 0.868, below the accurately computed ground value around 1.060. An independent variational Gaussian $\psi = (\beta/\pi)^{1/4} e^{-\beta x^2/2}$ has energy $\beta/2 + 3/(4\beta^2)$, minimised at $\beta^3 = 3$ and giving 1.082. Its proximity to the true ground energy has a different status: the Gaussian energy is an upper bound by the variational principle, while leading WKB provides no universal bound for this potential. Using agreement between two approximate numbers as proof of a rigorous interval would require actual lower and upper estimates.

At larger n the period relation provides an additional prediction. Since $A \propto E^{3/4}$,

$$T_{\mathrm{cl}} = 2\, dA/dE \propto E^{-1/4};$$

the frequency increases at larger amplitude, and the local spacing should grow as $E^{1/4}$. Numerically compute a handful of high levels with a direct finite-difference or spectral Hamiltonian, then plot $E_n^{3/4}$ against $n + 1/2$. A nearly linear trend is a more sensitive diagnostic of the predicted law than comparing a single apparent power from a log plot at low n. Increase domain size and basis cutoff independently. A truncation that

confines high-energy tails can falsely steepen the spacing, while a coarse grid can flatten the kinetic-energy dispersion. Both errors become more visible for rapidly oscillating states.

Relate a barrier action to a coherent population oscillation

Take two identical minima separated by a smooth barrier. At energies below the barrier top but above each isolated-well ground, there are two classically allowed intervals and a central forbidden region. If the barrier is sufficiently opaque, construct approximate localised states $|L\rangle, |R\rangle$ with equal one-well energy E_0. In their span the simplest symmetric Hamiltonian is $H = E_0 I - J(|L\rangle\langle R| + |R\rangle\langle L|)$ with $J > 0$ in a suitable phase convention. The even and odd combinations have energies $E_0 - J, E_0 + J$. The tunnel splitting is $2J$, set to leading exponential order by the overlap of amplitudes through the central forbidden interval.

A single under-barrier wavefunction amplitude carries e^{-I},

$$I = \int \kappa dx/\hbar.$$

For an open barrier the transmission probability is proportional to e^{-2I}. For a symmetric double-well splitting the relevant quantity is a coherent off-diagonal energy amplitude, so its leading exponential is $J \propto e^{-I}$, times a prefactor involving the oscillation scales and matching in the two wells. Confusing these exponents can lead to a severe error when using a calculated spatial barrier to predict a coherent tunnel frequency. The exact prefactor depends on the potential and turning-point normalisations. A direct symmetric numerical eigenproblem giving the difference of two nearly equal energies requires enough precision to resolve an exponentially small splitting.

Prepare $|L\rangle$ at time zero. Its evolution under the two-state Hamiltonian gives

$$P_R(t) = \sin^2(Jt/\hbar);$$

the first full transfer time is $\pi\hbar/(2J)$. If the observed energy splitting expressed as ordinary frequency is $2J/h = 20$ Hz, the first transfer occurs at 25 ms. Changing only the barrier action by $+0.70$ at fixed prefactor multiplies the splitting by $e^{-0.70} = 0.497$ and approximately doubles the transfer time. An open-barrier transmission experiment over the same change instead sees factor $e^{-1.4} = 0.247$. Both tests depend exponentially on barrier shape but interrogate different quantities.

Now add a calibrated tilt $\epsilon = E_L - E_R$. The 2×2 Hamiltonian after trace subtraction is $(\epsilon/2)\sigma_z - J\sigma_x$, and the maximum transfer falls to $4J^2/(\epsilon^2 + 4J^2)$. At $\epsilon = 2J$ it is one half while the oscillation angular frequency increases from $2J/\hbar$ to $2\sqrt{2}J/\hbar$. A loss of transfer contrast need not be environmental decoherence; static tilt alone yields this combination of increased frequency and reduced amplitude. Measuring both quantities and reversing the tilt tests the two-level model. If a higher intrawell level lies within the tilt or excitation range, a single tunnelling doublet no longer spans the relevant motion and a larger basis is required.

Understand the angular correction at a radial turning point

In three dimensions the reduced radial equation on $r > 0$ has a centrifugal term $\hbar^2 l(l+1)/(2mr^2)$. Applying the flat-coordinate WKB rule directly to this equation can give incorrect phases at its singular endpoint, especially for low l. A way to see the appropriate angular correction without guessing is to set

$r = r_0 e^x$, mapping the half-line to all real x, and write $u(r) = e^{x/2} w(x)$. The arbitrary reference r_0 keeps the logarithm dimensionless. Since $d/dr = r^{-1} d/dx$, differentiating twice yields

$$\frac{d^2u}{dr^2} = \frac{e^{x/2}}{r^2}\left(w'' - \frac{1}{4}w\right).$$

The resulting equation for w has squared local action momentum in x proportional to $2mr^2(E - V) - \hbar^2(l + 1/2)^2$. Thus returning its action $\int p_x dx$ to r uses $l(l+1) \to (l+1/2)^2$ in the radial semiclassical momentum. This is the Langer correction. It does not change the exact angular eigenvalue $L^2 = \hbar^2 l(l+1)$; it accounts for the coordinate transformation and endpoint behaviour of the semiclassical representation. Confusing those statements would alter the exact radial equation to repair an approximate integration rule.

An instructive check is the isotropic oscillator. For $V = m\omega^2 r^2/2$ and effective classical angular momentum $L = (l + 1/2)\hbar$, the radial action over its two roots is

$$A_r = (\pi/2)(E/\omega - L).$$

One can obtain this without an explicit contour integral by noting that radial motion repeats at twice the Cartesian frequency, so

$$dA_r/dE = \pi/(2\omega).$$

Fix the integration constant at the circular-orbit threshold $E = \omega L$, where the two radial turning points meet and $A_r = 0$. Quantising $A_r = \pi\hbar(n_r + 1/2)$ gives $E = \hbar\omega(2n_r + l + 3/2)$, matching the exact three-dimensional oscillator spectrum. For $l = 0$ the naive uncorrected centrifugal term has no inner turning point; transferring a generic two-smooth-turning-point formula into that half-line problem without reconsidering its origin is especially unsafe.

Calculate an exponentially small transmission without subtracting nearly equal numbers

In a classically forbidden interval the local solution contains a growing and a decaying branch. In a long interval numerical transfer matrices can contain elements as large as e^I, while the quantity sought is as small as e^{-2I}. Straight propagation of a decaying boundary condition in the unstable direction can contaminate it with a tiny growing roundoff component which eventually dominates. A plot matching the expected slope over the first few decay lengths gives no guarantee that a final tiny flux is accurate. Numerically stable alternatives include propagating a logarithmic derivative with controlled handling of its poles, matching independently normalised left and right solutions, or composing scattering matrices for short slices while retaining decaying propagation factors.

For a square barrier the exact transmission at $E < V_0$ in equal exterior regions is $T = [1 + V_0^2 \sinh^2(\kappa d/\hbar)/(4E(V_0 - E))]^{-1}$. With $E = V_0/2$ this simplifies to $\operatorname{sech}^2 I$. At $I = 20$ its value is approximately $4e^{-40} = 1.70 \times 10^{-17}$. Computing $T = 1 - R$ in ordinary double precision can give exactly zero since the reflection probability rounds to one. Compute transmitted amplitude or its logarithm directly and compare $\log T \simeq \log 4 - 2I$. At a moderate I, where both currents are accurately representable,

independently verify $R + T = 1$. Moving the benchmarking point across the barrier-opacity range tests both the physical approximation and the floating-point representation of the desired observable.

Resolve a wave through a classical turning point

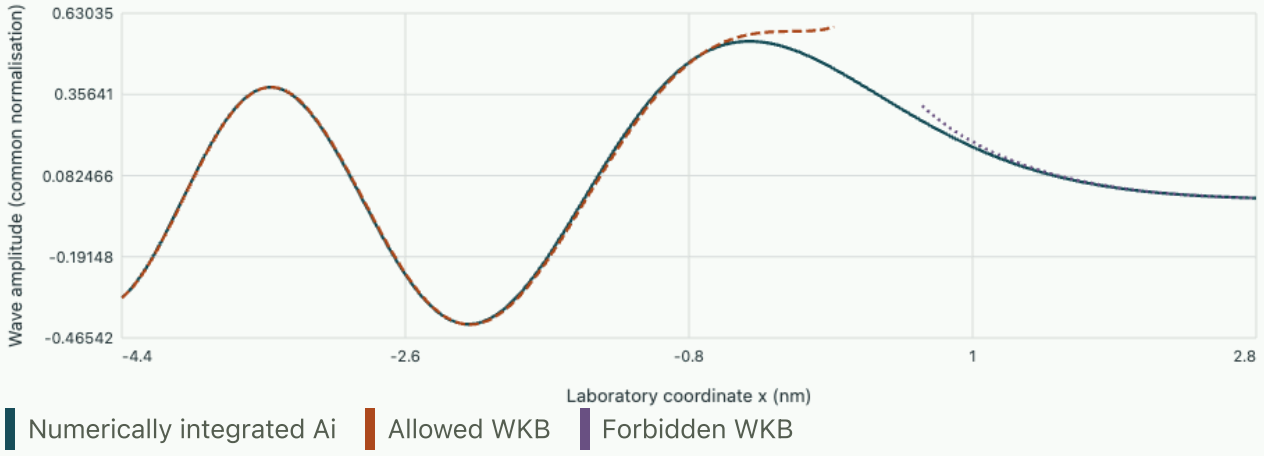
Vary the physical length scale in a locally linear potential. Compare the numerical Airy solution and the two semiclassical branches near and away from the turn.

Open this experiment online

Try the calculation

Turning-point length (nm) **0.8**

Turning-point position (nm) **0.4**



The turn at 0.4 nm has finite Ai value 0.35503. The characteristic transition length is 0.8 nm; the asymptotic curves omit the nearest 0.35 lengths.

Connect semiclassical action to counting states in phase space

The action quantisation rule can also be read as a statement about the number of energy levels below a chosen energy. In a one-dimensional smooth confining well the classically accessible region in (x, p) has area $\Omega(E) = \int dx \int_{-p(x)}^{p(x)} dp = 2A(E)$. Roughly one stationary state fits per phase-space area $2\pi\hbar$, with an endpoint correction from the turning-point phases. The smoothed density of states follows by differentiating $\bar{N}(E) \simeq \Omega(E)/(2\pi\hbar)$, giving $\bar{\rho}(E) = T_{\mathrm{cl}}/(2\pi\hbar)$. This counts levels after smoothing over individual spacing; the exact count is a staircase and its derivative a sum of delta functions. A formula for a smooth density cannot predict each state in a near-degenerate doublet without additional phase and tunnelling information.

For a particle in a two-dimensional rigid rectangular region, apply the same counting idea in four-dimensional phase space. With area $\mathcal{A} = L_x L_y$, accessible momentum disk $p_x^2 + p_y^2 < 2mE$, the scalar smoothed count is $\bar{N}(E) \simeq \mathcal{A}\pi(2mE)/(2\pi\hbar)^2 = \mathcal{A}mE/(2\pi\hbar^2)$. Its derivative is a constant, unlike the $E^{-1/2}$ free one-dimensional density and the $\sqrt{E}$ three-dimensional density. This leading area law can be checked by directly

counting positive integer lattice points satisfying $(n_x\pi/L_x)^2 + (n_y\pi/L_y)^2 < k^2$ in a Dirichlet rectangle. It works after smoothing when many modes fit in the domain and makes no assumption that the rectangular shape itself models all possible billiards.

A more sensitive check accounts for the excluded axes in that first-quadrant lattice count. For a Dirichlet rectangle subtract half of the positive-axis contributions at each boundary of the quadrant. In terms of perimeter $\mathcal{P} = 2(L_x + L_y)$, the resulting first two terms are $\bar{N}(k) \simeq \mathcal{A}k^2/(4\pi) - \mathcal{P}k/(4\pi) + O(1)$ after appropriate smoothing, with fluctuations from discrete modes beyond this local expansion. Neumann boundaries reverse the sign of the perimeter term because modes constant along one coordinate are admitted. Area alone determines the bulk growth, whereas boundary condition affects the next correction. The finite corner term and spectral fluctuations require more care than assigning one universal integer offset to every billiard.

The distinction between smoothing and exact prediction also explains why counting every computed eigenvalue only up to an arbitrarily sharp threshold can produce apparent convergence jumps as the mesh improves. If a true eigenvalue lies near the threshold, a small numerical shift changes an integer count by one. Compare a range of cumulative counts, track nearby eigenvalue residuals and study the smoothed density with a bandwidth large enough to include several levels but small compared with the energy scale of interest. Repeating for two geometries of equal area and different perimeter tests actual geometric information beyond an overall energy scale.

Measure the boundary correction in a square cavity

A scalar mode calculation uses a square of side 10.0 length units and reports all Dirichlet modes with $k < 5.00$ inverse length units. Find the leading area estimate, add the perimeter correction, and compare with a direct lattice-point count.

▼ **Derive and check the result**

The area contribution is $100(25)/(4\pi) = 198.94$; the perimeter subtraction is $40(5)/(4\pi) = 15.92$, giving a smoothed estimate 183.03 before corner and oscillatory terms. The exact count uses positive integers n_x, n_y satisfying $n_x^2 + n_y^2 < (50/\pi)^2 \simeq 253.30$. For each $n_x = 1, \ldots, 15$, count $n_y \le \lfloor \sqrt{253.30 - n_x^2} \rfloor$ and sum. The values are $15, 15, 15, 15, 15, 14, 14, 13, 13, 12, 11, 10, 9, 7, 5$, giving 183. Agreement at this threshold is close, while the leading area term alone is about sixteen high. Nearby thresholds can have different residual fluctuations, so the close integer agreement at this one wave number should not be treated as an exact two-term counting rule. The same calculation on a different aspect ratio at fixed area would change both the perimeter and the lattice pattern.

Measure a reflection phase separately from the travel action

In a one-dimensional cavity a quantisation condition can be written as a round-trip phase budget. Let an allowed region accumulate one-way phase $\theta(E)$ and let reflections at its left and right bounding regions have phase shifts $\phi_L(E), \phi_R(E)$ for unit-modulus reflection. A self-reproducing wave requires

$$2\theta(E) + \phi_L(E) + \phi_R(E) = 2\pi n,$$

with an integer depending on the chosen phase origin. A rigid Dirichlet wall reflects with amplitude -1; a smooth decaying turning point contributes a different reflection phase that the Airy matching fixed. Adding 2π to one reflection phase simply relabels the integer, but an energy-dependent boundary phase alters the spacing and cannot be removed by a constant relabelling.

A useful boundary that can be solved without approximation is a finite step $V = 0$ for $x < 0,\ V = V_0 > E$ for $x > 0$. With incident wave e^{ikx}, reflected amplitude re^{-ikx} and exterior evanescent $te^{-\kappa x}$, where k, κ here are inverse lengths, continuity of the value and derivative gives

$$1 + r = t,\ ik(1 - r) = -\kappa t.$$

Solving yields

$$r = (k - i\kappa)/(k + i\kappa).$$

Its magnitude is one and its phase can be written $-2\arctan(\kappa/k)$. As V_0 tends to infinity with E fixed, the phase tends to $-\pi$, giving the rigid-wall limit. Just below the step threshold it approaches zero. Two mirrors with equally complete reflection can therefore produce different cavity eigenfrequencies.

Near the rigid-wall limit expand $r \simeq -e^{2ik/\kappa}$. To leading order the exterior behaves like a rigid reflecting plane displaced a penetration length $1/\kappa$ beyond the interface. For a deep symmetric finite well of width L, the phase condition approximately replaces L by $L + 2/\kappa(E)$. This shift lowers levels relative to a rigid well of the same geometric width. It is only an approximation because penetration depends on energy. Matching logarithmic derivatives independently on the two sides is preferable near threshold or when the barrier shape varies over the penetration length.

Infer a boundary penetration from a measured free spectral interval

A long one-dimensional cavity with identical deep finite barriers has a measured low-mode wavenumber interval 2% smaller than π/L. Under the constant penetration approximation infer $1/\kappa$ relative to L and identify a check on the approximation.

▼ **Derive and check the result**

Set $\pi/(L + 2/\kappa) = 0.98\pi/L$. Then $2/\kappa L = 1/0.98 - 1 = 0.0204$, or a penetration distance $1/\kappa = 0.0102L$ at each wall. For $L = 100$ nm this is about 1.02 nm. Measure several successive intervals to see whether one penetration length describes them. An increasing penetration with energy changes the reflection-phase derivative and therefore the spacing; the physical group delay then contains travel time in the allowed region plus boundary delay. A geometrically longer rigid cavity would produce a similar single interval but a different energy dependence, so an isolated observation does not uniquely identify the cause.

Tutorial · determine what a semiclassical estimate can certify

Recover the period and level spacing from an action curve

For $A(E) = \int_{x_1}^{x_2} p\,dx$ in a smooth bound well, derive dA/dE and infer the local energy spacing. Apply it to a 100 kHz oscillator and express spacing in both joules and electronvolts.

▼ **Work through the solution**

The endpoint derivative terms vanish because $p = 0$ at both ends. Inside, $\partial p/\partial E = m/p = 1/v$, so dA/dE equals the classical one-way travel time $T_{\mathrm{cl}}/2$. From the quantisation rule increasing n by one gives local spacing $\Delta E \simeq 2\pi\hbar/T_{\mathrm{cl}} = h f_{\mathrm{cl}}$. At 100 kHz this is 6.626×10^{-29} J or 4.136×10^{-10} eV. In an anharmonic potential the classical period generally depends on energy; use the local slope or integrate between adjacent solutions rather than assuming a universal ladder spacing.

Check whether the Airy overlap interval exists

For a model atom with mass 1.44×10^{-25} kg let $F = 1.0 \times 10^{-21}$ N at the turning point. Find the Airy length. If $|V''| = 1.0 \times 10^{-16}\,\mathrm{N/m}$, estimate the relative quadratic correction at 5ℓ.

▼ **Work through the solution**

The length is $(\hbar^2/2mF)^{1/3} \simeq 3.38 \times 10^{-8}$ m. The ratio of quadratic potential term to linear term at 5ℓ is $|V''|5\ell/(2F) \simeq 0.00845$. Thus several Airy lengths can fit in a region with small curvature correction for these numbers. The parameter $|x - x_t|/\ell = 5$ should still be checked against the desired asymptotic precision; the result supports an overlap interval but does not guarantee a prescribed decimal accuracy. Bringing a second turning point within a few such lengths changes the matching problem qualitatively.

Compare a triangular action with a rectangular shortcut

A linearly falling barrier has initial forbidden wavenumber $\kappa_0/\hbar = 3.0\,\mathrm{nm}^{-1}$ and width $d = 2.0$ nm. Compare its exponential estimate with that of a rectangle using initial height throughout. What would a rectangle at the average potential height predict?

▼ **Work through the solution**

For the triangle, $\kappa(x) = \kappa_0\sqrt{1 - x/d}$, so $I = (2/3)(\kappa_0/\hbar)d = 4.0$, giving $e^{-8} = 3.35 \times 10^{-4}$. The initial-height rectangle gives $I = 6$ or $e^{-12} = 6.14 \times 10^{-6}$. Averaging the potential height first gives wavenumber $\kappa_0/\sqrt{2}$, $I = 4.24$ and $e^{-8.49} \simeq 2.06 \times 10^{-4}$. The action averages the square root of the local energy gap, not the gap itself. Agreement in mean barrier height is insufficient for predicting an exponential observable. Exact matching or a direct numerical probability current would be needed to determine the prefactor.

Further reading

- Fließbach · Näherungsmethoden
- Cambridge · WKB, Airy matching and semiclassical quantisation
- Course investigation · semiclassical quantisation and tunnel splitting

Quantum states, dynamics and measurement · 13. Measure geometric phase from three spin overlaps

A numerical eigensolver is free to choose a new complex phase for every eigenvector. A product of three measured overlaps removes these arbitrary choices. Relate its argument to a spherical triangle, then see why a vanishing overlap destroys phase information.

Close a loop before assigning a phase

Choose three normalised spinors $|A\rangle, |B\rangle, |C\rangle$. Their individual phases change under $|j\rangle \mapsto e^{i\gamma_j}|j\rangle$. In the cyclic product $Z = \langle A|B\rangle\langle B|C\rangle\langle C|A\rangle$ every phase occurs once with each sign. This product is a gauge-independent complex quantity although none of the three overlap phases separately is.

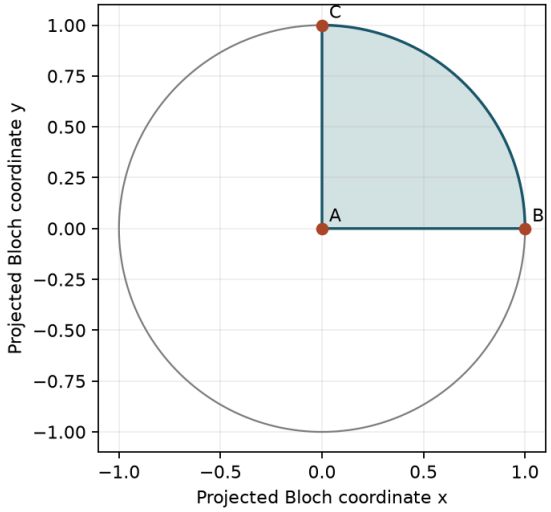
Take A at the north pole of the Bloch sphere, B on its equator at longitude zero and C on the equator at longitude φ with $-\pi < \varphi < \pi$. Choose $A = (1, 0)$, $B = (1, 1)/\sqrt{2}$ and $C = (1, e^{i\varphi})/\sqrt{2}$. Direct multiplication gives

$$Z = \frac{1 + e^{i\varphi}}{4} = \frac{\cos(\varphi/2)}{2} e^{i\varphi/2}.$$

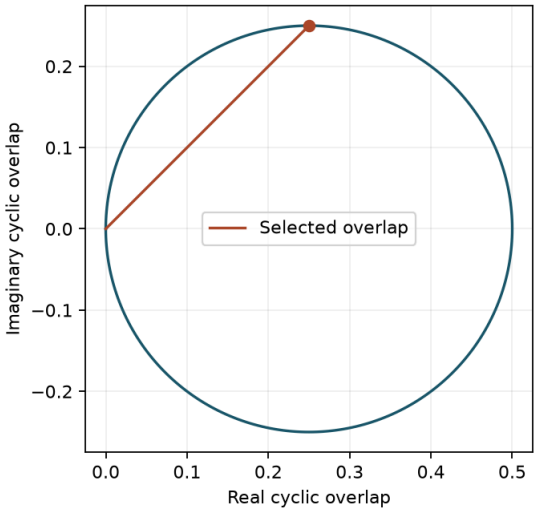
The oriented triangle bounded by the two meridians and the shortest equator arc has solid angle $\Omega = \int_0^{\varphi} d\phi \int_0^{\pi/2} \sin\theta \, d\theta = \varphi$. The overlap product therefore has argument $+\Omega/2$ for this order. The geometric phase of a ket parallel-transported along the oriented shortest geodesics is the negative of this overlap-product argument. Stating which sign is reported prevents an apparent contradiction. This construction requires no arbitrary differentiation of eigenvector phases.

Separate a well-defined angle from an observable signal

At 90 degrees longitude the triangle encloses $\pi/2$ steradians. The complex product is $(1 + i)/4$, its magnitude is about 0.354 and its argument is $\pi/4$. As longitude approaches 180 degrees, the equatorial states approach orthogonality. The magnitude tends to zero, and even a small absolute uncertainty in the measured complex product yields a large angular uncertainty. Exactly at orthogonality there is no unique shortest equatorial arc or measurable phase of the zero complex number.



The north pole projects to the centre and the equator to the rim. The filled planar region illustrates the path, whereas its solid angle is integrated on the sphere.



At the origin the overlap phase is undefined. Reversing the circuit reflects the complex product across the real axis.

Exercise · reverse the circuit

What happens to amplitude and phase if the experiment uses A, C, B in place of A, B, C?

▼ **Work through the solution**

Hermitian symmetry conjugates every overlap while the scalar factors can be reordered. The new product equals Z^*. Its magnitude stays fixed and both signed phase conventions reverse.

Exercise · estimate the angular uncertainty

A measured overlap has magnitude 0.02 and a small perpendicular complex uncertainty of magnitude 0.002. What is the first-order phase uncertainty? Compare with a magnitude of 0.4.

▼ **Work through the solution**

For a small transverse displacement the angular change is $\delta\theta \simeq |\delta Z_\perp|/|Z|$. The answers are 0.10 rad and 0.005 rad. Identical absolute detector noise therefore gives very different phase precision near an orthogonal pair.

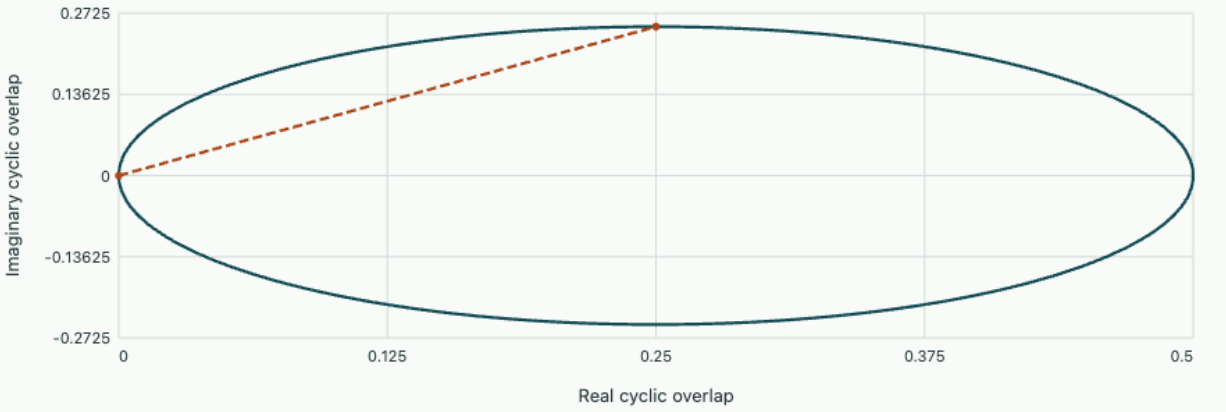
Try it · Geometric phase

Change the inputs and compare the recalculated curves with the preceding derivation and baseline figure. The axes give the units; the numerical readout states the model assumptions and any limiting cases. Reset the inputs to return to the reference setting.

Open this live calculation

Try the calculation

Third-state longitude (degrees) **90**



Cyclic-overlap locus Selected overlap

Overlap modulus 0.35355; overlap phase 0.7854 rad. Parallel-transport phase has the opposite sign. Arbitrary individual state phases cancel.

Download the corresponding editable notebook. The browser recalculates the reduced equations directly; the notebook exposes the full calculation and its checks.

Open editable notebook Download .ipynb

Quantum states, dynamics and measurement · 14. From electron exchange to atomic shells and molecular binding

An orbital model can explain why a closed atomic shell is special and why a shared electron can bind two protons. Both predictions need an energy as well as a rule for counting states. We construct the energies and check them against their separated-particle limits.

Count states and find what changes in an atom with many electrons

For a hydrogenic principal number n, allowed orbital quantum numbers run from 0 to $n-1$. Each l permits $2l+1$ magnetic projections. Two spin states accompany each orbital. An antisymmetric many-electron state vanishes if two occupied spin orbitals coincide, giving the shell capacity

$$N_n = 2\sum_{l=0}^{n-1}(2l+1) = 2n^2.$$

This is a counting bound. Hydrogen energies depend only on n in the nonrelativistic Coulomb problem. In a neutral many-electron atom a core screens the nucleus. An orbital that penetrates the core samples a larger net attraction. Self-consistent screening and exchange split subshells. A bare $2n^2$ table cannot predict the order of filling across all atoms or the configurations of all transition metals.

For carbon, a closed $1s^2 2s^2$ core leaves two electrons in $2p$. For distinct spatial states a, b, form normalised spatial combinations $(a(1)b(2) \pm b(1)a(2))/\sqrt{2}$. A symmetric repulsive interaction gives $E_\pm = E_0 + J \pm K$ for orthogonal orbitals, with J the direct integral and K the exchange integral. The antisymmetric spatial branch pairs with a symmetric spin triplet and often lies lower in a degenerate open subshell. This gives a mechanism for Hund's first rule. Large orbital splittings can favour double occupation despite exchange.

> **Recall · Why does an inert shell show a spectroscopic jump?**
>
> Adding an electron above a completed low shell and removing one from that shell involve orbitals with different spatial extent and binding energy. Closed-shell counting also gives zero total orbital and spin angular momentum for the filled subshell. Actual ionisation energies still include relaxation of the remaining electrons.

Construct a molecular-ion energy curve in its own nonorthogonal basis

Fix two protons at separation R and work in atomic units. The nuclei move much more slowly than the electron. The electronic Hamiltonian is $h = -\nabla^2/2 - 1/r_A - 1/r_B$. For each fixed R the total Born–Oppenheimer energy includes the proton repulsion $1/R$. Use two unit-charge hydrogenic $1s$ basis orbitals ϕ_A, ϕ_B. Their overlap matters whenever a bond might form.

$$S = e^{-R}(1 + R + R^2/3),$$
$$J = -1/R + (1 + 1/R)e^{-2R},$$
$$K = -(1 + R)e^{-R}.$$

Here $J = \langle A| - 1/r_B|A\rangle$ and $K = \langle A| - 1/r_A|B\rangle$. They follow by integrating the two decaying exponentials in the field of the other nucleus. For example, the spherical average of $1/r_B$ on a sphere about A is $1/\max(r_A, R)$. Splitting the J radial integral there gives the expression above. Using the isolated hydrogen equation acting on the ket now gives $H_{AA} = -1/2 + J$ and $H_{AB} = -S/2 + K$.

Vary the Rayleigh quotient with respect to the coefficients. The stationarity equation is $Hc = E_{\mathrm{el}}Sc$ where the matrix on the right has unit diagonal and off-diagonal overlap S. Reflection through the midpoint fixes the even and odd combinations and their normalisations:

$$\psi_\pm = \frac{\phi_A \pm \phi_B}{\sqrt{2(1 \pm S)}},$$
$$U_\pm(R) = \frac{H_{AA} \pm H_{AB}}{1 \pm S} + \frac{1}{R}.$$

As R grows, both curves tend to $-1/2$ hartree, the energy of a neutral H atom and a distant proton. At $R = 2$ bohr the even branch is about -0.554 hartree. Its energy below the dissociation threshold demonstrates binding even within this restricted trial space. The minimum of this curve determines a bond length only within the chosen basis and the fixed-nucleus approximation.

OneSimulation experiment · Two-centre variational energies for the hydrogen molecular ion

Try the molecular density between two nuclei

Move the nuclei and inspect how constructive and destructive interference change the electron density on their connecting line. The odd combination keeps a node at the centre. Compare the even-state energy with the separated-atom value of −0.5 hartree and locate a bound separation.

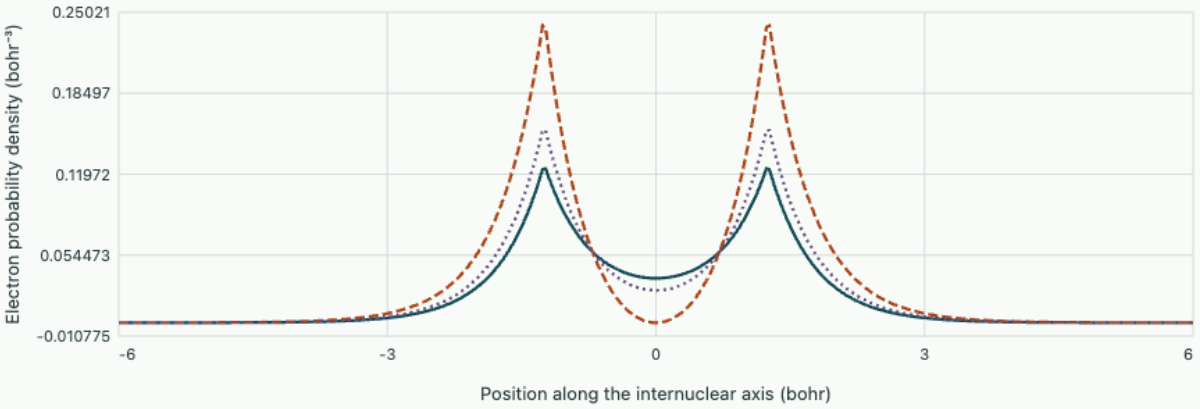
$$|\psi_\pm(x, 0, 0)|^2 = \frac{\left(e^{-|x+R/2|} \pm e^{-|x-R/2|}\right)^2}{2\pi(1 \pm S(R))}.$$

The orbitals are normalised in three dimensions and the plot is a line through that density. This is the same fixed two-orbital variational approximation as the OneSimulation notebook below. Nuclear motion and orbital relaxation are excluded. Use the notebook's eigenproblem to check the displayed total energies independently.

Open this experiment online

Try the calculation

Nuclear separation (bohr) **2.5**



Even combination |ψ+|² Odd combination |ψ−|² Incoherent half-and-half density

Nuclei at x = ±1.25 bohr. Overlap S = 0.458308. Total even/odd energies = -0.564829 / -0.290642 hartree. Even-state binding relative to H + proton = 1.7641 eV. The plotted line samples a three-dimensional density; its one-dimensional integral need not equal one.

Reproduce with OneSimulation

Change the range or sampling of nuclear separations. The solver orthonormalises the overlap metric before diagonalising. Compare its grid minimum with the even-state formula and distinguish grid error from the error inherent in the two-orbital basis.

Run the downloaded notebook with OneSimulation, NumPy and Matplotlib installed. The output below was recorded with the displayed calculation.

```
"""Hydrogen molecular ion in a fixed pair of hydrogenic 1s orbitals; atomic units."""
import numpy as np
import matplotlib.pyplot as plt
from onesim.numerics.linear.matrices.dense_linear_algebra import symmetric_eigenvalues

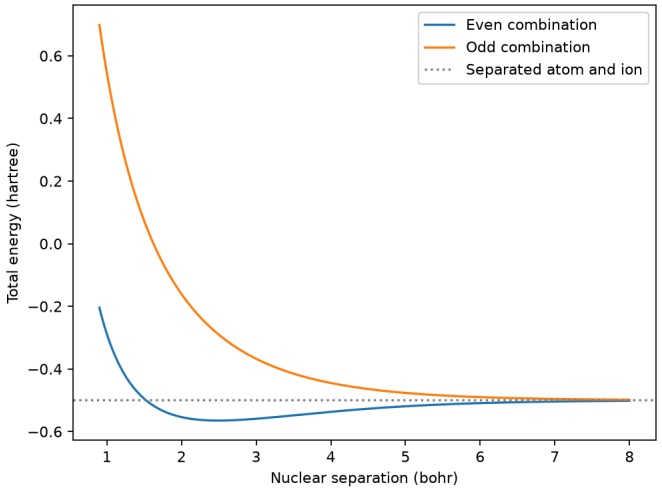
def total_energies(r):
    s = np.exp(-r) * (1 + r + r*r/3)
    j = -1/r + (1 + 1/r) * np.exp(-2*r)
    k = -(1 + r) * np.exp(-r)
    h = np.array([[-0.5+j, -0.5*s+k], [-0.5*s+k, -0.5+j]])
    metric = np.array([[1.0, s], [s, 1.0]])
    chol = np.linalg.cholesky(metric)
    left = np.linalg.solve(chol, h)
    orthogonal = np.linalg.solve(chol, left.T).T
    return symmetric_eigenvalues(orthogonal) + 1/r

distance = np.linspace(0.9, 8.0, 711)
bonding, antibonding = np.array([total_energies(r) for r in distance]).T
i = np.argmin(bonding)
print(f"Grid minimum R = {distance[i]:.3f} bohr")
print(f"Total energy = {bonding[i]:.6f} hartree")
print(f"Binding relative to H + proton = {(-0.5-bonding[i])*27.2114:.3f} eV")
plt.plot(distance, bonding, label="Even combination")
plt.plot(distance, antibonding, label="Odd combination")
plt.axhline(-0.5, linestyle=":", color="grey", label="Separated atom and ion")
```

```
plt.xlabel("Nuclear separation (bohr)")
plt.ylabel("Total energy (hartree)")
plt.legend()
plt.tight_layout()
plt.savefig("physics-molecular-ion.png", dpi=160)
```

Computed output

```
Grid minimum R = 2.490 bohr
Total energy = -0.564831 hartree
Binding relative to H + proton = 1.764 eV
```



Two-centre variational energies for the hydrogen molecular ion.

Download editable notebook · Download Python script

Add the second electron without assigning an electron to a nucleus

For neutral hydrogen include $1/r_{12}$ in the electronic Hamiltonian. The separated neutral-atom energy is now -1 hartree. With $u = \phi_A(1)\phi_B(2)$ and $v = \phi_B(1)\phi_A(2)$ the two assignments have overlap S^2. Spatial symmetrisation gives the covalent Heitler–London trial states and their energies:

$$U_{\pm}(R) = \frac{\langle u|H_{\mathrm{el}}|u\rangle \pm \langle u|H_{\mathrm{el}}|v\rangle}{1 \pm S^2} + \frac{1}{R}.$$

The plus state must carry the antisymmetric spin singlet. The off-diagonal matrix element includes electronic hopping and two-electron terms. Its sign and the overlap both enter the total energy. At large R, $S \to 0$ and each product contains one atom at each site. In contrast, a doubly occupied bonding molecular orbital expanded in the site basis contains ionic configurations with both electrons on one site. Optimising the relative weights of covalent and ionic configurations improves the dissociation limit.

As a worked matrix test take $R = 2$, $S^2 = 0.25$, $H_{uu} = -1.48$ and $H_{uv} = -0.45$ hartree. These are illustrative matrix elements, not tabulated hydrogen data. The singlet energy is -1.044 hartree after nuclear repulsion. The triplet yields about -0.873 hartree. Only the first trial value lies below the separated-atom threshold. A true equilibrium requires repeating the calculation over R.

Tutorial on shell models and bonds

1 · Count the microstates of two electrons in a p subshell

▼ **Work through the solution**

Six spin orbitals allow $\binom{6}{2} = 15$ antisymmetric two-electron determinants. For two parallel spins choose two distinct spatial orbitals in $\binom{3}{2} = 3$ ways for a fixed spin orientation. This counting alone provides no energy ordering.

---

2 · Diagnose a false bond from an omitted term

▼ **Work through the solution**

If a calculation reports only E_{el}, decreasing R can lower it through attraction to both nuclei. The force on the separation comes from $-d(E_{\mathrm{el}} + 1/R)/dR$. Omitting repulsion gives a false energy minimum or a collapse at short distance.

---

3 · Estimate the vibrational frequency near a computed minimum

▼ **Work through the solution**

Suppose $U''(R_e) = 0.10$ hartree/bohr² and the nuclear reduced mass is 918 electron masses. The angular frequency in atomic units is $\sqrt{0.10/918} = 0.0104$. In this harmonic model the vibrational energy spacing is 0.0104 hartree, or 0.284 eV. Replacing both protons by twice their mass divides the spacing by $\sqrt{2}$.

For further study see Griffiths and Schroeter, Introduction to Quantum Mechanics, 3rd edition, sections 5.2 and 8.2–8.4 on atomic configurations and variational molecular energies.

Quantum states, dynamics and measurement · 15. The scattering integral equation and successive Born terms

A weak potential often produces an angular pattern resembling its Fourier transform. What controls that approximation? A particle can propagate between two interactions with the same potential. Accounting for that propagation builds an integral equation and supplies a calculable second term.

Construct a Green function with the outgoing boundary condition

For a short-range potential and incident energy $E = \hbar^2 k^2/(2m) > 0$, move the potential to the right side of the stationary Schrödinger equation. The outgoing Helmholtz kernel satisfies $(\nabla^2 + k^2)e^{ikR}/R = -4\pi\delta(\mathbf{R})$. Its outward phase is appropriate for incident states normalised to a plane wave $e^{i\mathbf{k}\cdot\mathbf{r}}$ and time dependence $e^{-iEt/\hbar}$.

$$\psi(\mathbf{r}) = e^{i\mathbf{k}\cdot\mathbf{r}} - \frac{m}{2\pi\hbar^2}\int d^3r'\,\frac{e^{ik|\mathbf{r}-\mathbf{r}'|}}{|\mathbf{r}-\mathbf{r}'|}V(\mathbf{r}')\psi(\mathbf{r}').$$

Apply the differential operator to check the source and sign. Far outside the interaction region expand the distance in the phase as $r - \hat{\mathbf{r}}\cdot\mathbf{r}'$ and in the denominator as r. For elastic scattering $\mathbf{k}' = k\hat{\mathbf{r}}$, the coefficient of e^{ikr}/r is the amplitude.

$$f(\mathbf{k}',\mathbf{k}) = -\frac{m}{2\pi\hbar^2}\int d^3r'\,e^{-i\mathbf{k}'\cdot\mathbf{r}'}V(\mathbf{r}')\psi(\mathbf{r}').$$

Interpret each application of the free propagator

In operator notation the integral equation reads $|\psi\rangle = |\mathbf{k}\rangle + G_0^{(+)}V|\psi\rangle$. Substitution of its right side for $|\psi\rangle$ gives a plane wave, one intermediate propagation, then two propagations and so forth. The corresponding transition operator obeys

$$T = V + VG_0^{(+)}T = V + VG_0^{(+)}V + VG_0^{(+)}VG_0^{(+)}V + \cdots.$$

The first term measures the transform of V at the measured momentum transfer. In the second term an intermediate momentum is integrated over with denominator $E - \hbar^2p^2/(2m) + i0$ for p a wave number. It can differ from the incident momentum. Energy is conserved between the asymptotic states. The infinitesimal imaginary part retains the outgoing-wave condition in the integral.

> **Recall · A practical failure of first order**
>
> For a real potential the first Born forward amplitude is real. The exact optical theorem reads $\sigma_{\text{tot}} = (4\pi/k)\,\mathrm{Im}\,f(0)$. The first nonzero total cross section is order V^2. Its consistent forward contribution comes from second order, so combining orders indiscriminately can produce an apparent violation of flux conservation.

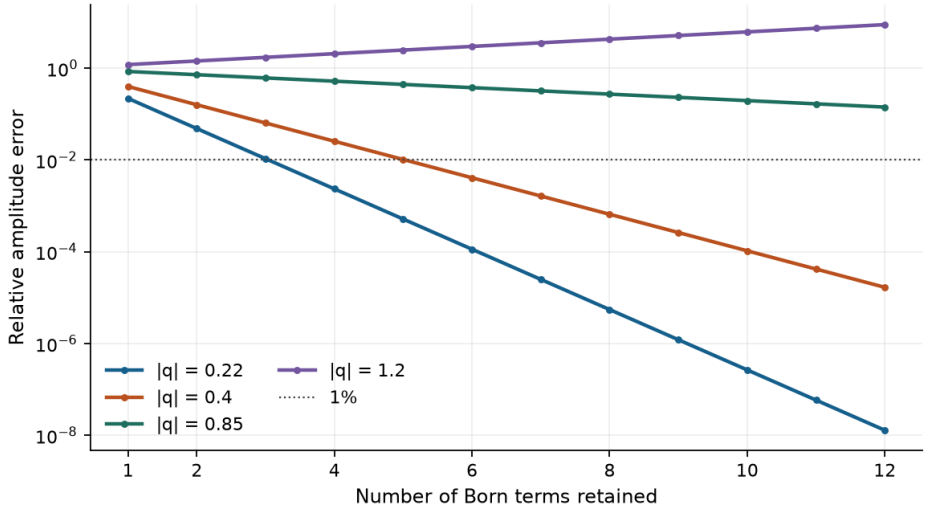
Sum a solvable sequence and test a numerical truncation

Consider a separable interaction $V = \lambda|g\rangle\langle g|$ with a square-integrable form factor. Each repeated propagation contributes the scalar $I(E) = \langle g|G_0^{(+)}(E)|g\rangle$. Trying $T = |g\rangle\tau\langle g|$ gives $\tau = \lambda + \lambda I\tau$ and hence

$$\tau = \frac{\lambda}{1 - \lambda I},$$

$$\tau_N = \lambda \sum_{j=0}^{N-1} (\lambda I)^j.$$

For $q = \lambda I = 0.20 - 0.10i$ the first-order relative amplitude error is $|q| = 0.224$. Truncating after two and three terms reduces it to $|q|^2 = 0.050$ and $|q|^3 = 0.0112$. A value approaching $q = 1$ signals strong enhancement. Exact poles follow by continuation to the correct energy domain. A small cross section in just one detector can arise from a form-factor zero even when the repeated-scattering factor is large.



Exact relative errors for the separable model. A small change in the magnitude of the repeated-scattering factor can greatly change how many Born terms are useful.

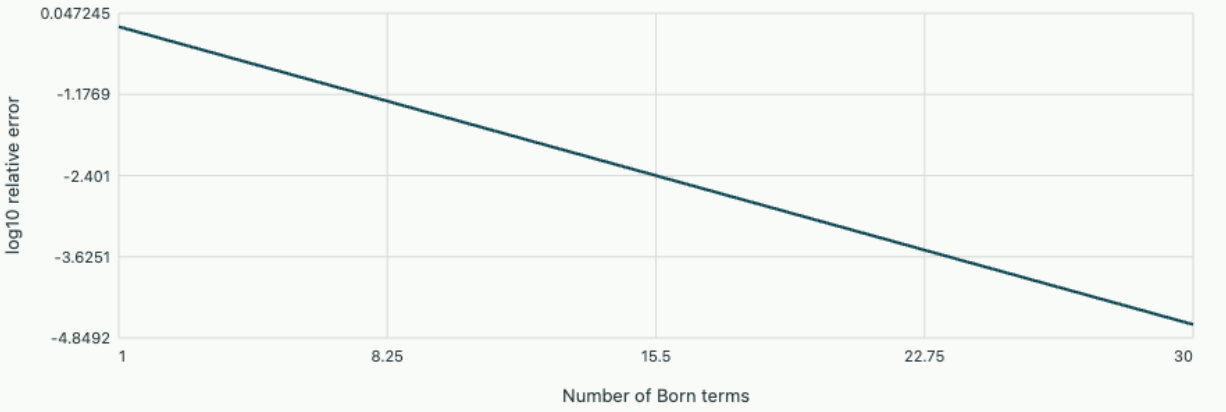
Try it · Born

Change the inputs and compare the recalculated curves with the preceding derivation and baseline figure. The axes give the units; the numerical readout states the model assumptions and any limiting cases. Reset the inputs to return to the reference setting.

Open this live calculation

Try the calculation

Repeated-scattering magnitude |λI| **0.7**



Exact separable-model truncation error

Relative error is |λI|^N. The geometric series converges.

Tutorial on recognising repeated scattering

1 · Check a Born-amplitude dimension

▼ Work through the solution

$m/\hbar^2$ has units of inverse energy times inverse length squared. Multiplying by an energy and a three-dimensional volume produces length. Squaring the amplitude gives the area per unit solid angle.

2 · Choose the number of terms

▼ Work through the solution

For a scalar $|q| = 0.40$, the relative truncation error is $|q|^N$. Five terms give 0.01024, slightly above 1%. Six give 0.00410. In a general potential no single scalar controls every channel, so repeat convergence tests with multiple incident energies and angles.

---

3 · Distinguish invertibility from convergence

▼ **Work through the solution**

At $q = -1.2$ the exact expression $\lambda/(1 - q)$ is finite. Individual Born terms grow and alternate. Failure of the expansion need not signal an infinite physical scattering amplitude. Solving the full integral equation and checking its residual are different tests from summing the series.

For further study see Griffiths and Schroeter, Introduction to Quantum Mechanics, 3rd edition, sections 10.3–10.4 on phase shifts, the integral equation and the Born series.

Quantum states, dynamics and measurement · 16. Spontaneous radiation, stimulated transitions and thermal detailed balance

A coherent laser can drive Rabi oscillations in two atomic levels. A large cavity filled with thermal radiation presents many modes with random phases. In this limit one can infer the ratios of absorption, stimulated emission and spontaneous emission coefficients by requiring the observed equilibrium to be independent of the atoms used to probe it.

Specify the convention for an Einstein coefficient

Let $E_2 - E_1 = h\nu$ and let g_i count the unresolved magnetic substates of level i. Define ρ_ν as energy per unit volume per hertz including both polarisations, and use coefficients averaged over equally populated lower or upper substates as appropriate. For an isolated narrow line in isotropic incoherent radiation the upward rate per atom is $B_{12}\rho_\nu$. The downward rate is $A_{21} + B_{21}\rho_\nu$. For a broad line average ρ_ν against a normalised line shape.

At equilibrium $N_2/N_1 = (g_2/g_1)\exp(-h\nu/k_BT)$ while stationarity requires $N_1 B_{12}\rho_\nu = N_2(A_{21} + B_{21}\rho_\nu)$. Isolate the unknown radiation density:

$$\rho_\nu = \frac{A_{21}/B_{21}}{(g_1 B_{12}/g_2 B_{21})e^{h\nu/k_BT} - 1}.$$

Count the cavity modes and identify the coefficients

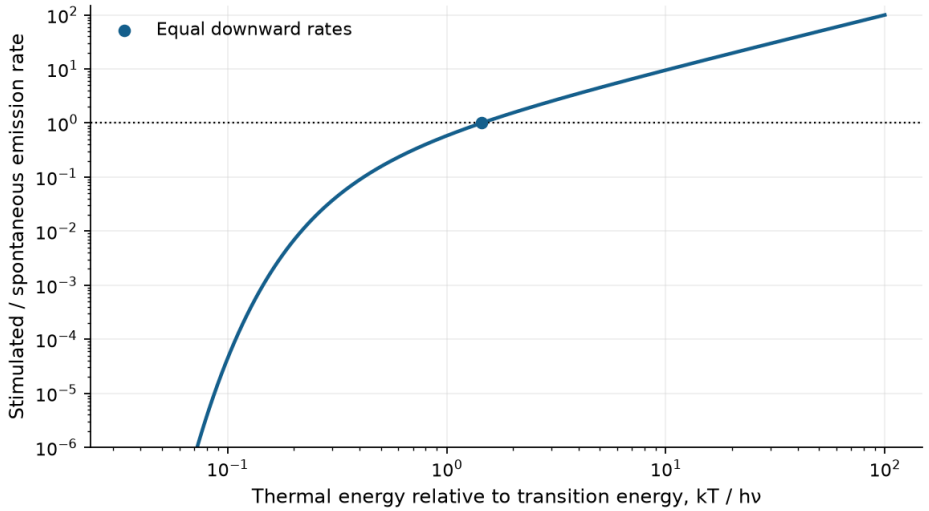
In a large periodic volume V the count of wave vectors in a shell is $V\,4\pi k^2 dk/(2\pi)^3$. Two transverse polarisations double it. With $k = 2\pi\nu/c$ this gives $8\pi\nu^2/c^3$ modes per volume per hertz. Each thermally occupied mode has mean energy $h\nu/(e^{h\nu/k_BT} - 1)$ above vacuum. Equality at every temperature fixes both independent factors in the rate expression.

$$g_1 B_{12} = g_2 B_{21},$$

$$\frac{A_{21}}{B_{21}} = \frac{8\pi h\nu^3}{c^3}.$$

The spontaneous-to-stimulated ratio in a blackbody is $e^{h\nu/k_BT} - 1$. Knowing the line frequency fixes a ratio of coefficients, not the dipole matrix element or the absolute lifetime. An isolated upper level with several radiative channels has total decay rate $\sum_j A_{2j}$ and emits into a specific channel with probability $A_{2j}/\sum_j A_{2j}$.

> **Recall · Frequency and angular frequency conventions**
>
> Spectral energies obey $\rho_\nu\,d\nu = \rho_\omega\,d\omega$. With $\omega = 2\pi\nu$, $\rho_\omega = \rho_\nu/(2\pi)$. A coefficient multiplying ρ_ω therefore changes by 2π. Comparing a printed A/B ratio requires checking this convention and whether intensity or energy density was used.



The relative importance of stimulation can be read from the ratio of bath energy to transition energy. The crossing fixes the bath temperature where the two downward rates agree.

Try it · Thermal emission

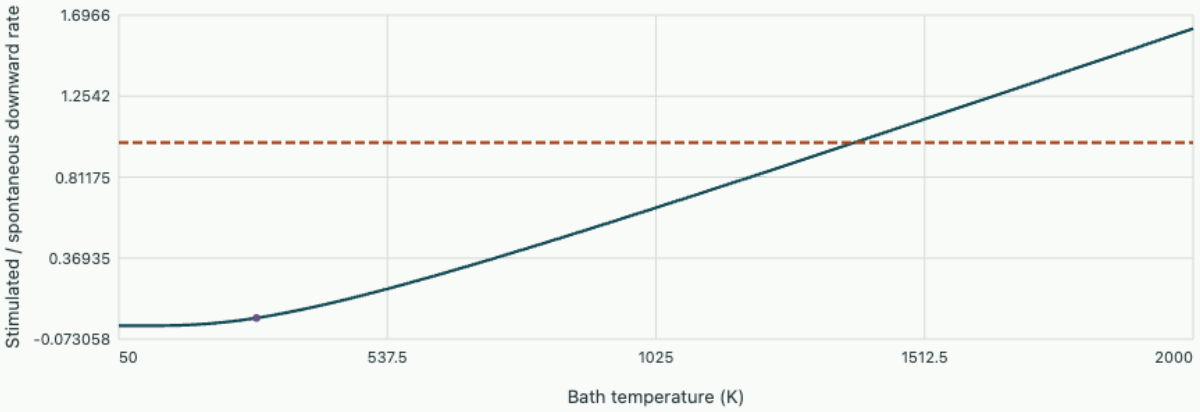
Change the inputs and compare the recalculated curves with the preceding derivation and baseline figure. The axes give the units; the numerical readout states the model assumptions and any limiting cases. Reset the inputs to return to the reference setting.

Open this live calculation

Try the calculation

Transition frequency (THz) **20**

Bath temperature (K) **300**



Thermal occupation · Equal downward rates · Selected bath

At selected bath stimulated/spontaneous = 0.042517. Equality occurs at 1384.8 K; the transition energy is hν.

Predict a lifetime and an equilibrium occupation

Consider a 10 GHz transition. Its characteristic temperature $h\nu/k_B$ is about 0.480 K. At 4 K the mean photon occupation is $1/(e^{0.120}-1) = 7.84$, so stimulated downward transitions dominate spontaneous ones. At 0.1 K the occupation is only 0.00830. A 600 THz optical transition at room temperature has $h\nu/k_BT \simeq 96$, leaving essentially no thermal photons at that frequency.

If an upper state has two decay channels of 4×10^7 and 1×10^7 s⁻¹, its vacuum population after a short excitation decays as $e^{-5\times10^7 t}$. The lifetime is 20 ns. The photon yield in the stronger branch is 0.80 in the absence of quenching and losses. Rates inferred from measured photon counts also need a detector-efficiency correction.

Tutorial on reading a line measurement

1 · Correct for unresolved degeneracies

▼ **Work through the solution**

If $g_1 = 2$, $g_2 = 6$, then $B_{12} = 3B_{21}$ in the convention of this chapter. Population inversion for net stimulated gain requires $N_2B_{21} > N_1B_{12}$, or $N_2/g_2 > N_1/g_1$.

---

2 · Find the bath temperature for equal downward contributions

▼ **Work through the solution**

Equality requires mean occupation one, hence $e^{h\nu/k_BT} = 2$. For 10 GHz, $T = 0.480/\ln 2 = 0.693$ K. Upward absorption may still occur at this temperature.

---

3 · Infer a missing nonradiative loss

▼ **Work through the solution**

An isolated excited population lasts 16 ns instead of 20 ns while calibrated radiative rates still sum to 5.0×10^7 s⁻¹. An independent nonradiative channel adds $1/(16\,\mathrm{ns}) - 5.0 \times 10^7 = 1.25 \times 10^7$ s⁻¹. The radiative quantum yield is 0.80.

For further study see Griffiths and Schroeter, Introduction to Quantum Mechanics, 3rd edition, section 11.3 on spontaneous emission and atomic lifetimes.

Quantum states, dynamics and measurement · 17. Which properties of an unknown spin can an instrument copy?

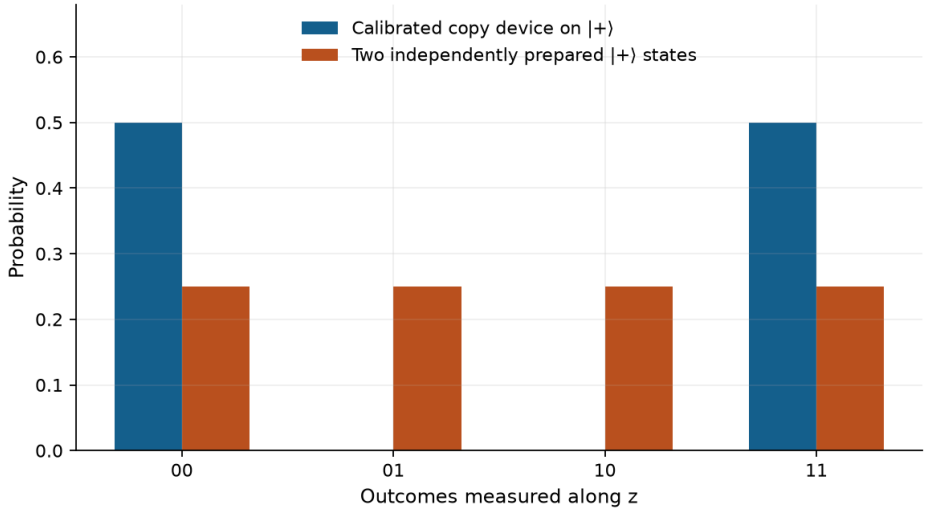
A device calibrated with spin up and down can write two perfectly distinguishable records. Asking what happens to a superposition reveals a limit on information extraction and explains why state tomography needs an ensemble.

Apply linearity to a calibrated copying apparatus

Let a blank qubit be prepared in $|0\rangle$. A unitary device might obey $U|0,0\rangle = |0,0\rangle$ and $U|1,0\rangle = |1,1\rangle$. Both rules are realised by a controlled NOT on the blank. Linearity determines the device on any superposition of these inputs. For $|+\rangle = (|0\rangle + |1\rangle)/\sqrt{2}$ the output is

$$U|+,0\rangle = (|0,0\rangle + |1,1\rangle)/\sqrt{2}.$$

The desired two-copy state would be $|+,+\rangle = (|0,0\rangle + |0,1\rangle + |1,0\rangle + |1,1\rangle)/2$. Measure both qubits along z. The actual output has zero probability of unequal results. The desired output has probability one half of unequal results. These are experimentally distinguishable preparations.



The calibrated copying device gives only matching spin records along the calibration axis. Two independently prepared superpositions also give the two unequal pairs.

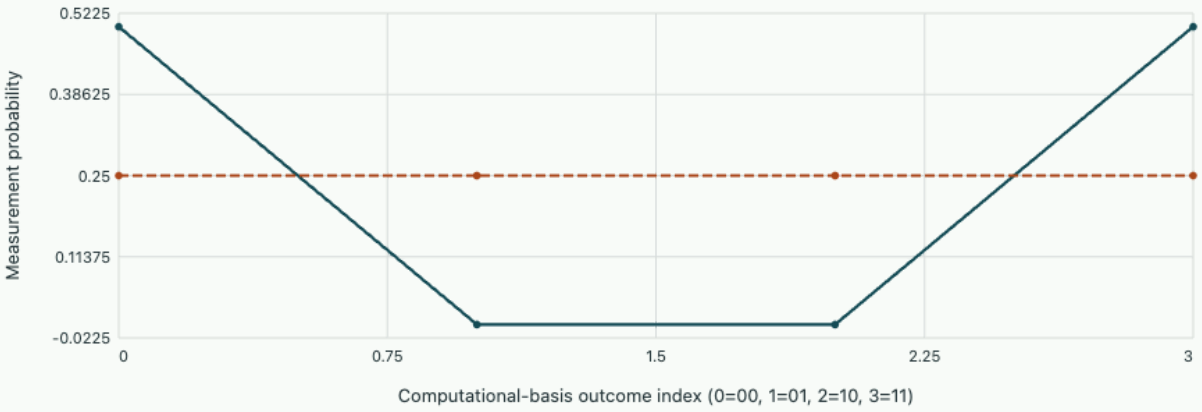
Try it · Spin copy

Change the inputs and compare the recalculated curves with the preceding derivation and baseline figure. The axes give the units; the numerical readout states the model assumptions and any limiting cases. Reset the inputs to return to the reference setting.

Open this live calculation

Try the calculation

Input polar angle (degrees) 90



Calibrated basis copier Two independently prepared copies

The copier creates correlated records. At a superposition input they differ from two independent copies; at either calibrated basis state they agree.

Derive the obstruction without assuming a particular basis

Suppose an apparatus with fixed blank and fixed prepared environment clones each of two pure states $|\psi\rangle$ and $|\phi\rangle$. After the operation any residual machine states may depend on the input. Because the two output copies are pure, they factor from the machine in each branch. Taking the magnitude of the inner product before and after unitary evolution gives

$$s = s^2\,|\langle M_\psi | M_\phi \rangle|,$$
$$s = |\langle \psi | \phi \rangle|.$$

The machine overlap is at most one, so inputs with $0 < s < 1$ cannot satisfy this equality. Orthogonal states form the special class for which exact, deterministic copying is possible. For $|0\rangle$ and $|+\rangle$, $s = 1/\sqrt{2}$ but two copies have overlap $1/2$ even before multiplying by the machine overlap. Additional hidden apparatus states cannot fix this discrepancy.

Recall · Pure, correlated and mixed outputs

Partial trace of the actual two-qubit entangled output gives each single qubit $\rho = I/2$. That result matches two fair z histograms, yet the pair has perfect z correlation. Single-axis marginals never certify that a pair consists of independent copies.

Relate disturbance to an observable record

A measurement trying to leave each state intact while recording its identity would have outputs $|\psi\rangle|m_\psi\rangle$ and $|\phi\rangle|m_\phi\rangle$. Inner-product preservation gives $\langle\psi|\phi\rangle = \langle\psi|\phi\rangle\langle m_\psi|m_\phi\rangle$. If the inputs overlap, a nondisturbing measurement of both must leave the same record up to phase. This argument assumes exact preservation. Weak or approximate measurements can provide partial information at the cost of a disturbance.

With independently prepared copies, spin tomography estimates different components on different trials. If N separate x measurements have expectation r_x, then $\hat{r}_x = (n_+ - n_-)/N$ has variance $(1 - r_x^2)/N$. At $r_x = 0$ one hundred trials give standard error 0.10. Copying a single unknown preparation could not produce these independent statistics.

Tutorial on spin records

1 · Predict a transverse measurement

▼ **Work through the solution**

For the Bell state above each individual x result is fair, but the product of the two x results is always $+1$. For the desired $|+,+\rangle$ both individual values are always $+1$. This separates the two preparations with repeated measurements.

---

2 · Distinguish a classical record from an unknown state

▼ **Work through the solution**

A classical bit is encoded in two distinguished orthogonal states. Controlled NOT copies that alphabet. Rotating the incoming state to an unknown basis introduces nonorthogonal alternatives relative to that alphabet, for which the same guarantee fails.

---

3 · How many new preparations are needed?

▼ **Work through the solution**

To estimate a spin component near zero to one standard error of 0.02 requires $N \simeq 1/0.02^2 = 2500$ independent preparations for that axis. Splitting the same budget among three axes increases each

component's error. Repeating a projective measurement on one qubit measures the prepared post-measurement state.

For further study see Griffiths and Schroeter, Introduction to Quantum Mechanics, 3rd edition, section 12.4 on the no-clone theorem.